Parasitic Molecular Strategies to Influence Host Plant Signaling and Gene Transcription

Dissertation

der Mathematisch-Naturwissenschaftlichen Fakultät

der Eberhard Karls Universität Tübingen

zur Erlangung des Grades eines

Doktors der Naturwissenschaften

(Dr. rer. Nat.)

vorgelegt von

M. Sc. Max Körner

aus Stuttgart

Tübingen

2022

Gedruckt mit Genehmigung der Mathematisch-Naturwissenschaftlichen Fakultät der Eberhard Karls Universität Tübingen.

Tag der mündlichen Prüfung:	17.01.2023
Dekan:	Prof. Dr. Thilo Stehle
1. Berichterstatter:	Prof. Dr. Markus Albert
2. Berichterstatter:	Prof. Dr. Georg Felix

Table of Content

1 Introduction 1
1.1 *Cuscuta reflexa* a vampire of the plant kingdom 1
1.2 How can parasitic plants communicate with their hosts? 4
1.3 Recognition of *Cuscuta reflexa* in the resistant tomato 5
1.4 Aim of this work 8
2 Molecular cues during susceptible Host-Parasite interaction 9
2.1 Results 9
2.1.1 Rapidly activated host gene expression during host-parasite interaction 9
2.1.2 Rapid host gene expression used as sensor to illuminate host plant signaling 12
2.1.3 Establishing a screening method to identify *Cuscuta*-derived molecular cues 14
2.1.3.1 Design and overview of the high througput bioassay 14
2.1.3.2 Detecting light emission pattern upon Cuscuta Extract treatment 15
2.1.3.3 *N. benthamiana* age effects on light emission 19
2.1.3.4 Detection range of the bioassay and the effects quenching 20
2.1.3.5 Influence of common plant components and stresses 21
2.1.3.6 Correlation of light and luciferase expression via qRT-PCR 23
2.1.3.7 Proof of concept - Comparison to attAGP 24
2.1.3.8 Alternative bioassay setup using stably transformed *A. thaliana* and *N. benthamiana* 25
2.1.4 Application of the sensor for the purification of the *Cuscuta*-derived molecular cue. 29
2.1.4.1 Properties of the *Cuscuta*-derived molecular cue during the pre-purification 29
2.1.4.2 Chromatographic purification 32
2.1.4.2.1 Purification of Cuscuta Extract 33
2.1.4.2.2 Purification of the active *Cuscuta*-derived molecular cue present in fraction 1A2 35
2.1.4.3 Proteinogenic properties of the molecular cue 38
2.1.4.4 Purification methods and technique summary 39
2.1.5 Alternative promoter-luciferase constructs - are multiple active components involved? 41
2.1.6 Investigation of *Cuscuta*-derived CLE peptides 43
2.2 Discussion 45
2.2.1 Rapidly activated host gene expression during parasitic- and host-plant interaction. 45
2.2.1.1 Transcriptomic changes in host plants during *C. refelxa* infection 45
2.2.1.2 Rapid host gene expression used as sensor to illuminate parasitic plant signaling. 47
2.2.2 Establishing the luciferase based high throughput bioassay 48

2.2.3 Purification of the parasitic signal 51
2.2.4 “A New Hope” What does Cuscuta influence in the host? 53
2.2.4.1 CLE peptides and their impact during *Cuscuta* spp. attachment 55
2.2.4.2 Summary 56
3 Analysis of the hydrophobic C-terminus of CuRe1 58
3.1 Results 58
3.1.1 Truncation of the CuRe1 C-terminal hydrophobic tail 58
3.1.1.1 Truncation of the hydrophobic tail of CuRe1 leads to reduced ethylene production 59
3.1.1.2 Truncated CuRe1 does not interact with SOBIR1 in mass-spectrometry analysis 60
3.1.1.3 Interaction of SlSOBIR1 with CuRe1 truncations 60
3.1.2 Truncation of the LRR-domain in addition to the hydrophobic tail 61
3.1.2.1 ΔLRR and ΔLRR-Δ2TM expression and ethylene production 62
3.1.2.2 Interaction of ΔLRR and ΔLRR-Δ2TM with SlSOBIR1 via Co-IP and mass-spectrometry 63
3.1.2.3 ΔLRR does not interact with SlSERK3a/b 65
3.2 Discussion 65
3.2.1 What is the role of the hydrophobic tail of CuRe1? 65
3.2.2 Truncation of the LRR-domain in addition to the hydrophobic tail 66
3.2.3 “Back to the Future”: What is the role of the hydrophobic tail of CuRe1? 68
4 Material and Methods 69
4.1 Material 69
4.1.1 Peptides 69
4.1.2 Media and Antibiotics 69
4.1.3 Bacterial strains 70
4.1.4 Plasmid lists 70
4.1.5 Oligonucleotide list 72
4.1.6 Antibodies 75
4.1.7 Plant genotypes 76
4.1.8 Chemicals and Consumables 76
4.1.9 Purification Columns and Buffers 76
4.2 Methods 77
4.2.1 DNA-Analysis 77
4.2.1.1 Plant genomic DNA preparation 77
4.2.1.2 Plant RNA preparation 77
4.2.1.3 cDNA preperation 77

4.2.1.4 Quantitative Real-Time PCR (qRT-PCR) 77
4.2.1.5 Phusion PCR 78
4.2.1.6 Colony PCR 78
4.2.1.7 Taq PCR 79
4.2.1.8 Plasmid Digest 79
4.2.1.9 Agarose-Gels 79
4.2.1.10 In Gel purification of DNA Fragments 79
4.2.1.11 Gateway TOPO cloning 79
4.2.1.12 Gateway L/R-reaction 80
4.2.1.13 GoldenGate cloning 80
4.2.1.14 Plasmid extraction from bacteria 81
4.2.1.15 Sequencing 81
4.2.1.15.1 RNA-Sequencing (provided by Krause Lab Tromsø) 81
4.2.2 Bacterial growth and transformation 81
4.2.2.1 Bacterial growth, O/N-cultures 81
4.2.2.2 Transformation of *Escherichia coli* 82
4.2.2.3 Transformation of *Agrobacterium thumefaciens* 82
4.2.3 Protein Analysis 82
4.2.3.1 Protein Extraction 82
4.2.3.1.1 Protein extraction for checking expression level 82
4.2.3.1.2 Protein extraction for Co-immunooprecipitation 82
4.2.3.1.3 Protein extraction for mass specrometry analysis 83
4.2.3.2 Protein Detection 83
4.2.3.2.1 SDS-Polyacrylamide gel electrophoresis (SDS-PAGE) 83
4.2.3.2.2 Coomassie gel staining 84
4.2.3.2.3 Gel preparation for mass specrometry analysis 84
4.2.3.2.4 Immunoblot analysis 84
4.2.3.2.5 Ponceau S 85
4.2.3.2.6 Protein concentration 85
4.2.4 Plant growth conditions and transformation 85
4.2.4.1 Plant growth conditions 85
4.2.4.2 Transient transformation of *Nicotiana benthamiana* 85
4.2.4.3 Stable transformation of Nicotiana benthamiana and A. thaliana 86
4.2.5 Functional assays 86
4.2.5.1 Proteinase digest 86
4.2.5.2 Promoter:Luciferase Bioassay 86

4.2.5.3 Ethylene biosynthesis 86
4.2.6 Technical devices 86
5 Summary 89
6 Zusammenfassung 91
7 References 93
8 Supplementary Information 100
8.1 List of Figures 100
8.2 List of Tables 102
8.3 Supplemental Datasets 103

1 Introduction

1.1 *Cuscuta reflexa* a vampire of the plant kingdom

Parasitism is a highly successful form of survival, that is visible in various forms throughout all areas of life (Westwood et al. 2010, Poulin and Morand 2000). Parasitism is based on the exploit of a host, without any regards toward the host survival. Parasitism in the plant kingdom is the switchback from an autotrophic lifestyle towards a heterotrophic lifestyle. The conversion from a self-sustaining plant into the dependency of another plant occurred 12 times during evolution and lead to approximately 292 genera and 4750 parasitic species which represent 1% of all land plants (Nickrent 2020).

Figure 1 *Cuscuta* spp. in different habitats growing on various host plants.

(A) *Cuscuta campestris* on *Coleus blumei* during flowering, greenhouse, Tübingen. (B) *Cuscuta campestris* growth on a susceptible host plant for extended time, leads to death of the host, greenhouse, Tübingen. (C) *Cuscuta europaea* growing on a *Daucus carota* field, garden near Ulm, 2020 (by Aylin Apostel). (D) *Cuscuta sp.* on susceptible host plant, Death Valley, USA, 2016. (E) Early scientific description: Würger im Pflanzenreich, Kosmos, Gesellschaft der Naturfreunde, Stuttgart, 1912

The switchback to a heterotrophic lifestyle is not an all or nothing process rather than a fine differentiation in different parasitic strategies. Based on the parasitic strategy, parasitic plants can be divided in different categories. Facultative parasitic plants do not depend on a host to complete their lifecycle but will happily parasitize neighboring plants if available (*Phtheirospermum japonicum*). On the other hand, obligate parasitic plants need a host and often depend on host derived molecules for germination (Yoneyama et al. 2010). Additionally, parasitic plants can be distinguished by their ability of photosynthesis. Hemiparasitic plants fully depend on water and nutrient supply by their host but are photosynthetic active, however with strong variation towards the efficiency. Parasitic plants that

are completely dependent on the host and do not have leaves, roots or any photosynthetic activity are holoparasitc plants. Holoparasitic plants withdraw in addition to water and nutrients carbohydrates from the host (dePamphilis and Palmer 1990, dePamphilis et al. 1997, Wicke et al. 2016). Parasitic plant species can grow rootless above or as “normal” plant with roots below the ground and can connect to the root system or the stem of their hosts (Figure 2).

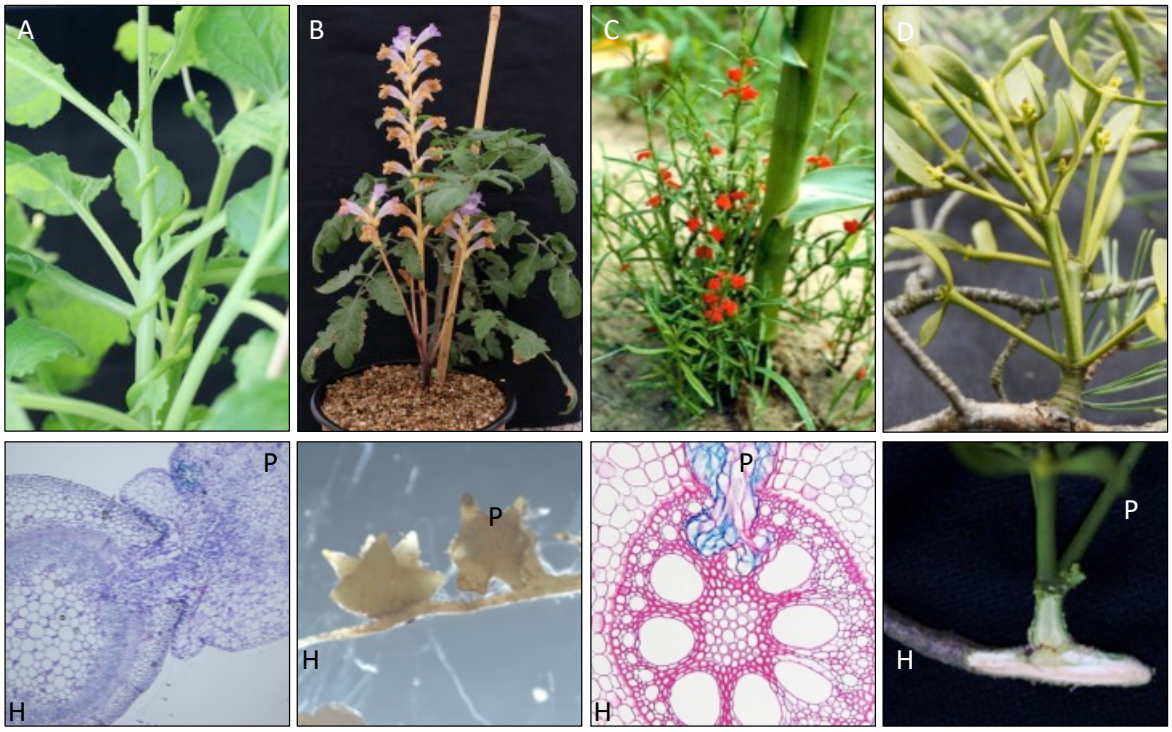

Figure 2 Parasitic plants attached to their host plants (top panel) and sections of the haustorium (bottom panel).

(A) Holoparasitic *C. reflexa* growing on *N. benthamiana* shoots. (B) Holoparasitic *P. ramosa* growing on *S. lycopersicum* roots (C). Hemiparasitic *Striga* spp. growing on maize roots (top: D.L. Nickrent, bottom: J. Scholes). (D) Hemiparasitic *Viscum* spp. growing on pine branches. H= host, P= parasite.

The obligate holoparasite *Cuscuta reflexa* is a green-yellowish, rootless and leafless vine that attaches to the stem of other plants. The lifecycle of *Cuscuta* spp. starts by sensing volatiles that are secreted by potential host plants (Runyon et al. 2006), upon sensing the volatiles *Cuscuta* spp. starts to germinate into a long thin vine that tries to get in touch with the host plant by behaving like snake of a snake charmer following the volatile leads (westwoodlab: https://www.youtube.com/watch?v=tZpjKemWalk). After making the initial contact *Cuscuta* spp. connects to the host plant by winding counter clockwise around the stem (Hegenauer et al. 2017). *Cuscuta* spp. then rapidly starts to develop so called haustoria that are a defining feature for all parasitic plants. The word haustorium originates from the Latin word haustor, which means water drawer. Haustoria, as lateral (e.g. *Cuscuta*

spp.) or terminal organs (e.g. *Striga* spp.), are the connection points between host and parasitic plant and facilitate the transfer between both plants (Yoshida et al. 2016).

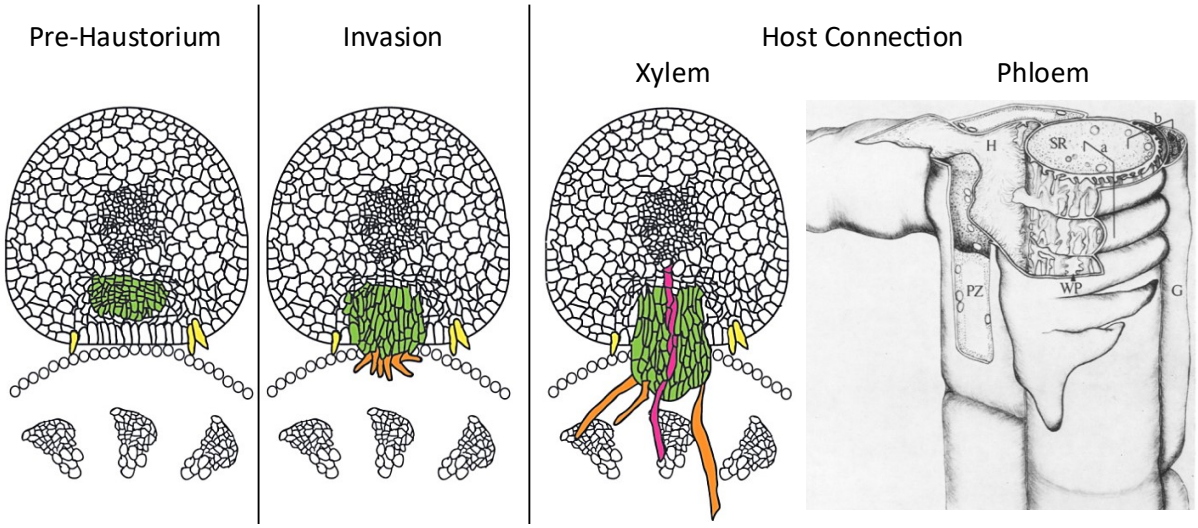

Figure 3 Haustoria development in *Cuscuta reflexa.*

The Haustoria development is initiated with by attaching to the host, the first step is the appearance of the disk like meristem (green) and trichome-like elongated cells (yellow) in the Pre-Haustorium. During the Invasive Phase the meristem cells penetrate the cortex of the host, once penetrated searching hyphae (orange) are formed and reach out for the vasculature. Searching hyphae connected to the Xylem form the Xylem bridge; Searching hyphae in touch with Phloem form hand like structures to establish the symplastic syncytium. Modified from Yoshida et al. 2016 and Dörr 1972.

The haustorium development generally can be divided in three separate phases: the formation of the prehaustorium, the invasion of the host and the connection to the host via the xylem and phloem. The haustoria formation in *Cuscuta* spp. is initiated by winding around the stem of the host and initiates the pre-haustorial phase that is accompanied by swelling and cell proliferation of a disc-like meristem structure. The development of elongated cells that start penetrating the host is the transition into the invasive phase. After the invasion of the host, specialized searching hyphae grow into the host and search for a connection to the vasculature. Searching hyphae in contact with the xylem transform into true xylem tissue, while the connection to the phloem is described as a hand like structure that wraps around the phloem and forms a symplastic syncytium (Yoshida et al. 2016, Dörr 1969, Dörr 1972). With an established connection *Cuscuta* spp. can withdraw solutes by lowering its own water potential (Hegenauer et al. 2017). This process is achieved by opening stomata to increase the water evaporation (more prominent in leafy parasites like the mistletoe) or by excreting sugars to direct the solute fluxes into the parasitic tissue (Lemoine et al. 2013, Yoshida et al. 2016, Hibbert and Jeschke 2001). *Cuscuta reflexa* is in addition able to withdraw nutrients by presenting itself as attractive sink that leads to a redirection of carbohydrates and nucleic acids into the parasite, and an exchange of

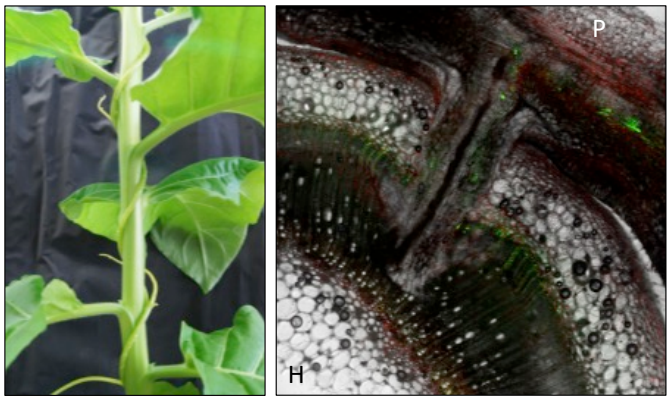

Figure 4 *C. reflexa* growing on *N. tabacum* shoots expressing pSUC2:GFP.

The transfer of GFP from host phloem cells into the parasitic tissue is an indicator for a connection of parasite and host vasculature. H= host, P= parasite (picture by Maleen Hartenstein based on Haupt et al. 2001).

amino acids and macromolecules between parasite and host (Alakonya et al. 2012, David-Schwartz et al. 2008, Haupt et al. 2001, Jeschke et al. 1994, Jeschke et al. 1997, Kim et al. 2014). The connection between *Cuscuta* spp. and host can be advantageous under certain circumstances due to the ability of *Cuscuta* spp. to connect several host plants and transferring stress signals over a long distance. Stress signaling induced by aphid feeding was shown to travel up to 1 centimeter per minute through several plants connected by *Cuscuta* spp. and could be detected throughout the plant network (Hettenhausen et al. 2017). *Cuscuta* spp. will exploit the host which leads to less biomass, less seeds and ultimately the death of the host plant.

Cuscuta spp. is known for a variety of hosts ranging from tomatoes, carrots and other crop plants. An infestation is difficult to control since slashing and manual removal is rather spreading *Cuscuta* spp. due to the ability to regenerate and over-winter from short partial veins or haustoria embedded in the host, respectively (Hegenauer et al. 2017, Truscott 1958). Cuscuta spp. seeds are known for their long hibernation in the soil that lets them germinate year after year. A general calculation of crop losses due to parasitic plants is estimated up to 1 billion US dollars which (Spallek et al. 2013, Gressel et al. 2004, Yoder and Scholes 2010) leads to a high interest in controlling *Cuscuta* spp. and studying the infection processes of *Cuscuta* spp. in detail.

1.2 How can parasitic plants communicate with their hosts?

Haustorium establishment results in an interspecific connection between host and parasite that requires the foregoing communication and orchestration as well as coordination of many developmental processes. How do parasite and host communicate with each other? What are the initial manipulative steps committed by the parasite and how do host cells sense and respond to parasitic encounters? *Orobanche* spp. initiate germination upon sensing strigolactones (Yoneyama et al. 2010) and then parasitize roots. The haustorium formation is guided by so called haustorium inducing factors (HIFs) that determine the future haustorium formation site (Chang and Lynn 1986,

Laohavisit et al. 2020 summarized in Körner et al. 2020). *Cuscuta* spp. is guided similarly to the soil distributed strigolactones of Orobanche by above ground volatiles, that escort *Cuscuta* spp. towards their host during germination (Runyon et al. 2006), after attachment no HIFs are known to help with the haustoria formation. Beside potentially unknown HIFs, Cuscuta is influenced by tactile as well as light stimuli that modulate the attachment rate and the number of initiated haustoria (Tada et al. 1996, Olsen et al.2016). Light ranging from blue to far red light was shown to influence the winding and haustorium formation rate depending on the combination of the different light sources (Furuhashi et al. 2021). Phototrophic effects could in addition induce shifts in the gradient of plant hormones like auxin (Liscum et al. 2014). Additionally, it was shown that external application of plant hormones like auxin, brassinolide and cytokinine could influence *Cuscuta* spp. behavior by increasing the number of formed haustoria and proper twining of around the host stem (Furuhashi et al. 2021). In the root parasite *P. japonicum* auxin biosynthesis was increased at the haustorium formation site during early haustorium development (Ishida et al. 2016) and during the later formation of the xylem bridge and tracheary element differentiation (Watake et al. 2020). Generally, plant hormones seem to be a target for different plant parasites that want to induce secondary growth (Matsumoto-Kitano et al. 2008). Especially cytokinine is known as mobile signal from the plant parasite *P. japonicum* to the host to induce morphological changes to influence root fitness (Spallek et al. 2017). Not only parasitic plants use cytokinines to influence the host reaction but also aphids use cytokinines to suppress the host immune system (Naessens et al. 2015). Since most of the parasite's communicative skills bases on the chemical level, the initial focus lies on the identification of the molecular cues that trigger haustoria formation and orchestrate the host connection.

1.3 Recognition of *Cuscuta reflexa* in the resistant tomato

Plants rely on two forms of innate immunity that can be divided in the PAMP-triggered immunity (PTI) and the effector triggered immunity (ETI) (Chrisholm et al. 2006, Jones and Dangle 2006). PTI is based on plasma membrane localized pattern recognition receptors (PRRs) to recognize pathogen-associated molecular patterns (PAMPs) such as the recognition of flagellin by the receptor-like kinase FLS2 (Gómez-Gómez and Boller 2000, Zipfel and Felix 2005). ETI is initiated by indirect or direct recognition of effectors by intracellular nucleotide binding leucine rich repeat (NB-LRR) resistant genes. The interplay of PTI and ETI leads to an immune syndrome that allows a variety of immune responses after detection of an intruder. While ETI is an accelerated PTI resulting in hypersensitive response (HR)(Jones and Dangle 2006), the PTI response can be divided in three stages starting with an immediate response covering the first 5 minutes after recognition, followed by the early response up to 30 minutes after recognition and the late response that can last for days (Boller and Felix 2009).

The immediate response includes changes in ion fluxes such as an increase of cytoplasmic calcium (Blume et al. 2000) and an oxidative burst (Chinchilla et al. 2007). During the following early response ethylene biosynthesis, receptor endocytosis and gene activation is initiated (Spanu et al. 1994, Robatzek et al. 2006 and Zipfel et al. 2004 respectively). The late response includes callose deposition and seedling growth inhibition (Gómez-Gómez et al. 1999 and Navarro et al. 2006 respectively). In the field of plant immunity, the microbe associated immunity is well investigated but less is known about the ongoing immunity during the interaction between a parasitic plant and its host. Parasitic *Cuscuta* spp. usually go unrecognized by host plants, however one exception is the cultivated tomato that can sense attacks by *C. reflexa*. The detection of *Cuscuta* spp. by tomato at least partially relies on the PRR Cuscuta Receptor 1 (CuRe1) that can detect the cell wall derived protein Cuscuta reflexa Glycine Rich Protein (CrGRP), containing the 21 amino acids long minimal motif CrCrip21. CrGRP is present in all *C. reflexa* cell walls including stem, haustoria and flowers, the full length CrGRP as well as CrCrip21 can induce ethylene and a hypersensitive reaction (HR) in tomato (Hegenauer et al. 2016, Hegenauer et al. 2020, Slaby et al. 2021). CuRe1 is a leucine-rich-repeat receptor-like protein (LRR-RLP) lacking an intracellular signaling domain. Therefore, the interaction with Suppressor of BIR1 (SOBIR1) providing the intracellular kinase is crucial for the signal transduction (Hegenauer et al. 2016, van der Burgh et al. 2019, Gust and Felix 2014). Upon ligand binding BRI1-Associated Receptor Kinase 1 (BAK1) was shown to be recruited sown in the well-studied RLP23 – SOBIR1 complex (Albert et al. 2015). It is expected that CuRe1 behaves in a similar fashion during CrCrip21 recognition and forms the CuRe1 – SlSOBIR – SlSERK3 (*S. lycopersicum* homologue of BAK1) complex. CuRe1 has an *in silico* predicted secondary intracellular domain that is of hydrophobic nature, compared to other RLPs e.g. RLP23 which is lacking a hypothetically second hydrophobic domain. This interesting feature led to a closer investigation of the possible role of the hydrophobic domain of CuRe1. Since RLP and SOBIR binding was shown to be dependent on the extracellular domain (Smakowska-Luzan et al. 2018, Mott et al. 2019) altered ethylene production or SlSOBIR1 binding via co-IP and MS/MS would uncover additional signaling pathways of CuRe1.

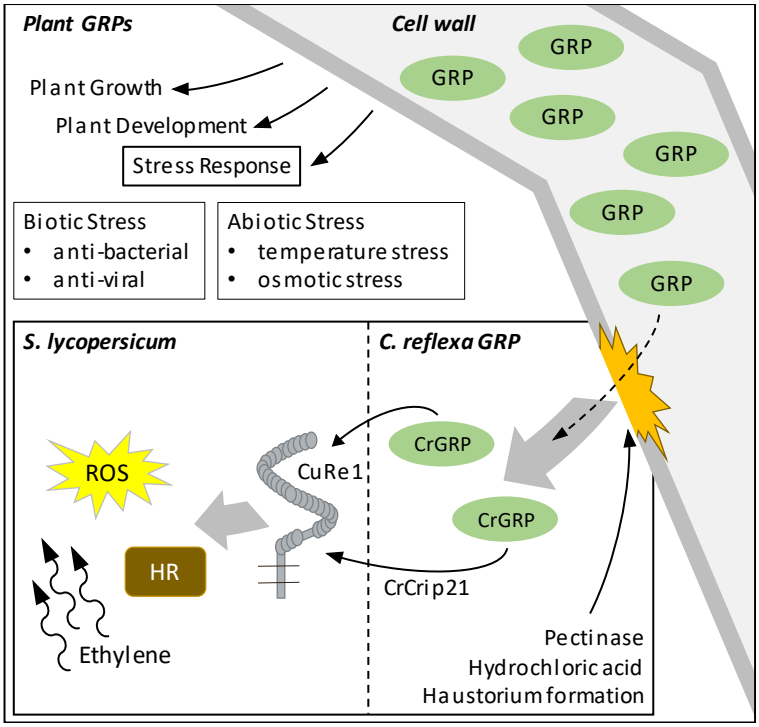

Figure 5 Roles of GRPs in plants and how CrGRP can initiate host defense during haustorium formation.

GRPs belong to a superfamily of proteins that can fulfill multiple roles in plant growth, plant development and stress responses. In *Cuscuta* spp.-host interactions, the cell wall derived CrGRP, or its minimal motif CrCrip21, is released naturally during host invasion or by pectinase and hydrochloric acid treatment. CrGRP/CrCrip21 is recognized by tomato CuRe1 and initiates defense responses like hypersensitive response (HR), reactive oxygen species (ROS) – and ethylene-production. (Slaby et al. 2021)

1.4 Aim of this work

The aims of this PhD thesis intend to shed light on the molecular processes during the interaction between the parasitic plant *C. reflexa* and host plants with special interest in the interplay of *Cuscuta*-derived molecular cues, their recognition and subsequently induced effects on the host cellular signaling and developmental processes.

***Cuscuta reflexa* – Susceptible host interaction:**

1. **Rapidly activated host gene-expression during the early stages of infection:** Transcriptome changes induced by *C. reflexa* during the early stages of infection should be analyzed and evaluated. To achieve this aim, an RNA sequencing approach is started in addition to literature screening.
2. **Establishing a high throughput bioassay to identify *Cuscuta*-derived molecular cues:** The information from the RNA sequencing and literature should be used to establish a high throughput bioassay. The bioassay is based on luciferase and the light emission upon promoter activation.
3. **Application of the bioassay to purify the *Cuscuta*-derived molecular cue:** The established assay should be used to find one or more molecular cues that are send out by *C. reflexa* to influence or hijack the susceptible host for their own benefit.

Characterization of CuRe1 downstream signaling

CuRe1 should be investigated in more detail with special interest in the downstream signaling, uncovering potential co-receptors and alternative binding partners.

2 Molecular cues during susceptible Host-Parasite interaction

2.1 Results

Haustorium establishment results in an interspecific connection between host and parasite that requires the communication and orchestration as well as coordination of many developmental processes. How do parasite and host communicate? What are the initial manipulative steps committed by the parasite and how do host cells sense and respond to parasitic encounters? Since most of the parasite's communicative skills bases on the chemical level, the initial focus lies on the identification of the molecular cues that trigger haustoria formation and orchestrate the host connection. To tackle this question, the transcriptomic regulation of the host needs to be investigated, to find induced genes that can be used in a bioassay to screen for the parasitic molecule that can initiate the communication with the host. To monitor the transcriptomic changes an RNA sequencing experiment was initiated that shows changes 2 hours after infiltration with an CrGRP containing extract. In addition, published data was used that investigated transcriptomic changes during different steps of *Cuscuta* spp. growing and attaching to its host. Based on the RNA sequencing, strongly induced host genes of the early phases of *Cuscuta* spp. attachment were found and implemented in a fast and easy bioassay that can process a high number of samples. The bioassay is based on promoters of the upregulated genes that are fused to the reporter gene luciferase.

Two major goals were to establish an appropriate bioassay and use it to find a molecular cue derived from *C. reflexa* that influences the host plant development. The major steps of the bioassay establishment were: (1) Finding rapidly activated host genes as sensor for parasitic signal detection, (2) Establishing a high throughput measuring system to identify *Cuscuta*-derived molecular cues and (3) Applying the system to purify and identify the *Cuscuta*-derived molecular cues.

2.1.1 Rapidly activated host gene expression during host-parasite interaction

To investigate rapidly activated host gene expression and use it as sensor for parasitic signal detection, the effects of an CrCrip21 (Hegenauer et al. 2020) containing extract on the transcriptome were tested. The experimental setup as well as the initial data analysis performed by the QBIC (Tübingen, Germany) is described in Körner 2016. A second evaluation was performed in cooperation with the Group of Kirsten Krause (Tromsø, Norway). The analysis by the Krause Group led to a strong decrease in regulated genes in all samples but increased confidence, due to increased thresholds the total count of regulated genes is 2049 (1536 upregulated and 512 downregulated) compared to the initial analysis with 34956 regulated genes.

The Principle Component Analysis (PCA) is used to predict a correlation between the compared plants genotypes (*N. benthamiana* wildtype (Wt), *N. benthamiana* stably transformed with CuRe1 (CuRe)), the treatment (CrGRP containing extract in MES buffer pH 5,5 (+), MES buffer pH 5,5 (-)) as well as the two time points (0h, 2h). Three distinct clusters are marked in Figure 6 while all plants at the 0-hour time point independent of treatment and genotype cluster in the lower half of the PCA (Figure 6: 0h), a shift is visible due to the treatment after 2 hours (Figure 6: 2h). One additional cluster is given by samples of *N. benthamiana* stably transformed with CuRe1 and treated with Cuscuta Extract after two hours (Figure 6: red circle: CuRe1 (+)).

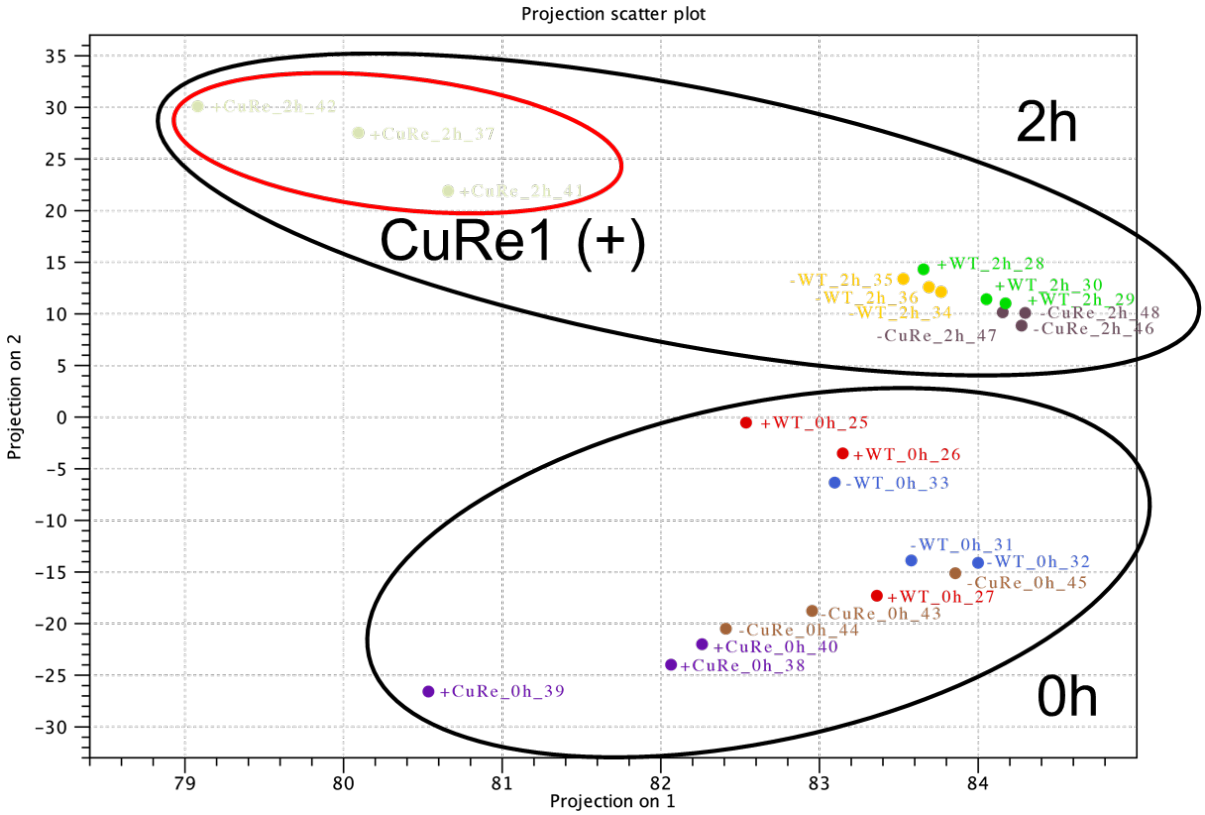

Figure 6 Principal Components Analysis of the individual samples.

Clusters are indicators of similar overall expression of the repetitions. Cluster 0h includes all plants and treatments at the 0h time point, Cluster 2h includes all samples and treatments at the 2h time point and Cluster CuRe1 (+) includes the 3 replications of *N. benthamiana* stably transformed with CuRe1 treated with CrGRP containing extract after 2 hours. Each individual sample, *N. benthmiana* wildtype (WT) and *N. benthmiana* stably transformed with CuRe1 (CuRe) each with (+) and without (-) treatment of CrGRP containing extract at time point 0h and 2h after infiltration, is shown in the PCA.

Based on the predicted changes in the PCA all regulated genes were sorted into upregulated vs downregulated genes and additionally binned into the following categories: genotype (*N. benthamiana* WT, *N. benthamiana* CuRe1), treatment (CrGRP containing extract in MES buffer pH 5,5 (+), MES buffer pH 5,5 (-)) and time point (0h, 2h). (Figure 7)

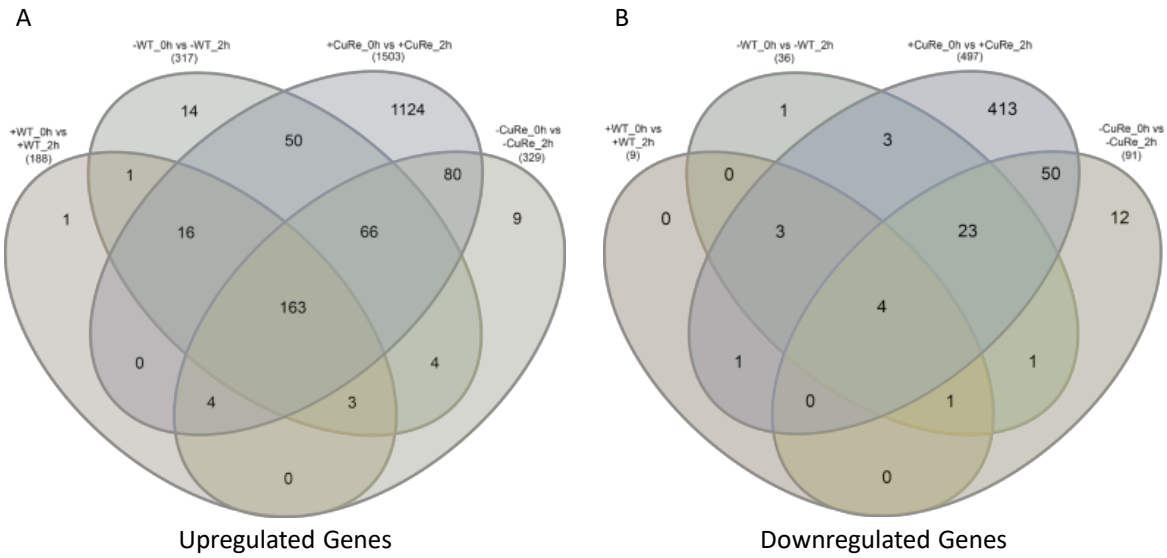

Upregulated Genes Downregulated Genes

Figure 7 Up- and Downregulation of host genes by exposition to Cuscuta Extract.

Most changes in regulation after 2 hours are visible in *N. benthamiana* stably transformed with CuRe1 treated with CrGRP containing extract. In wild type *N. benthamiana* CrGRP containing extract is not influencing the gene regulation. The two control treatments represent the CrGRP containing extract independent regulation due to infiltration process and the 2h incubation period. The regulated genes were sorted into upregulated genes (A) and downregulated genes (B). Both groups were binned into the categories wildtype *N. benthmiana* (WT) and stably with CuRe1 transformed *N. benthamiana* (CuRe1) each with (+) and without (-) treatment of the CrGRP containing extract. Samples were collected immediately after infiltration or 2h after infiltration (n=3). Total number of upregulated genes 1536, total number of downregulated genes 513.

Most changes occurred in stable transformed *N. benthamiana* CuRe1 treated with CrGRP containing extract, 1124 genes were specifically upregulated upon recognition by the CuRe1. These upregulated genes can be sorted in Gene Ontology (GO) categories if they are available, of the 1124 genes 505 had a designated molecular function and could be sorted in the corresponding group (Figure 7). The most influenced groups by Cuscuta Extract are protein modification, RNA biosynthesis and solute transport (Table 1).

Table 1 Upregulated genes sorted by their Gene Ontology (GO) molecular function in resistant plants (CuRe1 containing *N. benthamiana*) 2 hours after CrGRP containing extract infiltration (1124 genes were upregulated and 505 had a designated molecular function).

Molecular Function (GO, if available)	*N. benthamiana* CuRe1 + Cus Ex
Protein modification	77
RNA biosynthesis	63
Solute transport	49
Protein degradation	44
Membrane vesicle trafficking	36
Lipid metabolism	33
Cellular respiration	31
Reactive oxygen metabolism	21

Cell wall	21
Phytohormones	19
Protein biosynthesis	15
Secondary metabolism	14
Photosynthesis	13
Coenzyme metabolism	12
Nutrient uptake	8
Environmental stimuli response	8
Amino acid metabolism	8
Cytoskeleton	7
Protein translocation	6
Carbohydrate metabolism	6
RNA processing	5
Cell cycle	5
Chromatin assembly and remodeling	2
Polyamine metabolism	1
Nucleotide metabolism	1
DNA damage response	0
Number of genes with available molecular function	505
Number of regulated genes	1124

2.1.2 Rapid host gene expression used as sensor to illuminate host plant signaling

In 2015 a bioinformatic approach to distinguish plant parasite and host transcriptomes at the interface region has been published by Ikeue et al. and served as rich source for regulated host genes. The bioinformatic approach yielded regulated genes on a large scale in the host plant *Glycine max* as well the parasitic plant *Cuscuta japonica* for 5 parasitizing stages (24 hours after attachment (haa)), 48haa, 72haa, 96haa, 120haa). To detect genes that are regulated during the early stages of attachment, the focus lied on samples collected at 24haa (pre-haustorial phase) and 48haa (invasive phase) which mark the transition from no plant-plant connection to the first host tissue invasion. This transition was expected to have the initial transfer of possible molecular cues from the parasite to the host. Comparing 24haa and 48haa upon the induced transcriptomic changes therefore represent the regulated genes that are influenced by transferred molecular cues or other factors involved in *Cuscuta* spp.-host connection. The transcriptomic changes were ranked by their fold induction change. The promoters were selected based on the fold induction of regulated genes and additionally based on their genetic ontology molecular function to represent a broad spectrum of potential sensors. Upregulated genes involved in transport, RNA binding, plant hormone sensing and kinase-based sensing were selected (Körner 2016). The initial selection in Körner 2016 was extended by new candidates and resulted in 22 genes that were chosen. Promoters of the genes were cloned and tested for the ability to sense Cuscuta Extracts in this work. Other genes became of special interest due to

later insights (SWEET10, SUC2) and due to their already published function, e.g. at the interface region between parasite and host (Albert 2005).

Table 2 Genes selected for the bioassay

Nr.	Locus ID	Abbreviation	Arabidopsis Name
1	AT1G17240	RLP2	RECEPTOR LIKE PROTEIN 2
2	AT5G25610	RD22	RESPONSIVE TO DESICCATION 22
3	AT1G11650	RBP45B	RNA binding protein 45 B
4	AT1G55020	LOX1	LIPOXYGENASE 1
5	AT4G40060	HB16	HOMEOBOX PROTEIN 16
6	AT4G30960	SIP3	SNF1-RELATED PROTEIN KINASE 3
7	AT5G26340	STP13	SUGAR TRANSPORT PROTEIN 13
8	AT1G28110	SCPL45	SERINE CARBOXYPEPTIDASE-LIKE 45
9	AT4G34138	UGT73B1	UDP-GLUCOSYL TRANSFERASE 73B1
10	AT1G49820	MTK	5-METHYLTHIORIBOSE KINASE 1,
11	AT5G04040	SDP1	SUGAR-DEPENDENT1
12	AT1G09380	UMAMIT25	USUALLY MULTIPLE ACIDS MOVE IN AND OUT TRANSPORTERS 25
13	AT4G11650	OSM34	OSMOTIN 34
14	AT5G18030	SAUR21	SMALL AUXIN UP RNA 21
15	AT3G49940	LBD38	LOB DOMAIN-CONTAINING PROTEIN 38
16	AT2G13610	ABCG5	ATP-BINDING CASSETTE G5
17	AT3G03770	LRR protein kinase	Leucine-rich repeat protein kinase family
18	AT1G33811	GGL7	Guard-cell-enriched GDSL Lipases
19	AT2G38530	CDF3, LTP2	CELL GROWTH DEFECT FACTOR-3, LIPID TRANSFER PROTEIN 2
20	AT2G01860	EMB975	EMBRYO DEFECTIVE 975
21	AT2G19190	FRK1	FLG22-INDUCED RECEPTOR-LIKE KINASE 1
22	AT4G03230	G-LecRK	G-type lectin receptor kinase
	Special Interest		
23	AT1G22710	SUC2, SUT1	SUCROSE-PROTON SYMPORTER 2, SUCROSE TRANSPORTER 1
24	AT5G50790	SWEET10	SUGARS WILL EVENTUALLY BE EXPORTED TRANSPORTERS 10
25	Solyc08g078020	attAGP	attachment METHIONINE RICH ARABINOGALACTAN

It was assumed that regulatory elements stretch from -1bp to -1000bp from the transcriptional start (Yamamoto et al. 2007), other reports show an influence of promoters with a sized of up to 5700bp (Liu et al. 2014). The exact promoter length was not known, therefore this approach used a length of 2000bp (+/- 150bp) to include major regulatory elements and possibly stretched out elements that localize approximately -2000bp to -1500bp from the transcriptional start (Yu et al. 2016). Exceptions were established promoters where the described length was used (FRK1 (Asai et al. 2002), attAGP (Albert 2005), SUC2 (Haupt et al 2001), SWEET10 (Klatt 2021)).

To be used as sensors the cloned promoters were fused to luciferase via the established gateway cloning by Karimi et al. 2005.

2.1.3 Establishing a screening method to identify *Cuscuta*-derived molecular cues

2.1.3.1 Design and overview of the high througput bioassay

The bioassay is based on a Master Thesis (Körner 2016, Tübingen) to identify molecular cues that are secreted by *Cuscuta* spp. to the host to orchestrate the processes during parasite-host connection. The bioassay facilitates promoter-luciferase fusion reporter constructs (sensors) transiently transformed into *N. benthamiana* to detect *Cuscuta*-derived molecules. In a first step the transiently transformed *N. benthamiana* leaves were cut into small 3mm by 3mm pieces to fit into 96-well plates. The 96-well plates allowed a high sample size that could be detected full automatized by a plate reader. To find a bioactive molecular cue, various preparations were added to each leaf sample in the 96-well plates and the shift of light emission by the luciferase activation was measured with a Luminometer over time. The approach described in the Master Thesis (Körner 2016, Tübingen) differs in the setup and the light emission calculation. The transiently transformed leaf pieced were treated with Cuscuta Extract and incubated without the addition of luciferin. The luciferin was added with the inject pump of the luminometer and the light flash was measured and integrated for 5 seconds. The relative light units (RLU) of the light flash were higher in samples treated with Cuscuta Extract which lead to the assumption that this was due to a higher accumulation of the luciferase. Multiple variables raised concerns since the injection of luciferase could not be monitored. The application could vary due to droplets sticking to the side of the 96-well plate. Light measurements in well plates strongly depend on the surface of the measured liquid and the filling height, both were disturbed during the application via the inject pump and might have led to higher deviations of individual measurements. Additionally, time courses were not possible with this method because they needed the luciferase addition at the beginning to monitor individual time points during the measurement. To establish a bioassay that would be able to measure various time points as well as the single endpoint without altering the setup an alternative approach was considered. The bioassay approach described in the following result chapters represent the optimized bioassay setup.

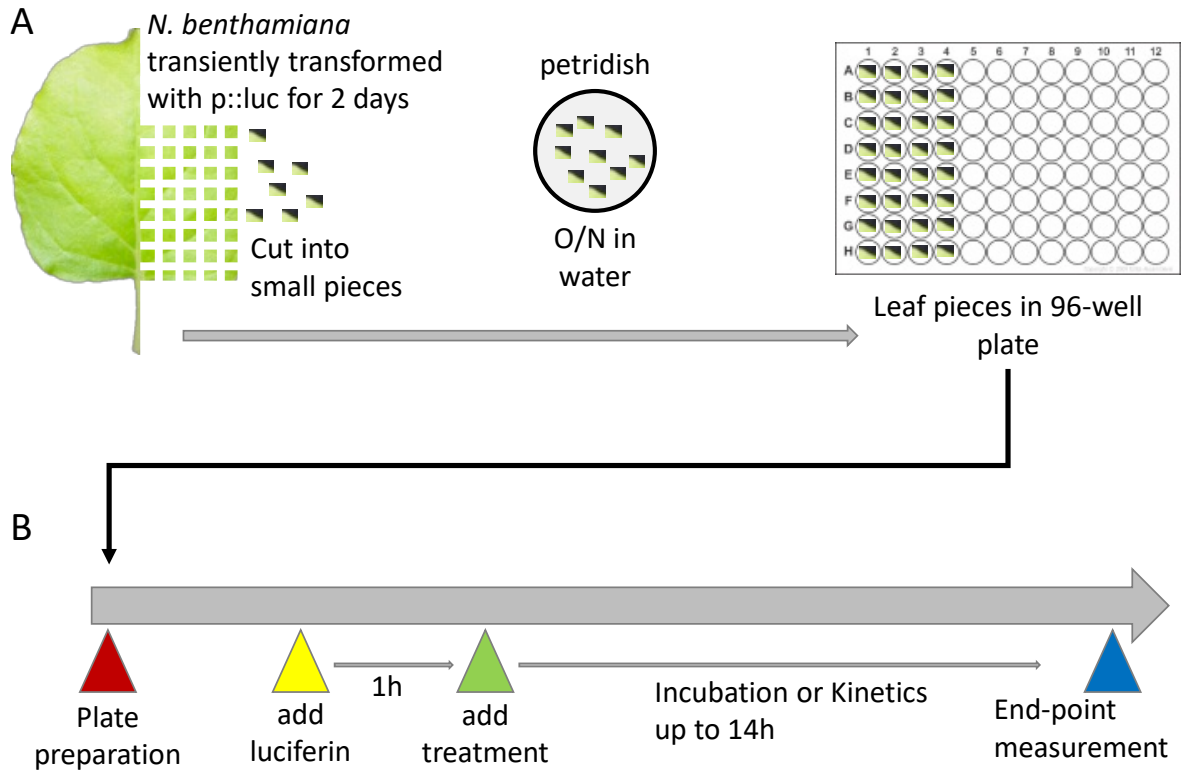

Figure 8 Plate preparation and measuring overview of the luciferase-based bioassay.

(A) Preparation for the bioassay include the transient expression of the selected sensor for 2 days, the transiently transformed leaves are cut into small pieces (3x3mm) and incubated over night to reduce stress reactions from cutting. The leaf pieces are distributed into a 96-well plate in 25mM MES pH 5,5. (B) For the bioassay luciferin is added to the 25mM MES pH 5,5 and after 1h the treatment (e.g. extracts, peptides and controls) is added. Light emission can be measured as endpoint measurement over time. The plate cannot stay for more hours in the luminometer due to high evaporation of the buffer.

2.1.3.2 Detecting light emission pattern upon Cuscuta Extract treatment

All promoter-luciferase sensors were screened for their ability to respond to Cuscuta Extract, since it was not known how and after what time the sensors would react they all have been tested over a few hours lasting time period. The measurement over time revealed the activation time point and the activation amplitude. The activation time point was determined as the first time the emitted light signal reached 2-3 times above the background. This ratio of 2-3 times of the light emission was calculated by the amplitude between background light and the light emission induced by an activation of the promoter. The used Cuscuta Extract is described in in the purification workflow (Figure 21).

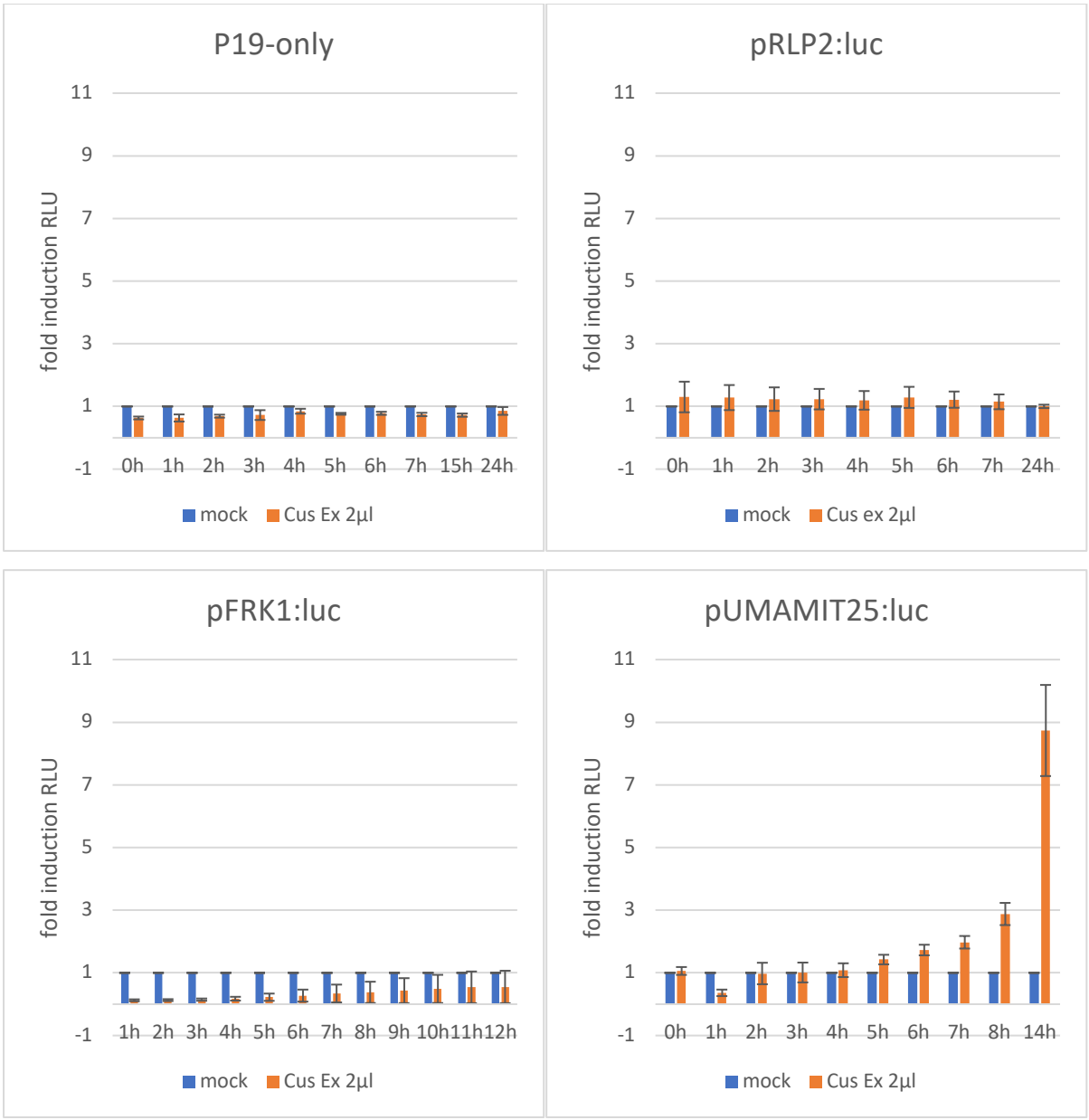

Figure 9 Light emission over time with one measurement per hour.

The functional pUMAMIT25 shows a steady increase of relative light units (RLU) during the measuring period, the non-functional pRLP2 and pFRK1 show no change in RLU over time. The silencing suppressor P19-only does not emit light. The bars show for each time point the fold induction based on the mock control of the same time point, mock= 2µl water, Cus Ex= 2µl Cuscuta Extract, pUMAMIT25 and pFRK1 N=3, pRLP2 N=4, P19 N=9, whiskers are standard deviation.

Based on the results of the time course experiments the sensors could be selected upon their ability to detect Cuscuta Extract. Sensors that did not give any difference of light output in comparison to the control treatment over time were classified as inactive, sensors that were able to detect Cuscuta Extract and induced a significant light increase (2-3 times above background) were classified as active.

Out of 22 initial candidates 17 were cloned and 3 showed a specific reaction to Cuscuta Extract (Table 3)

Table 3 Promoter-Luciferase construct cloned and tested in the bioassay to detect Cuscuta Extract

Nr.	Locus ID	Abbreviation	Cloned	Activation by Cus Ex
1	AT1G17240	RLP2	Yes	No
2	AT5G25610	RD22	Yes	No
3	AT1G11650	RBP45B	Yes	Yes
4	AT1G55020	LOX1	Yes	No
5	AT4G40060	HB16	Yes	No
6	AT4G30960	SIP3	No	No
7	AT5G26340	STP13	No	No
8	AT1G28110	SCPL45	Yes	No
9	AT4G34138	UGT73B1	No	No
10	AT1G49820	MTK	Yes	Yes
11	AT5G04040	SDP1	Yes	No
12	AT1G09380	UMAMIT25	Yes	Yes
13	AT4G11650	OSM34	Yes	No
14	AT5G18030	SAUR21	Yes	No
15	AT3G49940	LBD38	Yes	No
16	AT2G13610	ABCG5	No	No
17	AT3G03770	LRR protein kinase	No	No
18	AT1G33811	GGL7	Yes	No
19	AT2G38530	CDF3, LTP2	No	No
20	AT2G01860	EMB975	Yes	No
21	AT2G19190	FRK1	Yes	No
22	AT4G03230	G-LecRK	Yes	No
	Special Interest			
23	AT1G22710	SUC2, SUT1	Yes	Yes
24	AT5G50790	SWEET10	Yes	Yes
25	Solyc08g078020	attAGP	Yes	Yes

Based on the measurement over time the optimal time point for each sensor could be determined. For example, pUMAMIT25:luc shows a strong light emission after 14h of treatment (Figure 9) the same result is achieved by treating the samples and incubating them for 14h before the light measurements (Figure 10). Active as well as inactive sensors were repeated with additional controls. pFRK1:luc was previously used to monitor PAMP responses in *A. thaliana* protoplasts (Asai et al. 2002, Albert et al. 2010). Similarly, RLP2 was described in the context of resistance and susceptibility to fungus (Shen and Diener 2013). The ability of plants to react to PAMPs could trigger various downstream signaling pathway components, including the selected sensors. Since the aim of this work was the to study the susceptible interaction of parasitic plants and their hosts, distinguishing between known immune

response triggering peptides and an unknown component in the Cuscuta Extract was essential. Flg22 was used as well known PAMP and as a representative stimulant to switch on the LRR-RLK-related PTI pathway and as potential trigger of the previously described pFRK1:luc. CrCrip21 was the representative inducer for the LRR-RLP pathway and known as immune response inducing peptide originating from *Cuscuta* spp. (Figure 10).

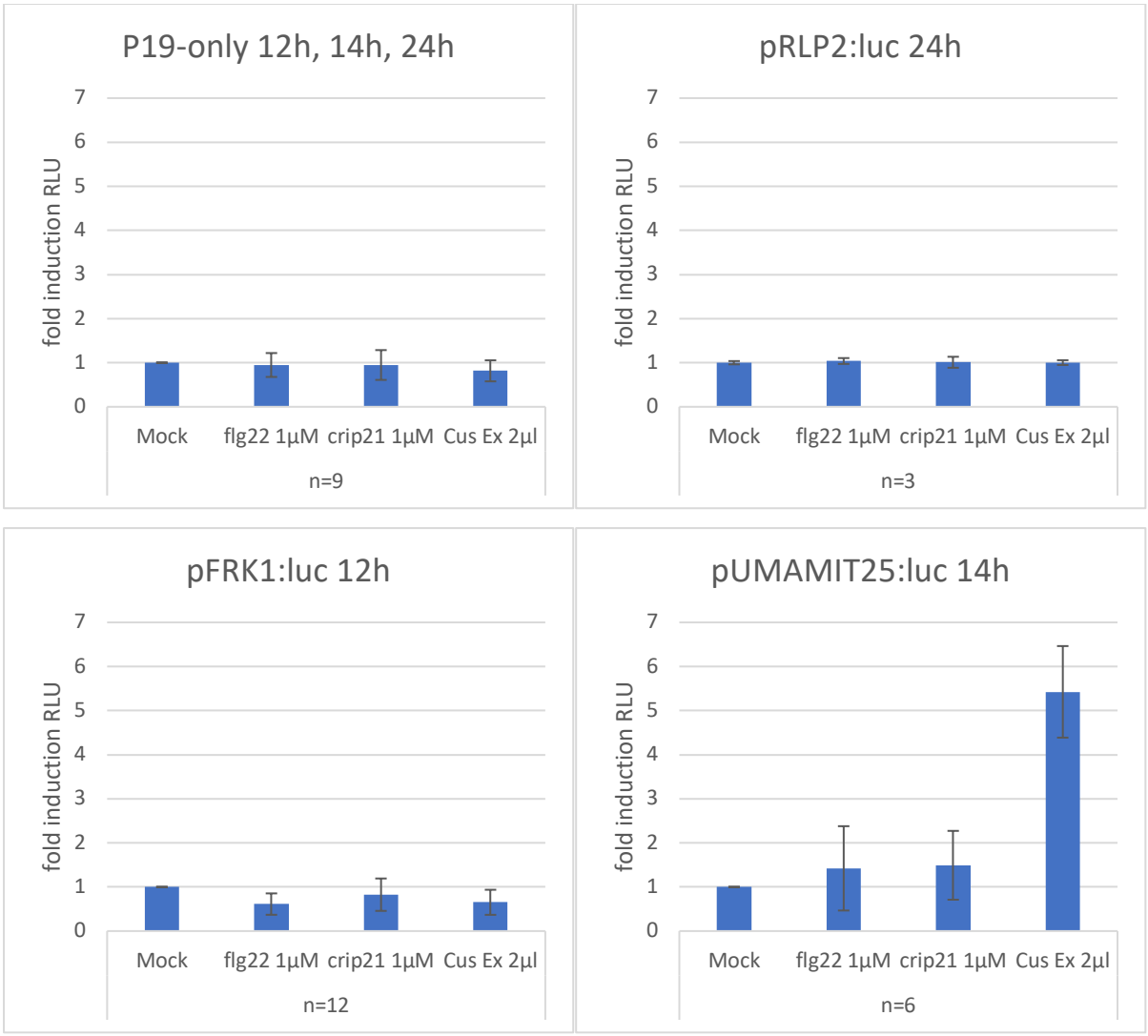

Figure 10 Light emission after incubation using an endpoint measurement (representative selection).

P19 was co-transformed as silencing suppressor and negative control, P19-only does not initiate light emission at any time. pFRK1 did not react in the described setup, after 12h. pRLP2 a non-suitable sensor construct has very low light emission. pUMAMIT25 has a significant increase of light production, 5-fold increase compared to mock treatment. Bars show relative light units (RLU) relative to the mock control measured after the same incubation time. Mock= 2µl water, Cus Ex= 2µl Cuscuta Extract, Peptide end conc 1µM, pUMAMIT25 and pFRK1 N=3, pRLP2 N=3, P19 N=9, whiskers are standard deviation.

In Figure 10 a selection of the tested sensors is shown, pFRK1:luc and pRLP2:luc are representative for complete inactive sensors that did not show a response after the Cuscuta Extract treatments and

interestingly they did not react to the PAMPs as well. In contrast, pUMAMIT25:luc is strongly upregulated and displays a high fold induction after stimulation with Cuscuta Extract compared to the control. Similarly, all the cloned promoter-luciferase constructs were tested for their capability to function as sensor and based on these results, selected sensors were used for further experiments, shown in Table 3. With all experiments P19, the suppressor of silencing, was transiently co-transformed in *N. benthamiana,* therefore plants containing only P19 were used as negative control to exclude spontaneous light emission by assay independent luciferin oxidation. P19 was tested identically to the sensors containing samples at the time points between 0h and 24h as indicated in Figure 9 and Figure 10.

Three sensors worked very well and did show a reaction to Cuscuta Extract but only pUMAMIT25:luc did offer a stable read out as well as clear and high ratio of light emission. For all further experiments pUMAMIT25:luc was used as it gave the clearest results.

2.1.3.3 *N. benthamiana* age effects on light emission

For further experiments the influence of the plant age of transformed *N. benthamiana* was determined. Two time points were tested, 4 week and 5 weeks, younger plants were too small to provide a reasonable number of leaf pieces and older plants started flowering and needed too much space when cultivated in the greenhouse. Therefore 4- and 5-week-old plants were transformed and tested with the Cuscuta Extract. In Figure 11 the 5-week-old plants show a light emission decrease in comparison to samples of 4-week-old plants, but still both sample pools showed a significant increase when compared to the mock control. Follow up experiments were performed with 4-week-old *N. benthamiana*.

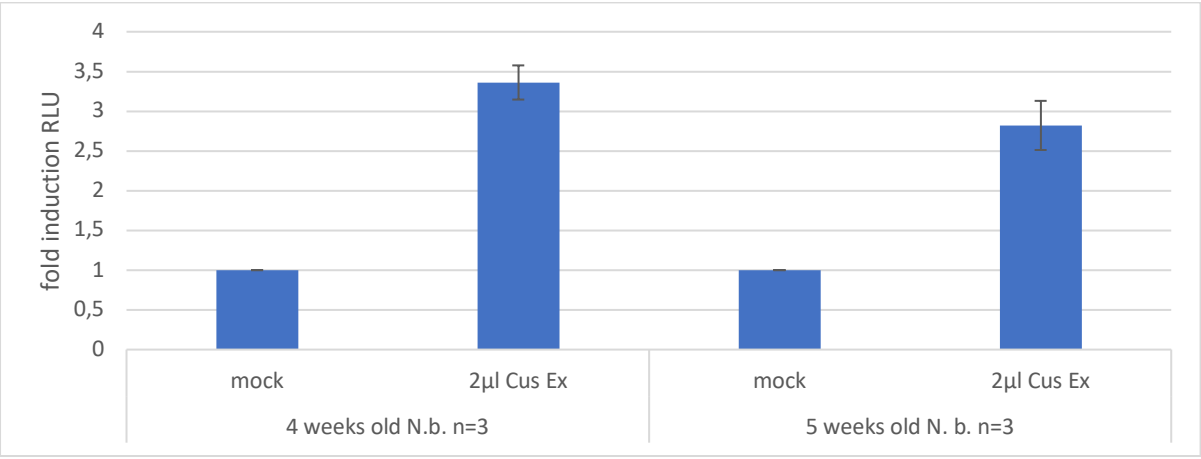

Figure 11 *N. benthamiana* plant age effects on the detection of Cuscuta Extract with transient transformed pUMAMIT25:luc.

Leaves of *N. benthamiana* were transiently transformed with pUMAMIT25:luc, treated as indicated and light emission was measured after 14h. Increasing age of *N. benthamiana* leads to a reduced light emission. Bars show average of relative light units (RLU) relative to the mock control after 14h, mock= 2µl water, Cus Ex= 2µl Cuscuta Extract, N=3, whiskers are standard deviation.

2.1.3.4 Detection range of the bioassay and the effects quenching

To evaluate the sensitivity of the assay to the Cuscuta Extract treatments, a dilution series from 10µl to 0,001µl was performed (Figure 12). Interestingly the higher volumes led to a reduction of light emission and with 10µl Cuscuta Extract to a complete loss of light signal intensity that was even below the mock control. In the lower range the sensor was able to detect the Cuscuta Extract at volumes as low as 0,03µl. Based on the dilution series the sweet spot for this sensor is between 1µl and 0,3µl. The high number of samples that were tested and the technical limitation of a multichannel pipet led to an application of 2µl Cuscuta Extract for further experiments, which still provides a high fold induction of approximately 3-fold while easing the bioassay setup.

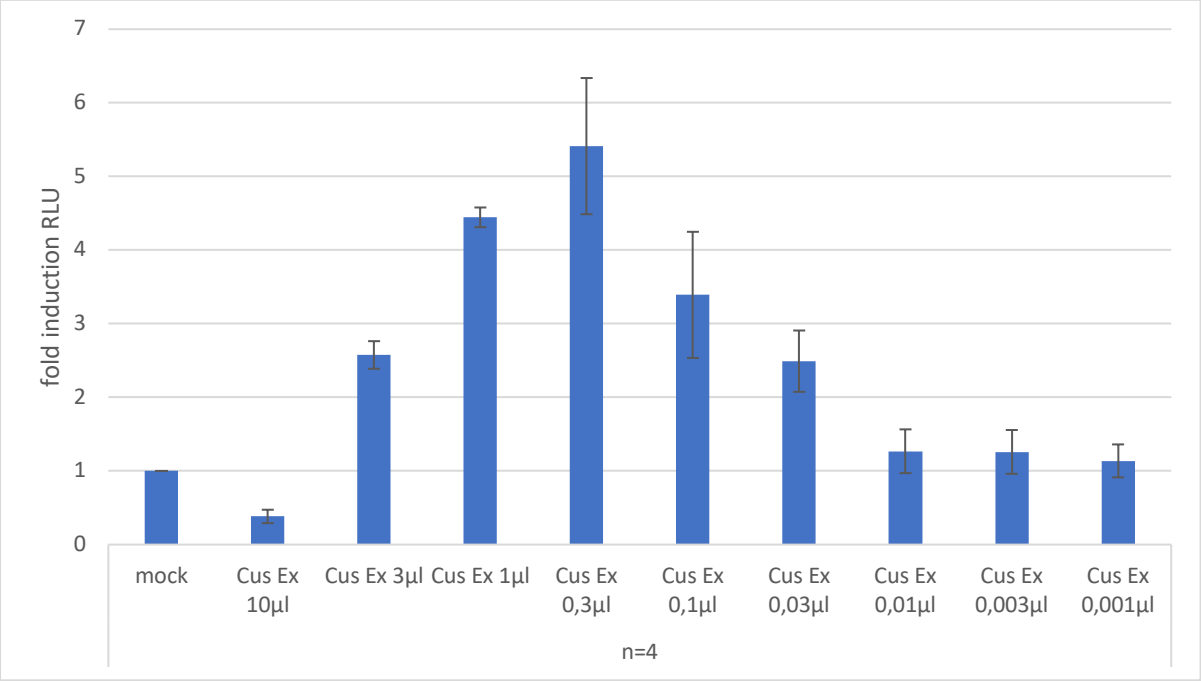

Figure 12 Dose dependent detection range of the sensor pUMAMIT25:luc to applied Cuscuta Extract.

The Cuscuta Extract was diluted up to 10 000 times. The assay shows a detection range down to 0,03µl, 0,01µl and lower volumes are not distinguishable from the mock control. Increased volumes of Cuscuta Extract lead to a reduction in the light emission. 10µl can reduce the light emission below mock control. Bars show relative light units (RLU) relative to the mock control after 14h, mock= 2µl water, Cus Ex= X µl Cuscuta Extract, N=4, whiskers are standard deviation.

2.1.3.5 Influence of common plant components and stresses

The most promising sensor candidate was run through several control tests to see the reaction to various plant-based metabolites, components used during the purification as well as classic PAMPs. Since a reaction to plant-based metabolites, purification agents and pathogens was undesirable for the purification of a novel susceptibility associated component.

pUMAMIT25:luc was tested with Cuscuta Extracts as well as flg22 and CrCrip21 to confirm sensibility to Cuscuta based extracts without any reaction to the known PAMPS. Flg22 is the minimal motif of the bacterial flagellum and known to induce an immunity response in the nM range with a broad host spectrum (Felix et al. 1999). CrCrip21 is the minimal motif of the cell wall localized, *Cuscuta*-derived CrGRP. CrCrip21 can trigger an immune response in the cultivated tomato in the nM range (Hegenauer et al.2016). Additionally, chitin a common component of the cell wall of fungi as well as insects was tested. Chitin perception is facilitated via Lysin motif receptor-like kinases (LysM-RLKs) and the Co-Receptor CERK1 that is involved in the response to various carbohydrates (Desaki et al. 2018, Desaki et al. 2019). Chitin oligomers were in addition shown to be involved in the symbiotic interaction of *M. truncatula* and arbuscular mycorrhiza (Genre et al. 2013). Sucrose produced during photosynthesis is transported from source (production) to sink (consumption) through phloem cells. Glucose and sucrose, the storage molecule of plants, were screened upon their ability to trigger the gene expression related to the chosen gene promoters (Smeekens 1998).

Osmotic stress was already shown to have no influence on the assay with other sensor constructs (Körner 2016), to confirm these results pUMAMIT25 was tested with additional concentrations of common osmotic stress inducers. The applied concentrations were based on the possible maximal concentration during purification steps, the high molarity solutions were then diluted in the same way as all other extracts. The final concentration is indicated in the figure description.

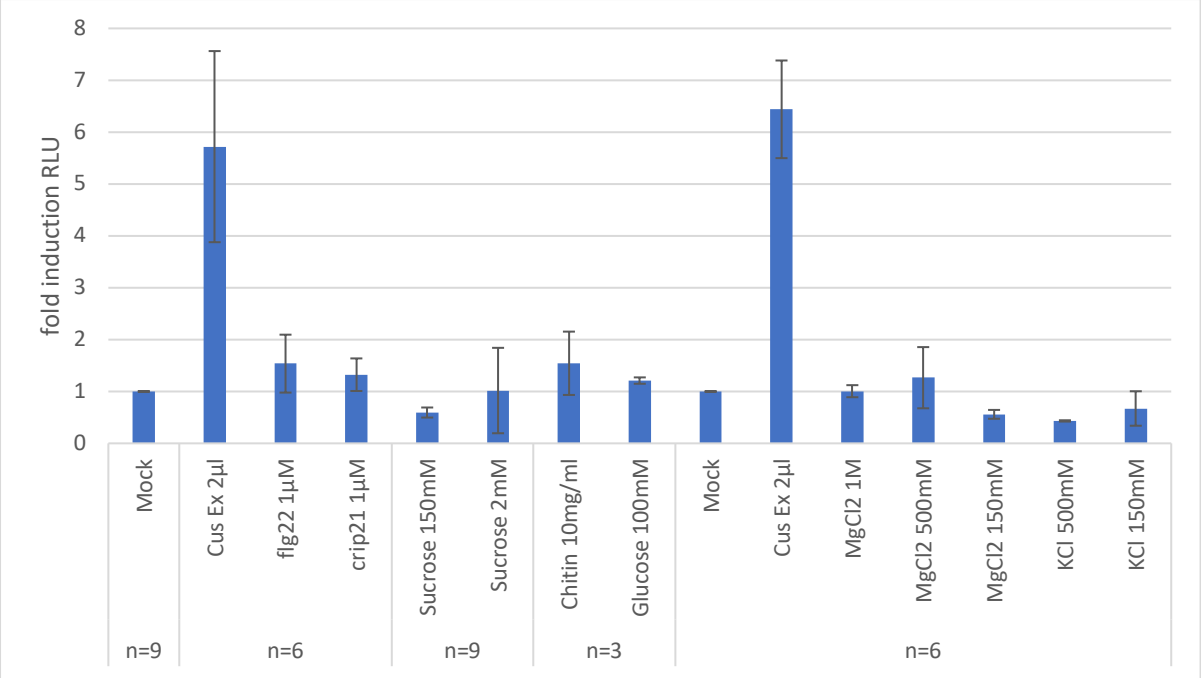

Figure 13 Effects of endogenous signals (carbohydrates, osmotic signals and pathogen related molecules) on pUMAMIT25:luc.

The endogenous signals such as Sucrose and Glucose as well as pathogen associated molecules did not initiate the light emission. $MgCl_2$ and KCl did not lead to a measurable light emission. Carbohydrates and osmotic signals were used with the described concentration and then diluted equally to the Cuscuta derive extracts to mimic real plant conditions. Sucrose 150mM (end conc 3mM); Sucrose 2mM (end conc 0,04mM); Chitin 10mg/ml (end conc 100µg/ml); Glucose 100mM (end conc 2mM). Osmotic stress. $MgCl_2$ and KCl were used in concentrations 1M, 500mM and 150mM (end conc 20mM, 10mM and 3mM respectively), peptides were applied with an end concentration of 1µM, whiskers are standard deviation

No significant increase of light emission was detected with pathogen associated peptides, the various carbohydrates and the osmotic stresses. The ability to induce ethylene biosynthesis was tested with flg22 and CrCrip21 (Figure 26) both could induce ethylene biosynthesis at similar concentrations but did not trigger any light emission. The tested carbohydrates and osmotic stresses do not induce light emission in respected samples (Figure 13).

Plant hormones play a major role in developmental processes and therefore may also switch on the sensors. In Körner 2016 the tested plant hormones did not activate the initially tested sensors but needed to be repeated for the new constructs. Therefore auxin, cytokinin and brassinosteroid that are widely involved in developmental processes but also known from other pathogens to be used for their own benefit were tested. Additionally, systemin that is involved in defense signaling during feeding of caterpillars was used (Wang et al. 2018). The synthetic strigolactone racGR24 which is known as germination trigger for root parasites was also tested. All tested plant hormones did not activate pUMAMIT25:luc (Figure 14).

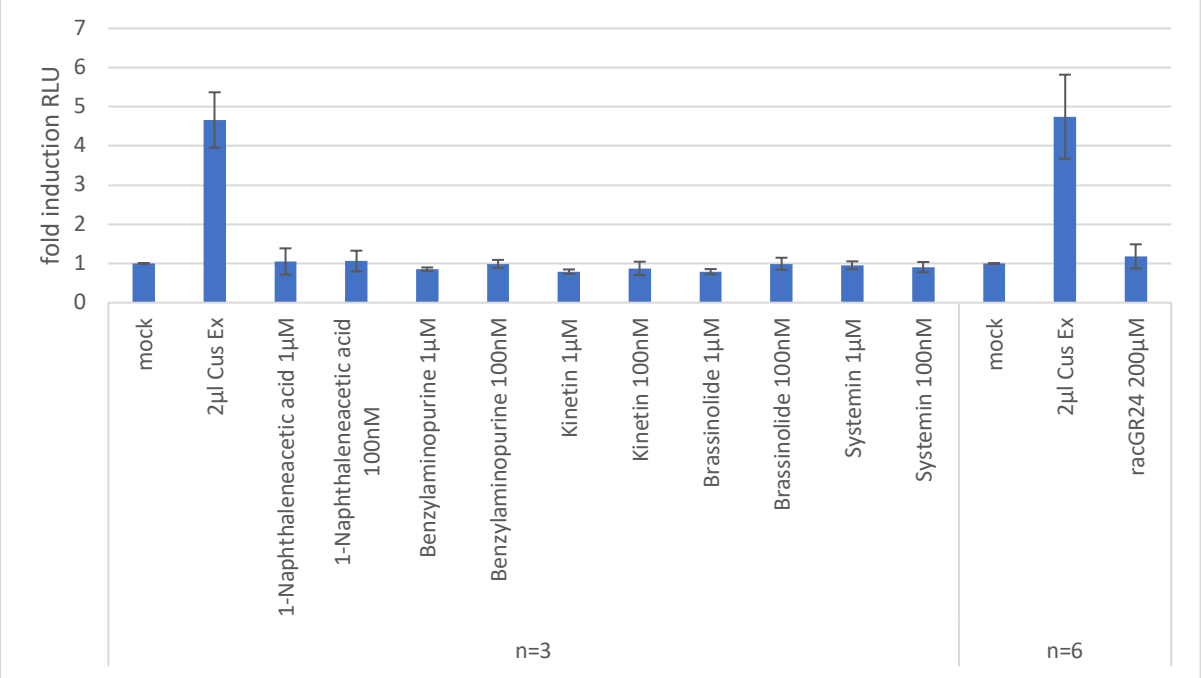

Figure 14 The effects of plant hormones on the sensor pUMAMIT25:luc.

The plant hormones were applied in two concentrations and independent of the concentration were not able to induce pUMAMIT25:luc which resulted in light emission similar to the negative control (Auxin: 1-Naphthaleneacetic acid (NAA); Cytokinin: Benzylammoniumpurine (BAP), Kinetin (N^6-furfuryladenine); Brassinosteroid: Brassinolide; Systemin (peptide hormone) and Strigolactone racGR24 (performed in an independent approach therefore has separate control measurements) Bars show relative light units (RLU) relative to the mock control after 14h, mock= 2µl water, Cus Ex= 2 µl Cuscuta Extract, plant hormones are end concentration N=3 (racGR24 N=6), whiskers are standard deviation.

2.1.3.6 Correlation of light and luciferase expression via qRT-PCR

Is light production in the assay directly linked to luciferase activity? To correlate the light output during the assay with the *luciferase* transcription qRT-PCR was performed. Three time pointsfor sample collection were chosen to represent the different stages during the assay. With 30 minutes the initial response was monitored, 2 hours as intermediate and 14 hours when the sensor is standardly tested in the assay. The *luciferase* transcription is clearly detectable 30 minutes after the Cuscuta Extract addition. The other time points do not differ from the controls, suggesting that the light output after 14h is mainly due to an early and strong activation of the transcription immediately after the addition of the Cuscuta Extract. It is assumed that the translational process is slower and ongoing which leads to a steady increase of light emission over time (Figure 15).

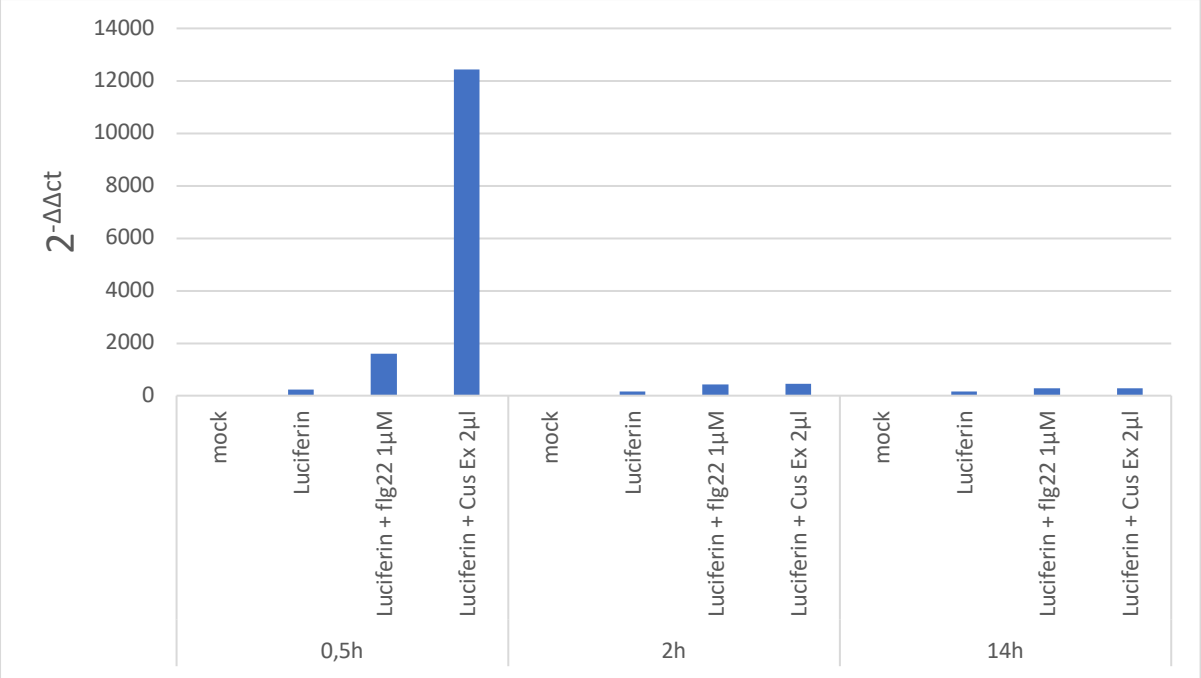

Figure 15 Quantitative analysis of luciferase transcription via qRT-PCR.

The luciferase is coupled to pUMAMIT25. The luciferase transcript is shortly after application of Cuscuta Extract detectable. The qRT-PCR shows a fast and strong upregulation of luciferase transcript levels after 0,5h. 2h and 14h after Cuscuta Extract application the transcript levels are indistinguishable of the controls. Light emission in the bioassay is measured after 14h for pUMAMIT25.

2.1.3.7 Proof of concept - Comparison to attAGP

One proven gene activation is the attachment Arabinogalactan Protein (attAGP) which was shown to play a role in the stickiness of *C. reflexa* to the resistant host, tomato (var. Money Maker). Spatiotemporal attAGP promoter activation at the attachment site was shown by GUS accumulation and staining in stable pattAGP:GUS transformants (Figure 16 from Albert 2005). *attAGP* expression might be activated by a *Cuscuta*-derived molecular cue, therefore pattAGP:luc was tested as a sensor construct. attAGP was shown to have an effect in resistant plants therefore a comparison between *N. benthamiana* WT and *N. benthamiana* stably transformed with CuRe1 is interesting to get insights into the possible detection of a molecular cue. With the experimental setup a possible CuRe1 related downstream signaling that might trigger or redirect to the sensor could be investigated. The promoter of attAGP is activated upon treatment with Cuscuta Extract and therefore confirms an activation via transfer of a molecular cue into the host. The comparison between the pattAGP in WT and CuRe1 containing *N. benthamiana* does not show any difference. attAGP is not influenced by or involved in the CuRe1 downstream signaling. The role of attAGP is still not fully understood but experiments indicate a reduction of attachment strength in case of a knockdown. The activation via Cuscuta Extract

indicates a *Cuscuta* spp. guided role of the attachment enhancer attAGP independent of the resistant or susceptible background of the host plant.

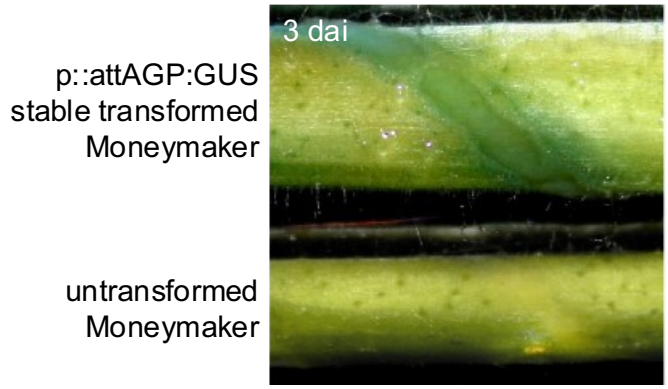

Figure 16 Promoter attAGP:GUS expression in stable transformed moneymaker.

Stable transformed moneymaker and wt Moneymaker tomato were infected with *C. reflexa*, 3 days after infection (dai) the *C. reflexa* was removed and the stem was stained. GUS staining at the area of attachment is visible only in the stable transformed tomato (modified from Albert 2005)

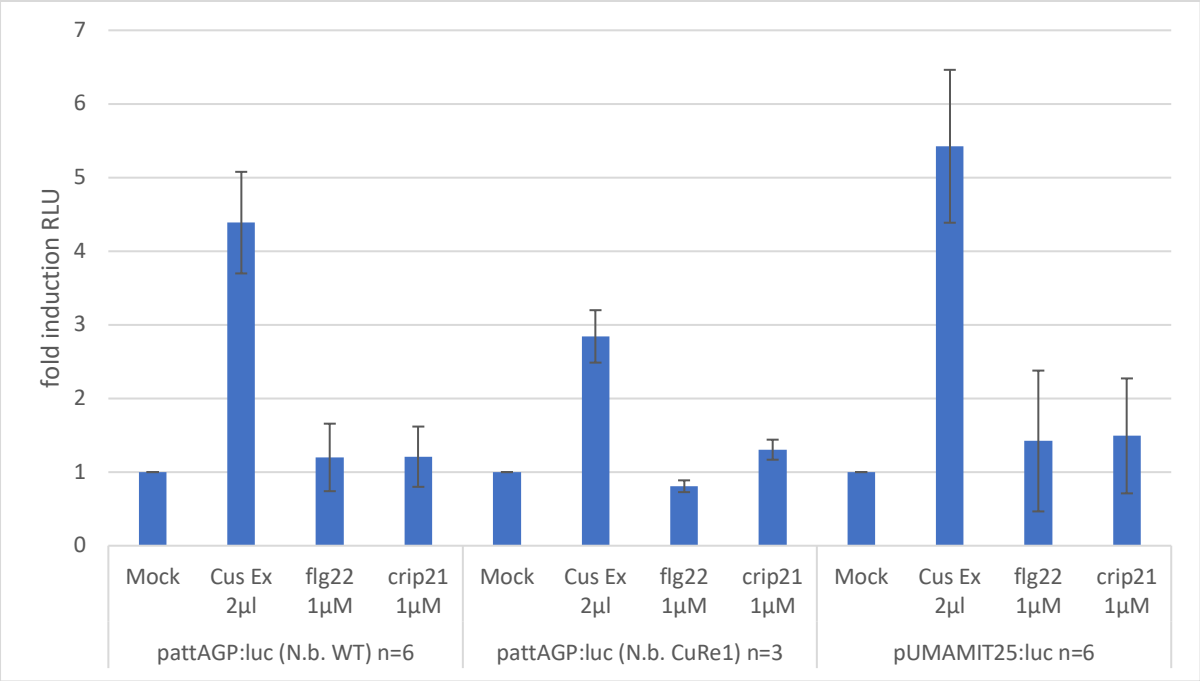

Figure 17 pattAGP in stable with CuRe1 transformed and wildtype *N. benthamina*.

pattAGP:luc has a similar activation pattern in wildtype and stable CuRe1 *N. benthamiana* plants that show a slightly lower fold induction. The light emission pattern is similar to pUMAMIT25:luc in wildtype background. Bars represent fold induction of light emission, peptides are applied with 1µM end concentration, whiskers are standard deviation.

2.1.3.8 Alternative bioassay setup using stably transformed *A. thaliana* and *N. benthamiana*

For the stable transformation of *A. thaliana* and *N. benthamiana* the most interesting sensor constructs were used. The vector pBGWL7 used for all transient transformations contains the BASTA selection marker and could be used for the stable transformation as well.

A. thaliana was floral dipped and collected seeds were sawed on soil and selected by spraying BASTA® and genotyped (not shown). The leaves of the selected plants were treated as described in Figure 8

and tested with Cuscuta Extract. The sensors in all tested individuals were inactive and did not give any increase of light emission upon treatment with Cuscuta Extract (Figure 18), since the bioassay was functional and approved in *N. benthamiana* new stable transformations were done in *N. benthamiana* with the meanwhile approved and well-working pUMAMIT25:luc sensor.

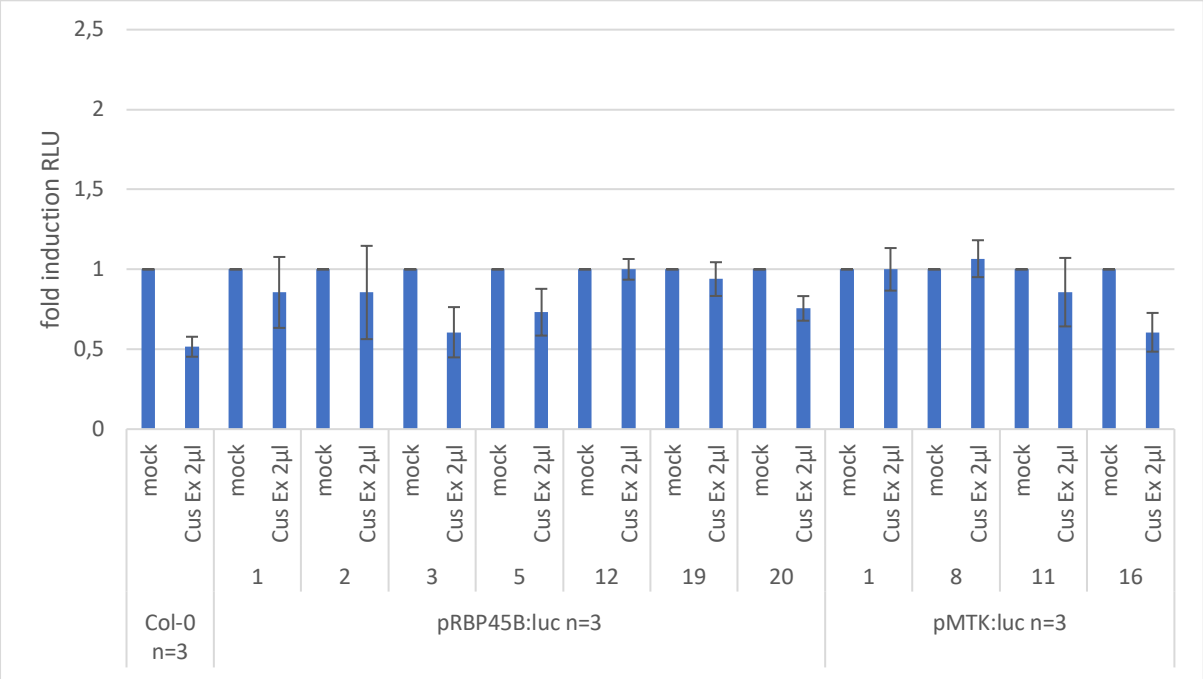

Figure 18 Stable transformed pRBP45B:luc and pMTK:luc in *A. thaliana* treated with Cuscuta Extract.

Stable transformed sensors in Col-0 background were genotyped and plants containing the senor were treated with 2µl of Cuscuta Extract and measured after 8h, numbers indicate independent transformants, no increased light emission is visible. The control is untransformed Col-0. Bars are fold induction of light emission; whiskers are standard deviation.

Stable transformed *N. benthamiana* were cultivated on selective BASTA® medium from callus cultures (T0), the seeds were collected, sawed and selected with BASTA® and after genotyping tested in the bioassay (T1). The light emission was detectable for the treatment with Cuscuta Extract (Figure 19). The positive tested transformants are used to generate the next generation (T2).

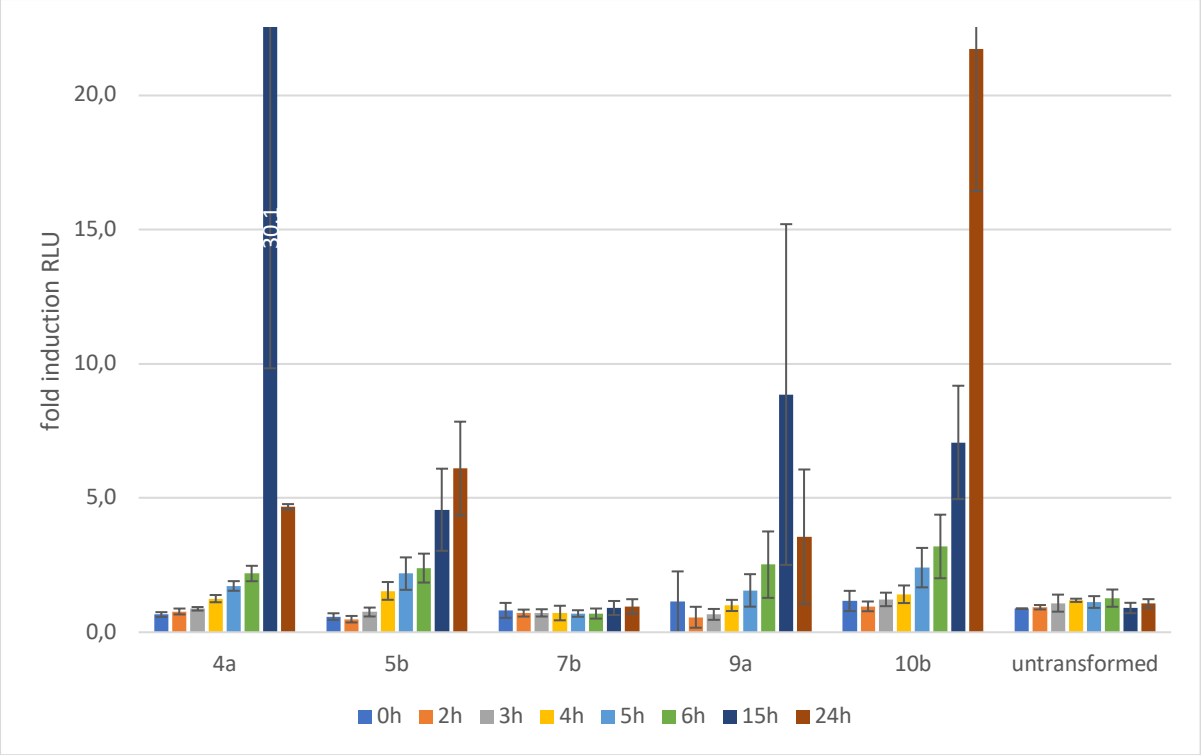

Figure 19 Stable transformed pUMAMIT25:luc in *N. benthamiana* treated with Cuscuta Extract.

Stable transformed plants (T1) were treated with 2µl of Cuscuta Extract and measured at 0h, 2h, 3h, 4h, 5h, 6h, 15h and 24h, the increase in light emission is clearly visible in 4a, 5b, 9a and 10b.The light emission differs in amplitude and the time of the maximal amplitude, 7b is comparable to untransformed *N. benthamiana.* Bars are fold induction of light emission, whiskers are standard deviation, 4a maxima after 15h is 30,1 fold induction RLU.

The T2 generation of line 5b was selected with BASTA again and then tested with Cuscuta Extract. The light emission is still visible but with lower amplitude in some lines this might be an effect of the plant innate gene silencing.

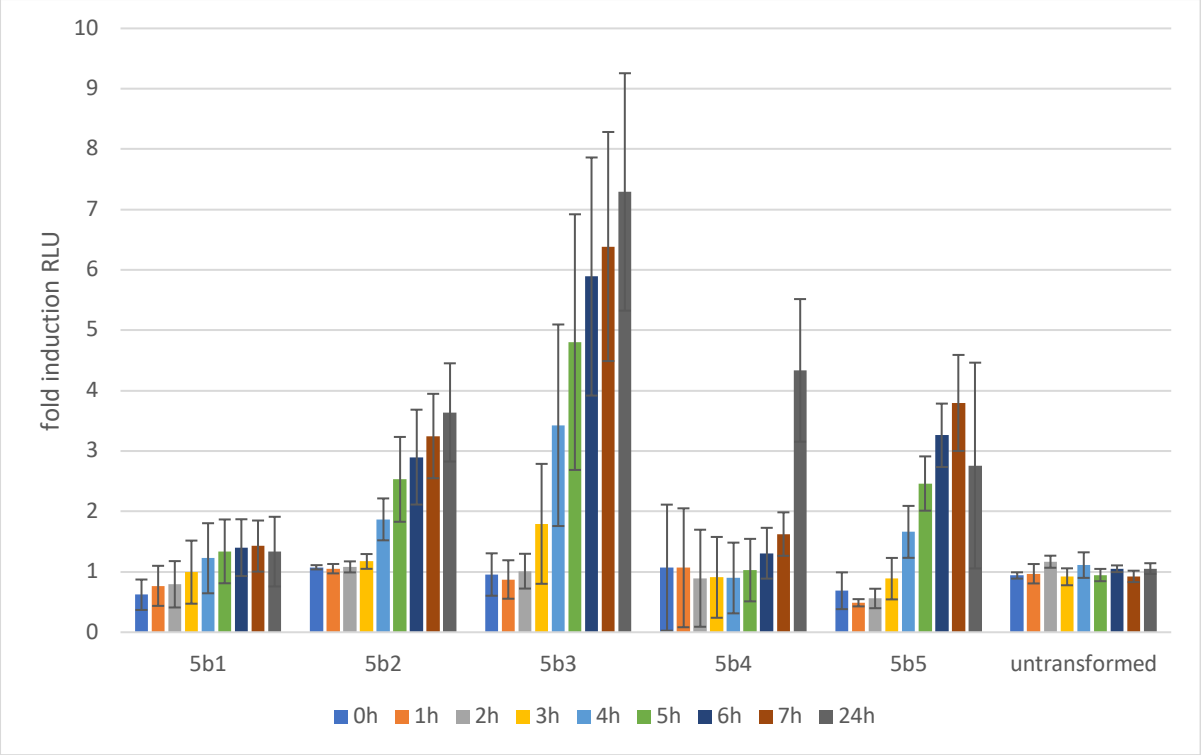

Figure 20 Stable transformed pUMAMIT25:luc in *N. benthamiana* treated with Cuscuta Extract.

Stable transformed plants (T2) were treated with 2µl of Cuscuta Extract and measured at 0h, 1h, 2h, 3h, 4h, 5h, 6h, 7h and 24h, the increase in light emission is clearly visible in the T2 generation of line 5b. The light emission differs in amplitude but is consistently activated. Bars are fold induction of light emission; whiskers are standard deviation.

2.1.4 Application of the sensor for the purification of the *Cuscuta*-derived molecular cue

The promotor:luciferase constructs proved to be sensitive and specific sensors to detect a *Cuscuta*-derived molecular cue which seems obviously present in the Cuscuta Extract. Therefore, the assay was applied to screen for and to identify one or more specific molecules of Cuscuta Extracts in various purification steps. The purification scheme can be divided in three separate steps. (1) The pre-purification includes all steps prior to the first chromatographic purification, including harvesting, extraction and preparing the extract for the chromatographic purification (Figure 21). (2) The chromatographic purification with the aim to enrich and polish the *Cuscuta*-derived molecular cue (Figure 24 A and B). (3) And the characterization that includes experiments to gain additional insights of the biochemical properties of the *Cuscuta*-derived molecular cue (Figure 24 C). Importantly, fractions of each purification step have been analyzed for their activity in the new established bioassay and obtained active fractions have been pooled for further analyses. Furthermore, in case active compounds could not be bound or eluted from the column, flow through and/or wash of chromatographic steps have been analyzed in more detail.

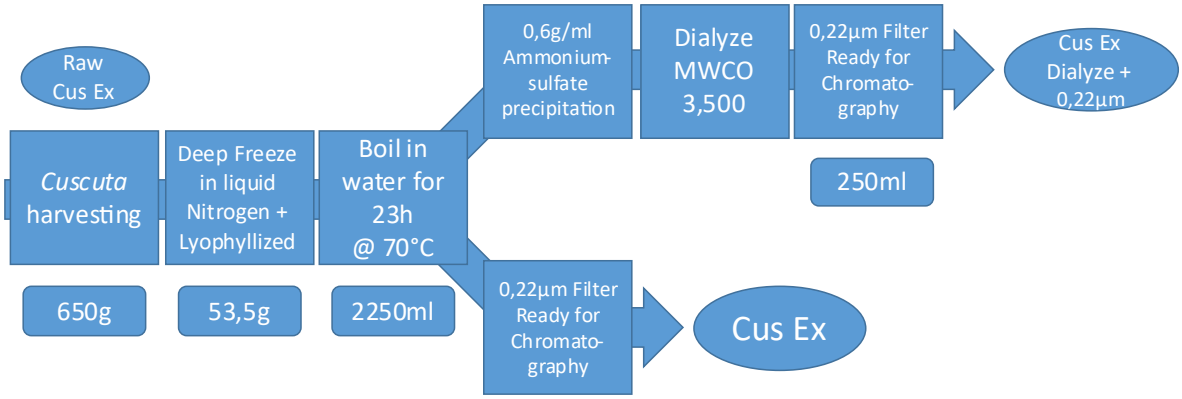

Figure 21 Workflow of the pre-purification.

Pre-purification of the Cuscuta Extract. The arrow indicates stepwise process. Two main approaches were used, Cuscuta Extract directly filtered after boiling and dialyzed Cuscuta Extract after Ammonium sulfate precipitation. Ovals contain the sample name for further identification. Round edged squares indicate Mass and Volumes of each step.

2.1.4.1 Properties of the *Cuscuta*-derived molecular cue during the pre-purification

First step was to compare the pre-purification steps in the bioassay to evaluate possible losses of the bioactive *Cuscuta*-derived molecular cues during the pre-purification. Major steps are the deep freezing, boiling and the dialyzing, therefore the freshly ground Cuscuta Extract (raw Cus Ex) was compared to deep frozen and boiled Cuscuta Extact (Cus Ex). Boiling leads to the denaturation of

proteins and therefore might reduce the activity or could also help to stabilize bioactive *Cuscuta*-derived molecular cues due to the denaturing of otherwise degrading enzymes. Additionally, the ammonium sulfate precipitation that reduces unwanted compounds as well as increases the protein concentration followed by dialysis was investigated. To get insights in a possible correlation of protein content and light emission the protein concentration was determined for all pre-purification steps (Figure 22).

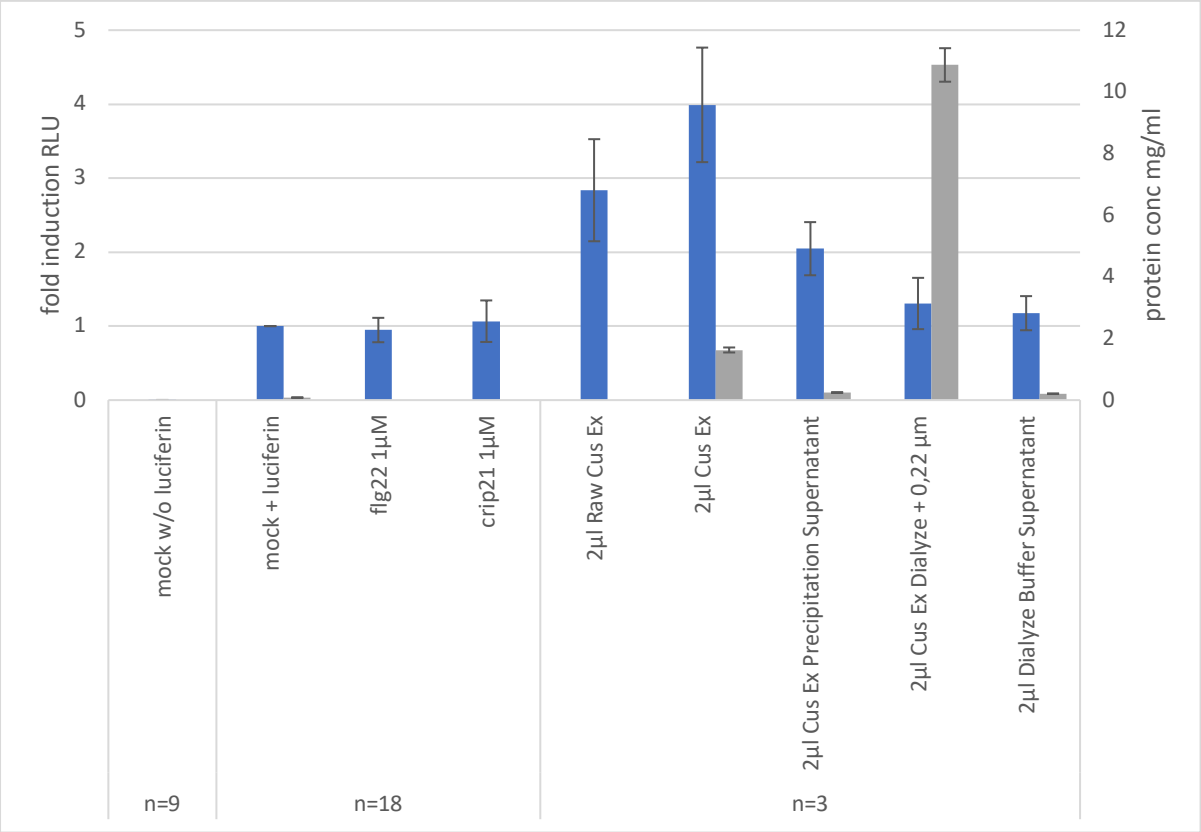

Figure 22 Correlation of protein concentration and the induced light emission of the pre-purification steps (pUMAMIT25:luc, 14h).

The pre-purification steps were tested up on their ability to induce light (blue bars) in compression to the protein concentration (gray bars). The light emission was measured in transiently with pUMAMIT25:luc transformed *N. benthamiana* leaves. The protein concentration was measured by Bradford's protein assay ($OD_{595/450}$) with a BSA calibration series. The freeze dried and boiled Cuscuta Extract (Cus Ex) can induce a similar and slightly higher light emission compared to the fresh ground Raw Cuscuta Extract (Raw Cus Ex). The ammonium sulfate precipitation increased the protein concentration but did not activate the promoter and could not be used for the chromatic purification. Cuscuta Extract Precipitation Supernatant is Cuscuta Extract incubated with saturated ammonium sulfate at 4°C for 24h, centrifuged at 10 000g and the supernatant is collected. The precipitation is resuspended in water and dialyzed in 10 liter 25mM MES pH 5.5 (Dialyze Buffer). The Dialyze Buffer supernatant sample is collected from the 10 liter Dialyze Buffer. Mock w/o luciferin (0,0017 fold induction RLU), bars are fold induction of light emission, whiskers are standard deviation.

The raw Cuscuta Extract can activate the promoter to a similar fold induction as the Cuscuta Extract after boiling, therefore the deep frozen and boiled Cuscuta Extract could be used for further investigations. While the protein concentration was increased after the dialysis of the ammonium sulfate precipitation the light emission was not increased, therefore the protein concentration does not seem to have an influence on the activation pattern in the luciferase bioassay (Figure 22).

Further the ability to induce ethylene was investigated and the Raw Cuscuta Extract and processed Cuscuta Extract that activate the bioassay additionally induce ethylene production. The precipitation supernatant that shows reduced light emission is not active in the ethylene assay, the dialyzed ammonium sulfate precipitation that is inactive in the bioassay can activate ethylene production. The differential activation pattern indicates that the molecular cues that activates the promoter-luciferase bioassay is not the CrGRP that can be measured in the ethylene assay (Figure 23).

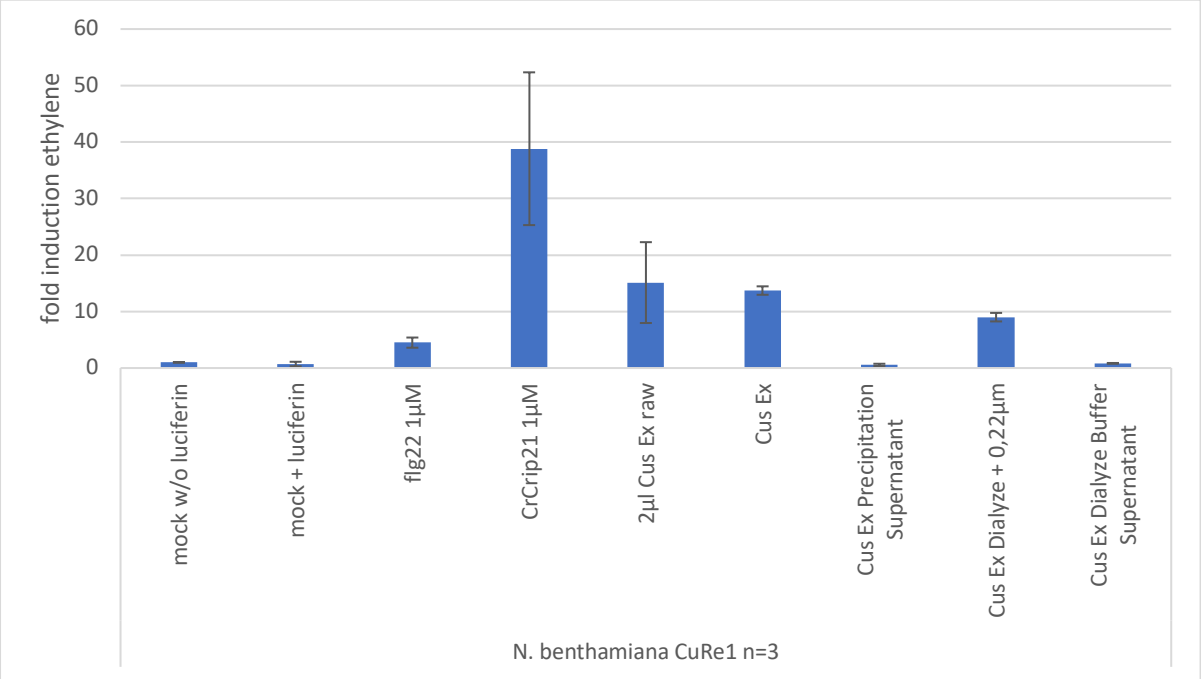

Figure 23 Ethylene production in *N. benthamiana* leaves expressing CuRe1 treated with the Cuscuta Extract pre-purification preparations.

Stable CuRe1 expressing *N. benthamiana* leaf samples initiate ethylene production upon treatment with CrCrip21 which is detected by Cure1 as well as after treatment with the full length CrGRP in raw (Raw Cus Ex) and boiled Cuscuta Extract (Cus Ex). The dialyzed ammonium sulfate precipitation did activate the ethylene production. The Supernatants during both processes did not activate the ethylene production. Positive control is flg22. Bars represent fold induction of ethylene, peptides have an end concentration of 1µM, 2µl of extract preparation were used, luciferin 0.2mM (same and concentration as the bioassay), ethylene was measured after 3 hours incubation with the treatment, 1ml gas phase of a 6ml tube were measured, whiskers are standard deviation.

2.1.4.2 Chromatographic purification

The pre-purification yielded the basic extract, that was aimed to be as pure as possible without any chromatographic steps. The dialysis that increased the protein concentration did not increase the amount of promoter triggering Cuscuta Extract but rather resulted in a complete loss of activity, therefore it was not used in further purification methods (Figure 24).

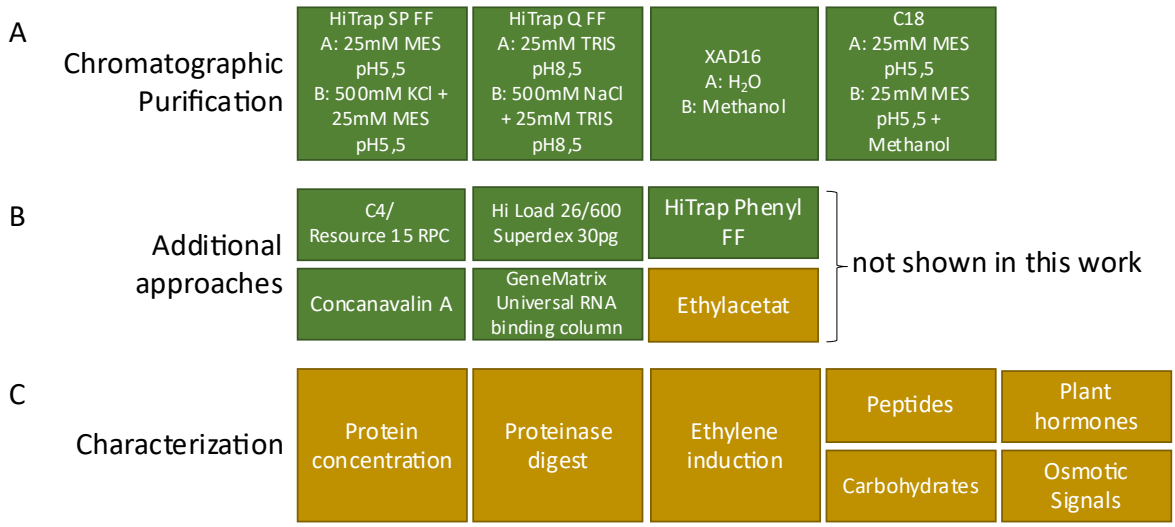

Figure 24 Workflow of the chromatographic purification and characterization

(A) Chromatographic purifications methods used with the pre-purified extracts. For the chromatic purification the Cuscuta Extract was adjusted to the buffers indicated in the green boxes. (B) Additional approaches not shown due to their comparability to the shown experiments, results of the additional approaches are summarized in Table 4. (C) Characterization of the *Cuscuta*-derived molecular cue. (green: chromatographic purification methods, brown: characterization methods).

The Cuscuta Extract was adjusted to a column specific buffer, which allowed the application of the extract directly onto a column of choice. For further purification the ÄKTA pure FPLC system was used and the column preparations recommended by the manufacturer were followed. The Cuscuta Extract was loaded onto the column, Cuscuta Extract that directly ran through the column during the loading is the flow through followed by a short wash with the running buffer. The gradient elution was collected in 96-well plates and followed by a 100% elution buffer wash. Therefore, all following figures display the following 4 steps that were tested in the bioassay: 1) Cuscuta Extract, 2) flow through and running buffer wash, 3) fractionation (96-well plate) and 4) elution buffer wash.

2.1.4.2.1 Purification of Cuscuta Extract

Ion exchange is often used in protein purifications and perfectly suited for method scouting. Therefore, cation exchange as well as anion exchange techniques were used to try the enrichment of the molecular cue. Strong cation exchange chromatography were already used in Hegenauer et al. 2016 and proved to be a successful step to enrich molecular cues originating from *Cuscuta* spp.. In Hegenauer et al. 2016 and 2020 the elution from the strong cation exchange column was containing the molecular component now known as CrGRP (minimal motif CrCrip21).

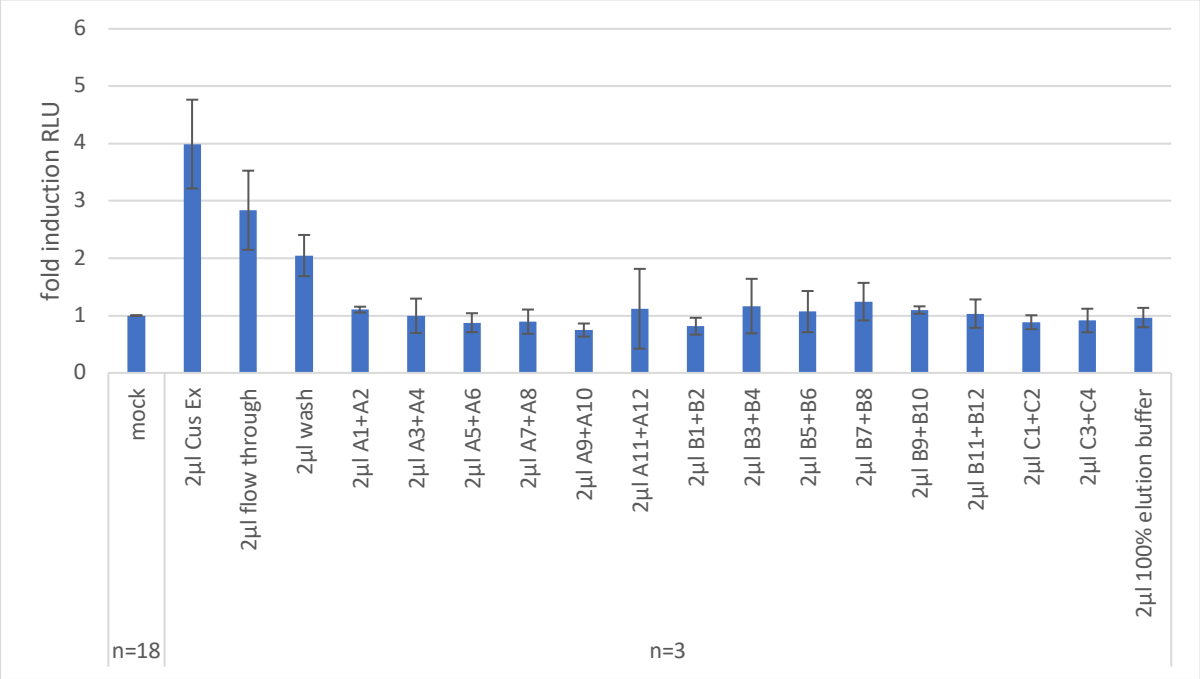

Figure 25 Cation Exchange column (HiTrap SP-FF, 5ml) fractions applied to the sensor pUMAMIT25:luc.

The *Cuscuta*-derived molecular cue that activates pUMAMIT25:luc can flow directly through the cation exchange column and is retrievable in the flow through and the wash, all eluted fractions are inactive. Cation Exchange column buffer was 25mM MES buffer pH 5.5 (elution 500mM KCl). Cuscuta Extract was loaded (250ml). Flow through 250ml; wash 10ml; fractions 1ml two following fractions were combined; bars are fold induction of light emission; whiskers are standard deviation.

The strong cation exchange column is not able to bind the *Cuscuta*-derived molecular cue, since the strongest activation is in the flow through (Figure 25). The fractions do not contain the molecular cue or a very low concentration that is not detectable in the bioassay. The Cuscuta Extract preparations were tested for their ability to induce ethylene and therefore act in the immunity pathway like other known PAMPs. Interestingly the flow through of the cation exchange column was inactive in the ethylene assay but active in the promoter-luciferase bioassay, which implies proper binding of CrGRP and its minimal peptide CrCrip21 (Figure 26). These results suggest a divergence regarding the properties of CrGRP and the novel molecular cue detected by the promoter-luciferase bioassay.

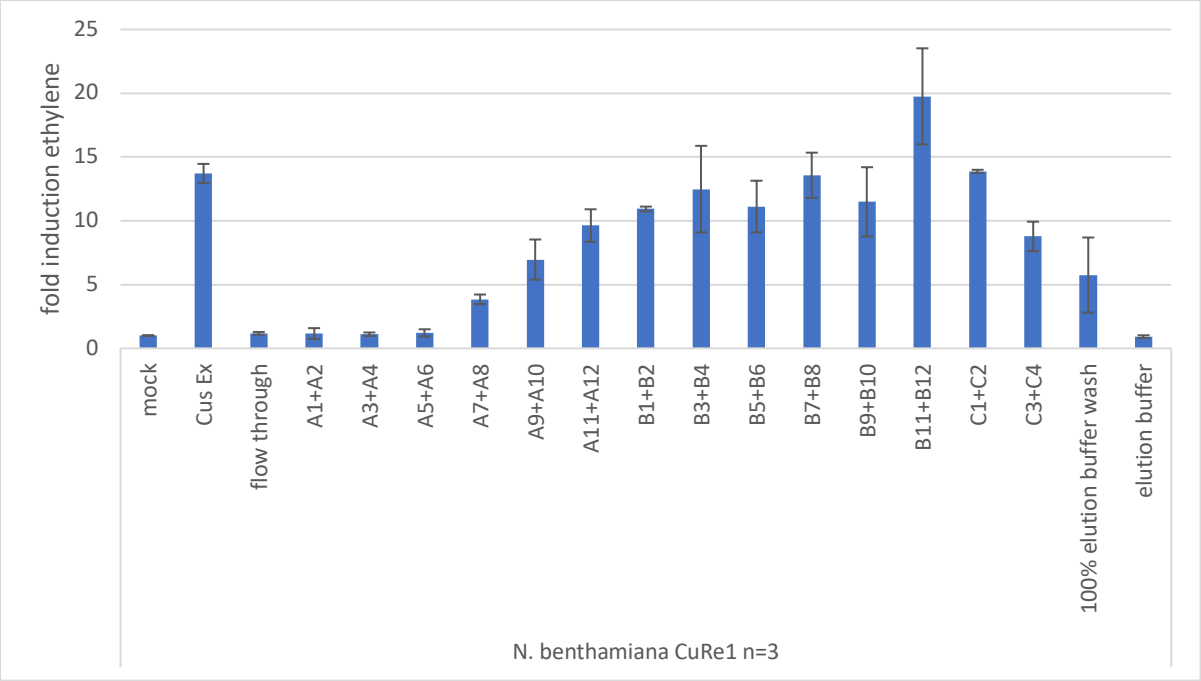

Figure 26 Ethylene production of *N. benthamiana* expressing CuRe1, treated with Cuscuta Extract preparations from the cation exchange column.

Stable CuRe1 expressing *N. benthamiana* leaf samples initiate ethylene production upon treatment with the fractions of the cation exchange column containing the full length CrGRP. The flow through of the cation exchange column (HiTrap SP-FF, 5ml) is not able to initiate ethylene production. Cation Exchange column buffer was 25mM MES buffer pH 5.5 (elution 500mM KCl). Cuscuta Extract was loaded (250ml). Flow through 250ml; wash 10ml; fractions 1ml two following fractions were combined, bars represent fold induction of ethylene over the mock control, 2µl of extract preparation were used, ethylene was measured after 3 hours incubation with the treatment, 1ml gas phase of a 6ml tube were measured, whiskers are standard deviation.

The molecular cue cannot be enriched by cation exchange chromatography, which might be an indicator for a negative net charge of the *Cuscuta*-derived molecular cue at a pH of 5.5. Therefore, an anion exchange column with a buffer pH of 8.5 was used to utilize a negative net charge of the proteins (Figure 27).

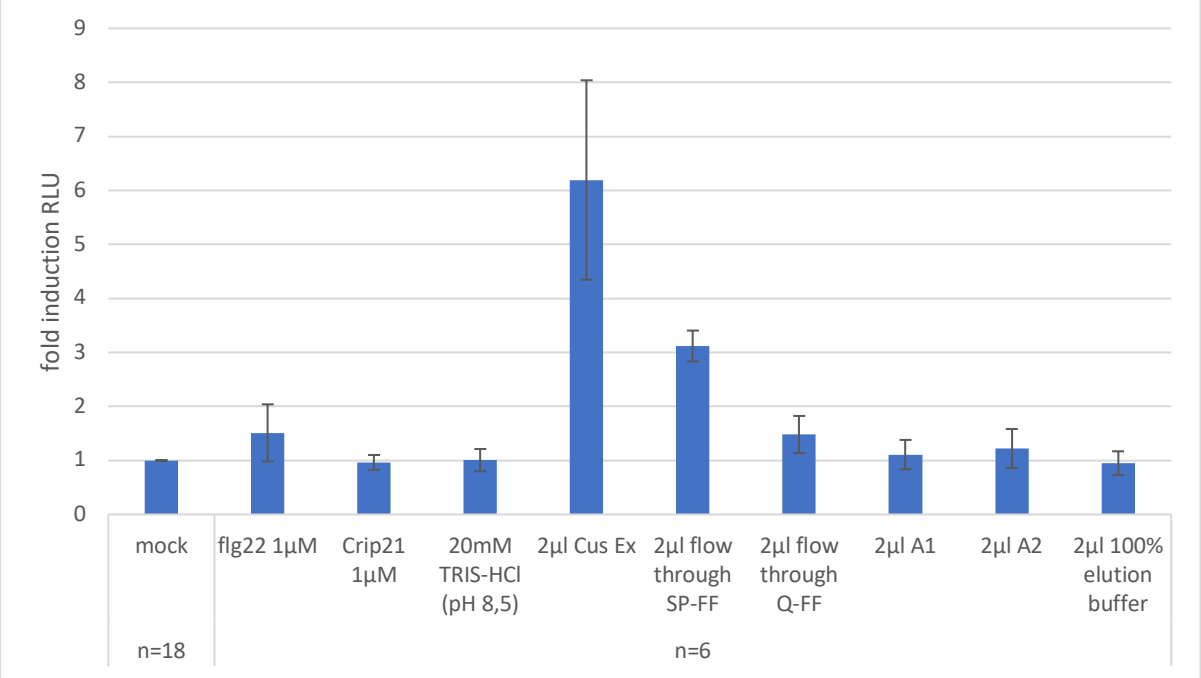

Figure 27 Anion Exchange column (HiTrap Q-FF, 5ml) fractions applied to the sensor pUMAMIT25:luc.

The *Cuscuta*-derived molecular cue that activates pUMAMIT25:luc can flow directly through the anion exchange column and is retrievable in the flow through, all eluted fractions are inactive. Anion exchange buffer was 20mM TRIS buffer pH 8.5 (elution 1M NaCl), running buffer and elution buffer were loaded 2µl (end conc 0.4mM TRIS-HCl (elution 20mM NaCl)). The flow through of the SP-FF was pH adjusted and loaded. Load 40ml; flow through 40ml; fraction 8ml; bars are fold induction of light emission; whiskers are standard deviation.

The anion exchange column was independently in a secondary try equilibrated with MES buffer pH 5.5 and revealed similar results (not shown) with a *Cuscuta*-derived molecular cue running through the column without binding to the matrix. The conditions for the ion exchange columns did not yield an active fraction and most of the activity was detectable in the flow through of the columns independent of charge and buffer conditions.

2.1.4.2.2 Purification of the active *Cuscuta*-derived molecular cue present in fraction 1A2

The chromatography column XAD16 is used as an absorbent for organic substances and is often used to reduce and remove cleaning agents in protein purifications. The XAD16 was used in a custom filled column and was run manually and collecting in higher fraction volumes. The XAD16 is a rather crude multipurpose high surface column bed that is also known from fruit juice upgrading. The binding of the active *Cuscuta*-derived molecular cue seems to be low since most activity was again found in the flow through and collected washing buffer (Figure 28).

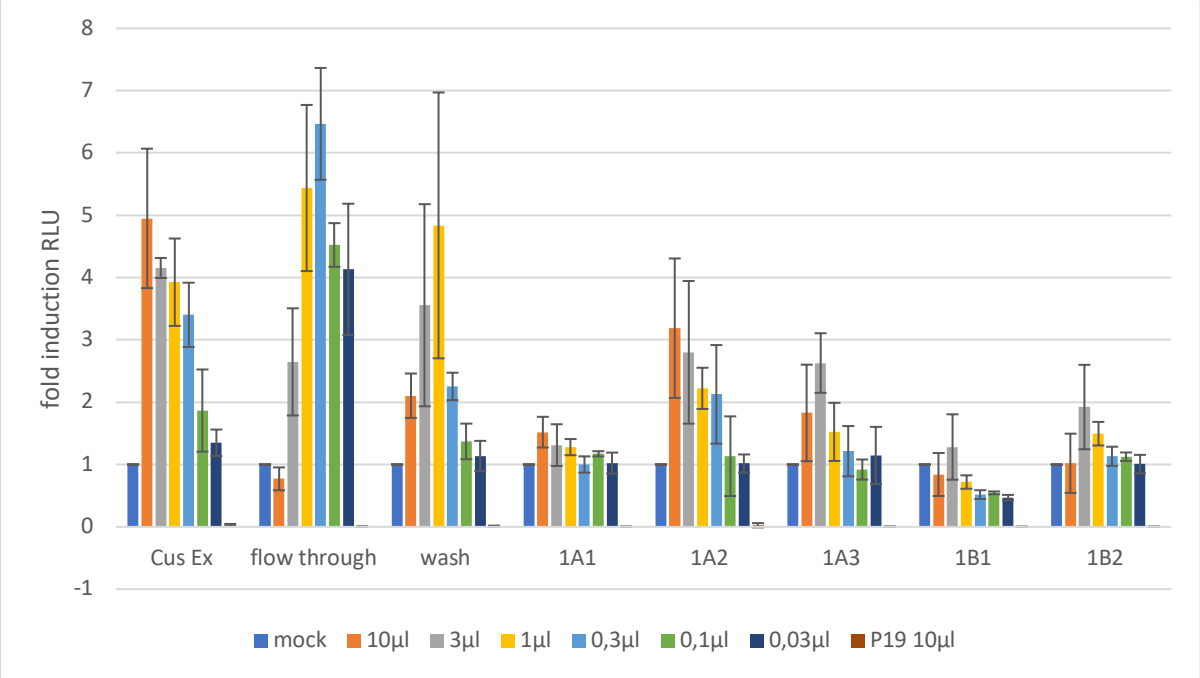

Figure 28 Activity of XAD16 fractions and dilutions applied to the sensor pUMAMIT25:luc

XAD16 is in common use to absorb organic substances from aqueous solutions and polar solvents in a low to medium molecular weight. Binds polar substances often used during purification of proteins, amino acids, and steroids. The Cuscuta molecular cue can be found in the flow through, the wash and the eluted fractions 1A2 and 1A3. Load total 300ml; flow through total 300ml; wash total 150ml, fraction size 50ml; volumes applied as indicated; bars represent fold induction of light emission; whiskers show standard deviation.

After chromatography with the XAD16 column the eluted fraction 1A2 seemed to contain enriched *Cuscuta*-derived molecular cue. To purify the eluted fraction 1A2 further, it was loaded to the cation exchange column. The purified fraction 1A2 in comparison to the Cuscuta Extract might not contain disturbing agents, that reduce or prevent the binding of the *Cuscuta*-derived molecular cue to the cation exchange column. Therefore, the *Cuscuta*-derived molecular cue was loaded to the cation exchange column. The activity of fraction 1A2 ran through the cation exchange column without binding and was retrievable in the flow through. The eluted fractions were inactive due to high standard deviation, therefore the active *Cuscuta*-derived molecular cue from the 1A2 fraction could not be enriched by cation exchange chromatography (Figure 29).

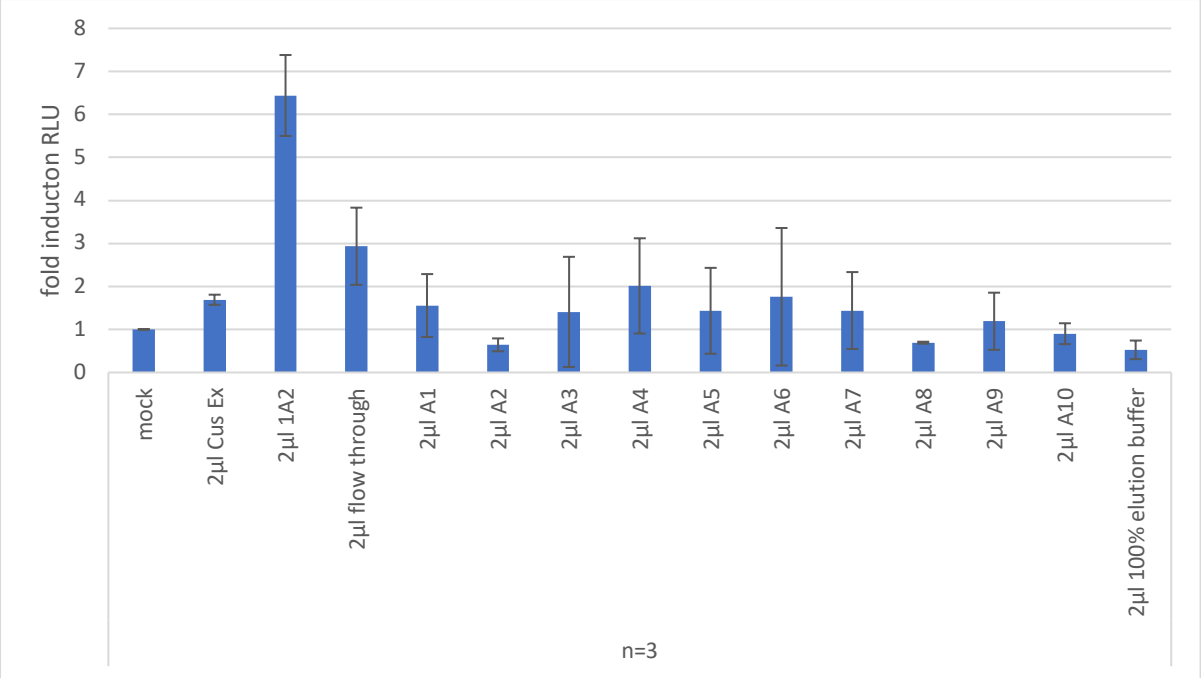

Figure 29 Luciferase-dependent light production in leaves containing the sensor pUMAMIT25:luc and treated with fractions from the CEC (HiTrap SP-FF, 1ml).

The active *Cuscuta*-derived molecular cue from fraction 1A2 of the XAD16 column can flow directly through the cation exchange column and is detectable with reduced activity in the flow through, all eluted fractions are inactive. Cation Exchange column was run with 25mM MES buffer pH 5.5 (elution 500mM KCl). 1A2 from the XAD16 was loaded. Load 4ml; flow through 4ml; fraction 1ml; volumes applied as indicated; bars represent fold induction of light emission; whiskers show standard deviation.

The purification based on ion exchange did not yield the expected enrichment of the *Cuscuta*-derived molecular cue, therefore reversed phase chromatography was tested. Reversed phase columns can bind hydrophobic molecules to the lipophilic C18 bed, while salt buffers run directly through the column. The C18 is mostly used to prepare an extract for mass spectrometry. The reversed phase C18 column was prepared with a relatively weak elution agent (MeOH). Additional tests with stronger elution buffers like acetonitrile revealed the same picture, the activity is easily detectable in the flow through but not in an elution fraction. Due to the good and high evaporation rate of the elution buffer all 2ml fractions were reduced in volume in a vacuum evaporator to 20µl (Figure 30).

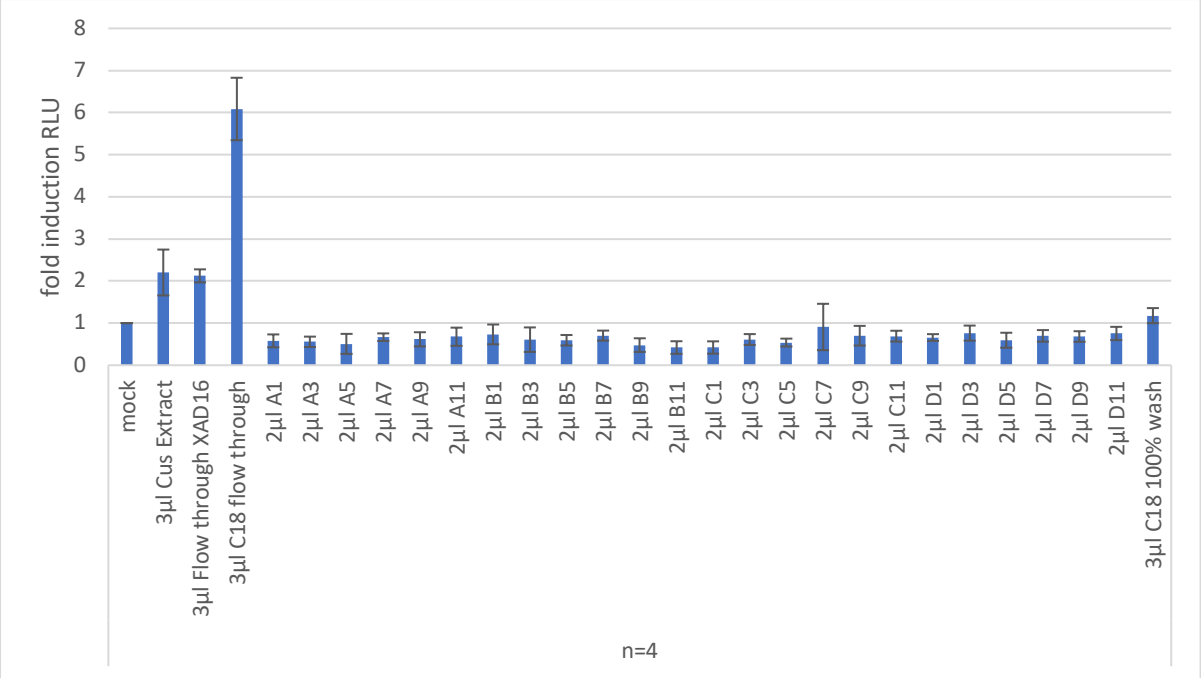

Figure 30 Light emission of the sensor pUMAMIT25:luc after application to the fractions from the C18 column (Supelcosil LC-18 HPLC).

The flow through of the XAD16 column was loaded, active fraction is only the flow through. The C18 column was run with 25mM MES pH 5.5 (elution methanol) fractions were collected in 2ml steps and reduced by vacuum evaporation to 20µl, volumes applied as indicated. Load total 100ml; flow through total 100ml; bars represent fold induction of light emission; whiskers are standard deviation.

2.1.4.3 Proteinogenic properties of the molecular cue

Since the initially performed approaches were not successful to enrich the *Cuscuta*-derived molecular cue it was assumed that the molecule may be of other character and not a protein. Therefore, samples were treated with Proteinase K and compared to untreated samples. If the *Cuscuta*-derived molecular cue is a protein or peptide it should be degraded by Proteinase K. As seen in Figure 31 the Proteinase K is not able to destroy the activity of the molecular cue, therefore it seems not to be of proteinaceous nature or strongly protected from Proteinase K digest.

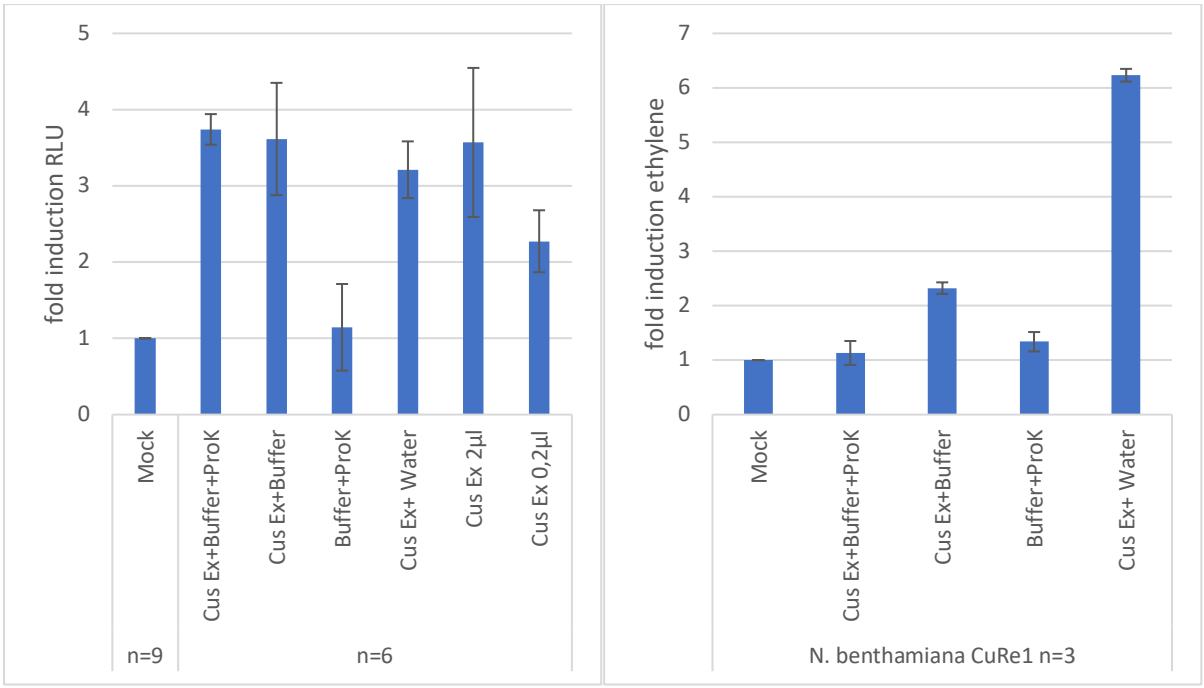

Figure 31 Light emission induced by Proteinase K digested Cuscuta Extract applied to the sensor pUMAMIT25:luc (left) and ethylene production of Proteinase K digested Cuscuta Extract applied to CuRe1 expressing *N. benthamiana* (right)

For the digestion with Proteinase K the 10µl of Cuscuta Extract were mixed with the reaction buffer (5mM $CaCl_2$ and 50mM Tris/ HCl pH 7,5) and Proteinase K (50µl/ml), incubated over night at 37°C and deactivated at 95°C (Cus Ex+Buffer+ProK) as control Cuscuta Extract and the reaction buffer (Cus Ex+Buffer) and reaction buffer and Proteinase K (Buffer+ProK) were used. In parallel 10µl Cuscuta Extract were mixed with water and treated the same as the digest (Cus Ex+water), additionally for the luciferase bioassay 10µl Cuscuta Extract was treated the same as the digest without dilution. All samples were reduced in volume by vacuum concentration. Mock = 25mM MES pH 5.5; Left: Bars represent fold induction of light emission of the sensor pUMAMIT25:luc in *N. benthamiana*; Right: Bars represent fold induction of ethylene production in *N. benthamiana* expressing Cure1; Both: whiskers are standard deviation.

The Proteinase K was additionally applied to Cuscuta Extract that was shown to be vulnerable to Proteinase K digestion (Hegenauer et al. 2016) and tested in the ethylene assay (Figure 31). The ethylene assay was chosen to confirm the activity of the Proteinase K and therefore supported the results of the luciferase bioassay, that the novel *Cuscuta*-derived molecular cue is not degraded by Proteinase K.

2.1.4.4 Purification methods and technique summary

The experiments shown before representing major steps but were further extended by additional conditions and columns to exploit all technical possibilities. Further methods and columns including conditions that are not shown in detail throughout this thesis are summarized in Table 4

Table 4 Purification Methods tested for the enrichment of the molecular cue.

Method	Column	Running Buffer/ Elution Buffer	Activity found in
Ion exchange	HiTrap SP-FF 5ml *	25mM MES (pH 5.5)/ 500mM KCl	flow through
	HiTrap Q-FF 5ml *	25mM TRIS-HCl (pH 8.5)/ 500mM NaCl	flow through
		25mM MES (pH 5.5)/ 500mM KCl	
Reversed Phase	C4 (no brand)	0.1% formic acid (pH 2.7)/ Acetonitrile	flow through or lost
	Supelcosil LC-18 HPLC *	25mM MES (pH 5.5)/ MeOH	
	Resource 15 RPC	25mM MES (pH 5.5)/ Acetonitrile	
		100mM TRIS (pH 10.2)/ Acetonitrile	
Gel Filtration	Hi Load 26/600 Superdex 30pg	without buffer (water)	elution at half column volume ~5kDa
		0.1% formic acid (pH 2.7); 100mM KCl	
		25mM MES (pH 5.5); 100mM KCl	
		25mM Ammonium acetate (pH 6.5); 100mM KCl	
Hydrophobic Interaction	HiTrap Phenyl FF	3M Ammonium sulfate/ 50mM $MgSO_4$	Not found in either fraction or flow through
Various	XAD16N *	25mM MES (pH 5.5)/ MeOH	flow through and 1A2
	Concanavalin A	50mM Na-Acetate, 200mM NaCl, 1mM $CaCl_2$, pH5.3/ 100mM α-Metylglucopyranoside	flow through
	GeneMatrix Universal RNA binding column	100µl DNA Binding Buffer+ 100µl Cuscuta Extrakt / 70% EtOH/ water	flow through
	Ethyl acetate	Ethyl acetate - Cuscuta Extract (1:1)	aqueous phase
	Ammonium sulfate *	0.6g/ml	supernatant
	Ethylene Assay *	25mM MES (pH 5.5) in *N.b.* CuRe1	no ethylene production
	Proteinase K digest (50µl/ml) *	5mM $CaCl_2$ and 50mM Tris/ HCl pH 7.5	no digest

* shown in this work

2.1.5 Alternative promoter-luciferase constructs - are multiple active components involved?

The purification did not yield the expected results, therefore an evaluation of the promoter properties in detail was initiated to exclude eventually occurring problems arising from miss-regulated prom:luc activity. UMAMIT25 was shown to play a major role in the amino acid export and seed loading (Besnard et al. 2017). Amino acid transporter as well as sugar exporter are important to provide essential nutrients for *Cuscuta* spp., therefore the promoters of the sugar transporters SWEET10 and SUC2 were used to investigate their ability to be activated by Cuscuta Extracts.

The bidirectional sucrose transporter SWEET10 is activated during the floral transition by flowering locus T and located mostly in leaf veins. Ectopic expression of SWEET10 induces flowering time related genes in the shoot apex (Andrés et al. 2020). Sucrose from the photosynthetic active tissues is exported by SWEET10 into the apoplast and from the apoplast loaded into the phloem via SUC2 (Chen et al. 2012). SUC2 was used to show a true phloem connection between *Cuscuta* spp. and the host plant via expression of GFP under control of pSUC2. GFP was loaded into the host phloem and could migrate through the haustorium connection into *Cuscuta* spp. (Haupt et al. 2001, Figure 4).

Since these genes are involved in the sucrose and amino acid transport during periods of high demand, they might be a rewarding target for *Cuscuta* spp. to exploit or to be abused.

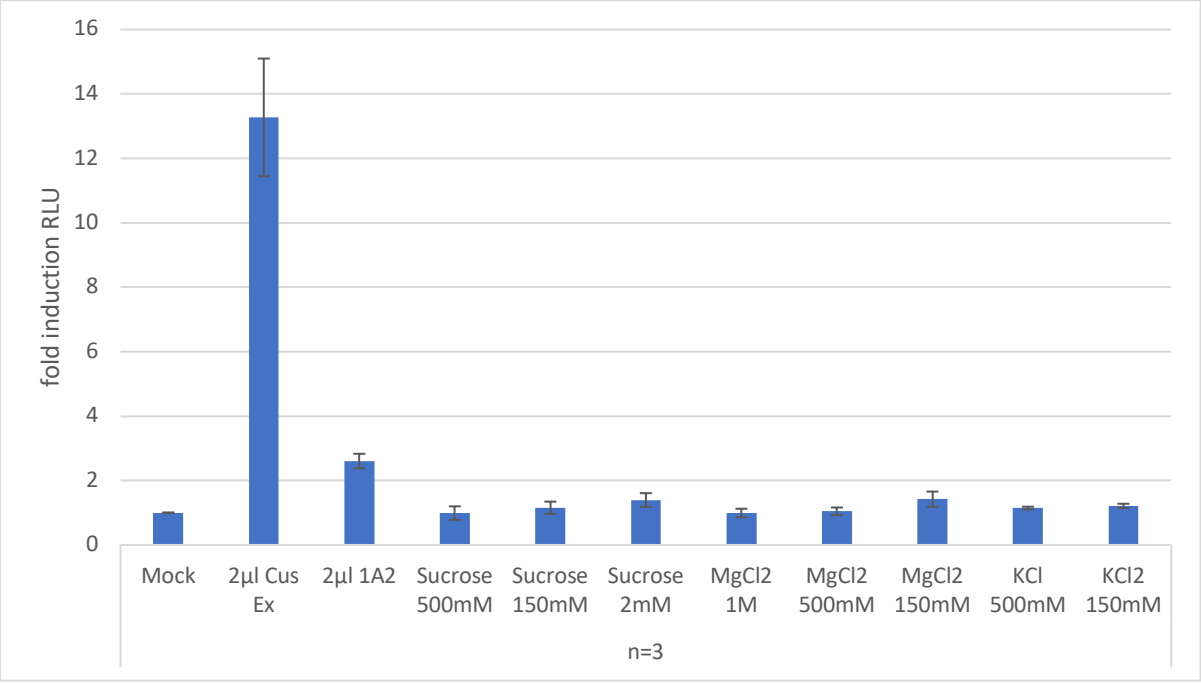

Figure 32 The promoter of the bidirectional sucrose transporter SWEET10 coupled to luciferase initiates light emission upon treatment with Cuscuta Extract but not with the established stresses.

N. benthamiana leaves transiently expressing pSWEET10:luc were treated with Sucrose 500mM (end conc 10mM); 150mM (end conc 3mM); Sucrose 2mM (end conc 0,04mM) and $MgCl_2$ and KCl with concentrations of

1M, 500mM and 150mM (end conc 20mM, 10mM and 3mM respectively); N=3; volumes are applied as indicated; bars represent fold induction of light emission after 23h; whiskers are standard deviation.

pSWEET10:luc is strongly activated by Cuscuta Extract that is visible with the high fold induction of over 13-fold. SWEETS are known to be hijacked by pathogens via TAL-effectors and function as susceptibly enhancing factors (Verdier et al. 2012) and root nematodes (Zhao et al. 2018). This puts SWEET10 into the position of being a target for a parasitic plant to be hijacked. SWEETS might be indirectly activated and in literature salt level changes (Sellami et al. 2019) as well as sugar level changes (Matsukura et al. 2000) were described to induce pSWEET10. This is, however not visible in the bioassay using pSWEET10:luc after treatments with salt- or sugar controls (Figure 32).

Interestingly, the time course with Cuscuta Extract treated pSUC2:luc samples showed a unique promoter activation pattern distinct from the activation of pUMAMIT25:luc (Figure 33). There, it is clearly visible that the activation upon the two purified extracts turns out to have a distinct pattern. Cuscuta Extract shows the late upregulation comparable to pUMAMIT25:luc (Figure 9) whereas the fraction 1A2 triggers an early increase of gene expression, that results in an increased light emission after 4 hours that is peaking at around 8 hours and flattens towards the 14h time point. This new pattern might indicate multiple components in the extract with distinct properties that might be purified differently and could act in different pathways.

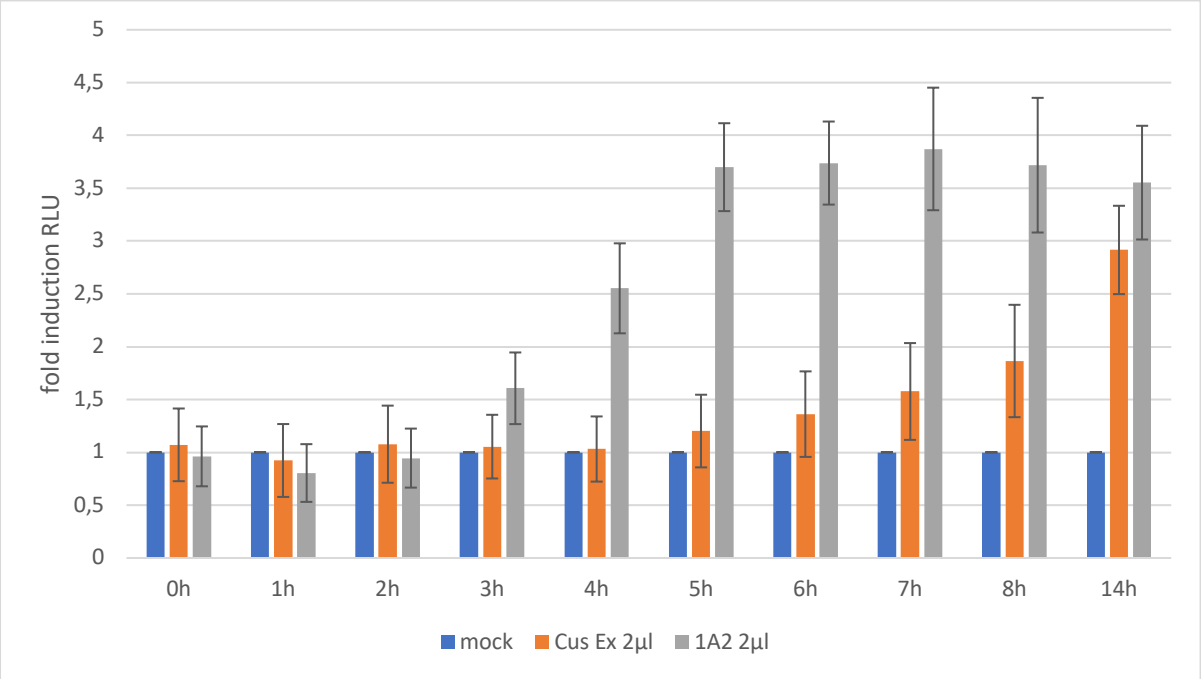

Figure 33 The promoter of the sucrose transporter SUC2, responsible for phloem loading and long-distance transport, coupled to luciferase initiates a distinct light emission after treatment with Cuscuta Extract or Fraction 1A2.

N. benthamiana leaves transiently expressing pSUC2:luc were treated with Cuscuta Extract and Fraction 1A2 form the XAD16 column elution. Cuscuta Extract is induced over time peaking after 14 hours, 1A2 is early induced and flattens towards the 14-hour time point. N=3; volumes are applied as indicated; light measurements were taken every hour; bars represent fold induction of light emission; whiskers are standard deviation.

Luciferase coupled to the promoter of SUC2 is expressed upon treatment with Cuscuta Extract and the measured light emission is increased, in addition a high sucrose concentration activates the gene expression and leads to a high light emission (Figure 34).

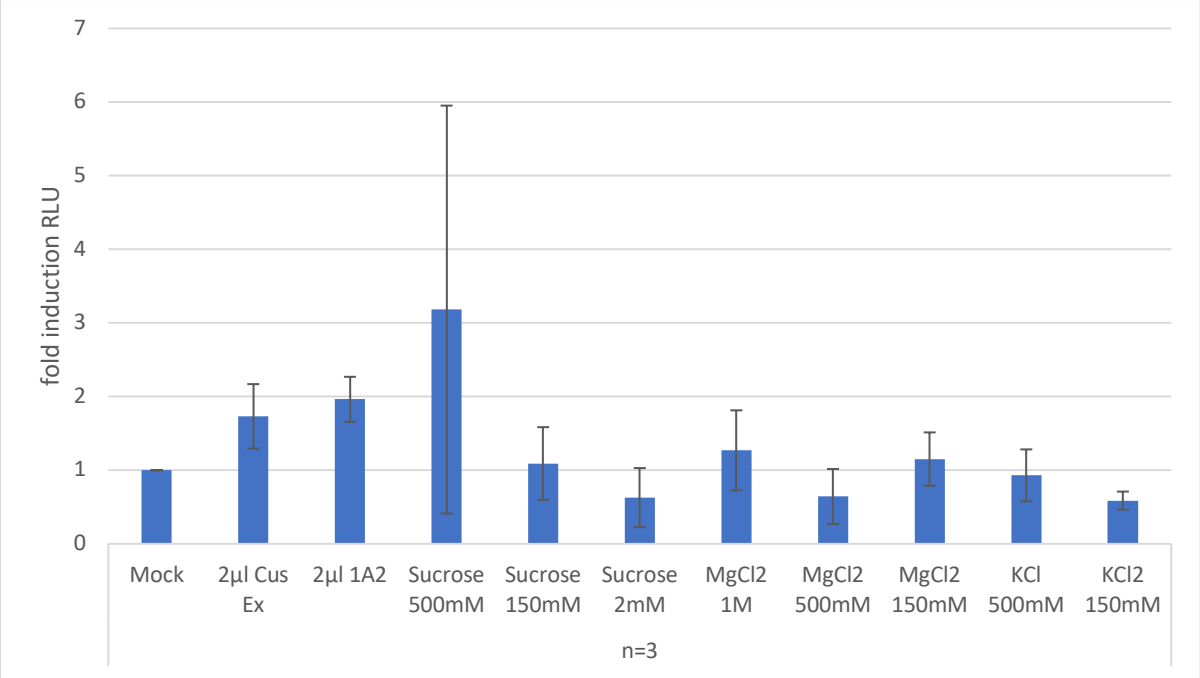

Figure 34 Light emission of *N. benthamiana* leaves transiently expressing pSUC2:luc is initiated by Cuscuta Extract and a high concentration of Sucrose.

N. benthamiana leaves transiently expressing pSUC2:luc were treated with Sucrose 500mM (end conc 10mM); 150mM (end conc 3mM); Sucrose 2mM (end conc 0,04mM) and $MgCl_2$ and KCl with concentrations of 1M, 500mM and 150mM (end conc 20mM, 10mM and 3mM respectively); N=3; volumes are applied as indicated; bars represent fold induction of light emission after 14h; whiskers are standard deviation.

2.1.6 Investigation of *Cuscuta*-derived CLE peptides

CLE peptides were shown to be involved in various developmental processes, especially in the shoot meristem CLE peptides are involved in the balance between cell proliferation and cell differentiation (Fletcher et al. 1999). In the vascular meristem CLE's are involved in the tracheary element differentiation (Hirakawa et al. 2008) and during lateral root formation CLE's guide the cell elongation (Depuydt et al. 2013, Rodriguez-Villalon et al. 2014). During the response to abiotic stresses CLE peptides regulate the preserving processes and contribute to the survival of the plant (Araya et al

2014). Besides the internal plant developmental guidance, CLE peptides are involved in root nodule formation during symbiosis (reviewed in Oka-Kira and Kawaguchi 2006). A special form of CLE-like peptides is even used by parasitic nematodes to hijack the host plant and create for the nematode favorable conditions (Guo et al. 2011, Roles of CLE peptides reviewed in Yamaguchi et al. 2016). In *Cuscuta japonica* CLE peptides were shown to influence xylem formation in haustorial cells (Shimizu et al. 2018). To investigate possible effects of CLE peptides during a susceptible interaction, *Cuscuta campestris* and *Cuscuta australis* were screened for CLE peptides. The screen revealed 7 *C. campestris* (CcCle) and 7 *C. australis* (CaCle) derived CLE peptide sequences that were synthesized and the peptides were then further tested in the promoter-luciferase bioassay (Figure 35).

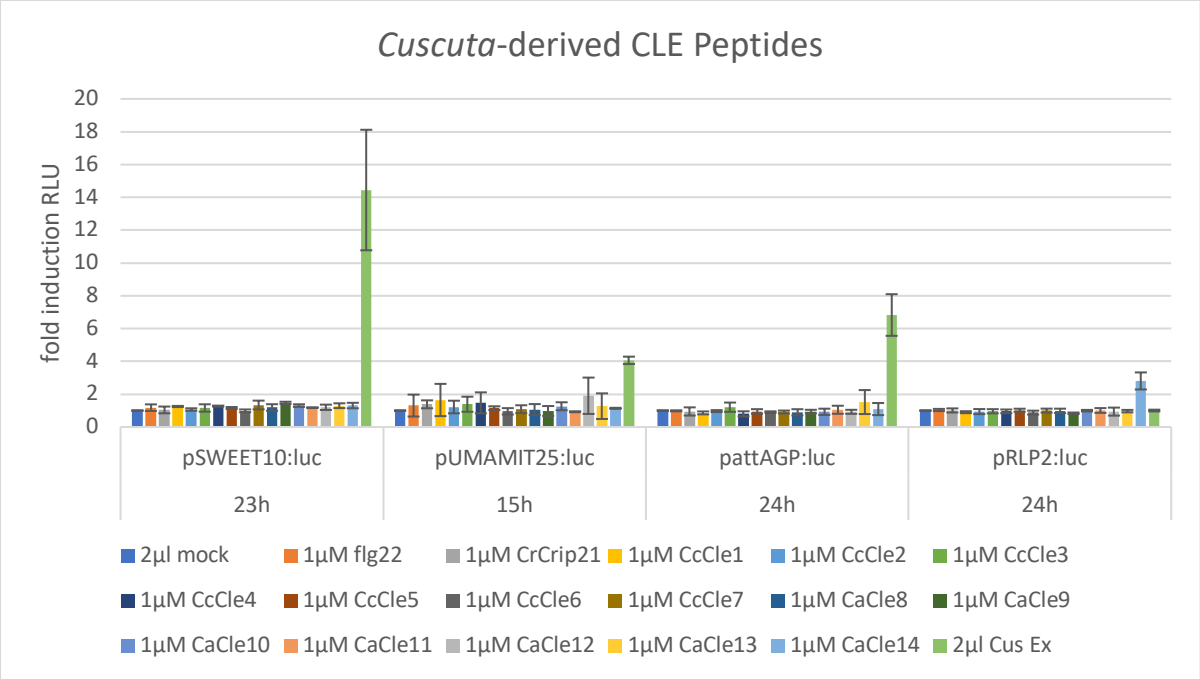

Figure 35 Light emission of promoter-luciferase constructs treated with *Cuscuta*-derived CLE peptides.

Synthesized CLE-like peptides from *C. australis* (CaCLE8-CaCLE14) and *C. campestris* (CcCLE1-CcCLE7) were applied to *N. benthamiana* leaves transiently expressing pSWEET10:luc, pUMAMIT25:luc, pattAGP:luc and pRLP2:luc. *Cuscuta*-derived CLE peptides did not initiate the light emission for pSWEET10:luc, pUMAMIT25:luc and pattAGP:luc. CaCLE14 did initiate the light emission for pRLP2:luc. Peptides (end concentration) and Extracts (volume) are applied as indicated; light emission measurements were taken as indicated; N=3; mock= peptide dilution medium; bars represent fold induction of light emission; whiskers are standard deviation.

The *Cuscuta*-derived CLE peptides did not trigger the promoters that were usually able to detect the Cuscuta Extract, but one promoter pRLP2:luc that is not able to detect Cuscuta Extract showed increased light emission after CaCLE14 application (Figure 35). This activation will be interesting in future experiments and has not been followed through.

2.2 Discussion

2.2.1 Rapidly activated host gene expression during parasitic- and host-plant interaction

2.2.1.1 Transcriptomic changes in host plants during *C. refelxa* infection

The RNA-Sequencing approach started by Körner 2016 and further evaluated in this thesis is used to get insights in the early transcriptomic changes in the host *N. benthamiana* during infection with *C. reflexa*. The aim was to uncover the differential transcriptomic changes that are regulated in a susceptible or resistant context. Therefore, the wildtype *N. benthamiana* was compared to the stably *CuRe1* expressing *N. benthamina*. The comparison between a susceptible plant and a partially resistant plant could help to distinguish between immunity related pathways and developmental pathways that are activated independently from the parasite recognition and therefore might be advantageous for the host-parasite connection. To uncover early changes *C. reflexa* extract preparation containing the immune response inducing CrGRP was infiltrated (CrGRP containing extract). The infiltration with CrGRP containing extract mimics the invasion of *C. reflexa* and should contain *Cuscuta*-derived molecular cues. To monitor the rapid adjustment and transcriptomic changes of the host plant, samples were taken directly after infiltration (0-hour) and after 2 hours.

The samples were initially analyzed by a team of the QBIC (Tübingen, Germany) with no scientific background in plant biology that led to an inconclusive data output as captured and discussed in Körner 2016. A new opportunity opened with collaboration partners that had an extended knowledge in RNA-sequencing analysis as well as a scientific interest in *Cuscuta* spp. interactions with hosts. The analysis revealed a completely different sample distribution in the PCA analysis and painted a novel picture of the activation pattern. All samples of the 0-hour timepoint form one cluster that is clearly separated horizontally from the 2-hour cluster. The 0-hour cluster contains all plants and treatments which is an indicator for a similar behavior of the plants at the beginning of the experiment. No major differences are visible in *N. benthamiana* expressing CuRe1 in comparison to wild type plants due to the stable expression of CuRe1. Additionally, the 0-hour cluster shows that the treatment with CrGRP containing extract followed by an immediate and rapid harvesting is too fast to result in any transcriptional changes. The clear separation of the two clusters 0-hour and 2-hour indicates that the infiltration process itself and the following incubation leads to a visible transcriptomic change in all samples. The wild type plants treated with the CrGRP containing extract cluster together with wild type plants and the CuRe1 expressing plants that were treated with control treatment. Clearly separated and forming their own cluster after 2 hours of treatment are the CuRe1 expressing plants treated with CrGRP containing extract. This pattern indicates that the strong and rapid changes in CuRe1 expressing plants are mostly due to the recognition of CrGRP that is recognized by CuRe1 and activates the immunity cascade. CuRe1-independent damage associated patterns (DAMP) could be

excluded since these DAMP-responses would be visible in wild type plants treated with the CrGRP containing extract (Figure 6).

CrGRP recognition by CuRe1 induces rapid transcriptomic reprogramming that leads to the upregulation of 1124 genes and the downregulation of 413 genes. The significant total regulation of 1537 genes are specific for CuRe1 expressing plants (Table 1). The number of regulated genes corresponds to studies showing that during the flg22 perception in *A. thaliana* approximately a total of 1200 genes were significantly regulated after 30 minutes, similar results were obtained by treating *A. thaliana* with EF-Tu-derived peptides where after 30 minutes 450 and genes were significant regulated (Zipfel et al. 2004, Zipfel et al. 2006). A recent study shows a set of 900 core genes regulated upon flg22 treatment shared between Brassicaceae (Winkelmüller et al. 2021). The intense reprogramming upon flg22 recognition in *A. thaliana* shows similarities to *N. benthamina* treated with CrGRP in form of the well-known immunity response genes SERK3 and SOBIR1 as well as the upregulation of very early and early response pathways in form of oxidative stress genes (RbohD), MAPKs and WRKY-type transcription factors (WRKY33). Additionally, the CrGRP treatment led to an increased transcription of plant hormone related genes involved in ethylene and salicylic acid signaling (NPR3) (Boller und Felix 2009, Boller and He 2009, Winkelmüller et al. 2021). The intense reprogramming upon CrGRP recognition is not restricted to stress related genes and shows a strong bias for genes involved in protein modification, RNA biosynthesis and solute transport (Table 1). The RNA-Seq was performed before the now known immune response inducing factor CrGRP has been discovered, therefore an interesting approach would be a repetition with the synthesized minimal peptide CrCrip21 to reduce possible background gene activation by other components in the CrGRP containing extract.

The experiment was not solely aimed on the immunity related transcriptomic changes but also in susceptibility related changes. Since the wild type plants treated with CrGRP containing extract clustered with the control treatments of wild type plants and stably with CuRe1 transformed plants, a closer look which genes were activated in each sample was necessary. A Venn-Diagram was used to visualize the relationship between the different samples. This style of visualization reveals the relation between gene and sample and therefore allows to identify specifically upregulated genes in each treatment and genotype (Figure 7). The Venn-Diagram revealed that only one gene: GAE1 (UDP-D-GLUCURONATE 4-EPIMERASE 1) seemed to be regulated in wild type background upon CrGRP containing extract treatment. GAE1 is known to be involved in the pectin biosynthesis of cell walls and repressed by *Pseudomonas syringae* during the infection (Bethke et al. 2016). GAE1 was in addition shown to co-localize with arabinogalactan biosynthesis pathway components (Poulson et al. 2015). The promoter of GAE1 was cloned and is part of an ongoing project that is testing and establishing

pGAE1:luc as novel reporter in the luciferase bioassay. The RNA-sequencing analysis might be interesting for future investigations of CuRe1 related signaling, but as this work focuses on the susceptible side of host reactions the analysis did not reveal the expected regulation of genes in a CuRe1 independent and susceptible context.

2.2.1.2 Rapid host gene expression used as sensor to illuminate parasitic plant signaling

The selection of gene promoters is mainly based on the publication of Ikeue et al. 2015, especially upregulated genes during the early pre-haustorial phase and invasive phase were interesting due their direct role in the establishment of a new functional plant-plant connection and their role during haustorium induction. Later gene regulation might be due to the restructuring of tissue, developmental reprogramming and the involvement in slower processes that might need more time to be activated. The major aim was to find strongly regulated genes that are involved in the initial reaction of the host plant to *Cuscuta* spp.. The regulated genes should be suitable for a promoter-reporter bioassay that sheds light on *Cuscuta*-derived molecular cues involved in the susceptible interaction (Table 2).

In Ikeue et al. 2015 *Cuscuta japonica* was grown on the host *Glycine max* and the differential expression patterns in the undissected interface region were analyzed. The growth of *C. japonica* was monitored for 5 days with samples taken 24h, 48h 72h, 96h and 120h after attachment (haa). The earliest timepoint for a transfer of *Cuscuta*-derived molecular cues is 48haa since *C. japonica* needs approximately two days to establish the haustorium and invade the host. Therefore, the differential upregulation between 24haa, no invasion of the host, and 48haa, first invasion of the host, was compared and the datasets were screened in silico for interesting gene candidates. Upregulated genes were sorted by their fold increase to get the highest upregulated genes and afterwards the genes were selected to get representatives of as many molecular functions as possible.

The upregulated genes that have been chosen for the bioassay showed a broad spectrum of biological functions and different subcellular localizations, since it was not known which genes might be guided or highjacked by *C. reflexa* a broad spectrum of genes was expected to include possible candidate genes that might be activated by the *Cuscuta*-derived molecular cue. Most upregulated genes had no clearly assigned functions and their corresponding promoters were unknown. Therefore, the promoter region was defined as 2000bp upstream of the start codon since most regulatory elements are located 0bp to 2000bp upstream of the transcription start. This approach involves the risk of missing the full-length promoters but the high number of candidate genes assured that a small number of promoters would be usable in the bioassay. Hence, if promoters are unfunctional due to missing

regulative elements, the sensor would not react in the bioassay and the promoter construct would be sorted out. All promoters were fused to luciferase and could be used to sense *Cuscuta*-derived molecular cues by emitting light. The major aim was to find at least one promoter that would be induced by a *Cuscuta*-derived molecular cue and therefore could be used to screen for unknown molecular cues that are able to manipulate, guide the haustorium or support the hijack of the host plant by parasites (Table 3).

2.2.2 Establishing the luciferase based high throughput bioassay

The bioassay was planned to be as fast, reproducible and easy to handle also in a high throughput manner. Therefore, the assay was designed in a 96-well plate format. The setup of the bioassay was part of Körner 2016 but was strongly revised and optimized. The initial approach (Körner 2016) based on the inject function of the luminometer, where the luciferin was added into each well with the built-in injector. The approach had two downsides; it consumed high volumes of luciferin due to the system priming and the injection was lacking a visible control. It could happen that the luciferin was injected on top of the leaf and therefore did not reach the reaction buffer in the 96-well plate. Additionally, the inject method allowed only one time point per plate and each timepoint needed a new plate with samples. By changing the assay into a luciferase glow assay with the addition of the luciferin at the beginning, different time points could be evaluated and a timeline of light emission was possible. Hence, this method allowed to see different activation patterns that gained importance later in the process (Figure 8).

Due to the transient transformation of *N. benthamiana* leaves, the total light output was influenced by age, transformation efficiency and additional stresses for example higher temperatures during summer or less light during winter. These alterations resulted in a change of the total relative light units (RLUs) measured by the luminometer, to compare the results the RLUs were normalized and transformed in fold induction RLUs. Fold induction RLUs proved to be more comparable than non-transformed RLUs but showed the disadvantage of not displaying the promoter background activity. Some promoter-luciferase constructs had a generally higher background RLU level than others, therefore the viability of a promoter-luciferase construct, as functional sensor, to sensitively respond to a *Cuscuta*-derived cue, was defined by the fold increase of light emission levels compared to the background levels when triggered with Cuscuta Extract.

The exemplarily shown activation of pUMAMIT25:luc, pFRK1:luc and pRLP2:luc in 1-hour steps demonstrates the difference between active, increased light emission after Cuscuta Extract treatment and inactive, same light emission as the untreated control. The time course was used to see possible

early or late activation patterns for the tested sensors. All sensors were measured over time for up to 24 hours to find a promoter-luciferase construct that had increased light emission (Figure 9). Based on the measurements over time the ideal incubation time for the readout was determined. In case of the pUMAMIT25:luc the ideal timepoint was 14 hours after elicitation, the other sensors exemplarily pFRK1:luc and pRLP2:luc did not react to this type of Cuscuta Extract at any timepoint. Once the ideal incubation time was found, promising promoter-luciferase constructs were exposed to immunity related peptides. The tested peptides flg22 and CrCrip21 are known to induce ethylene production in *A. thaliana* and *N. benthamiana* with concentrations in the nM range, respectively (Chinchilla et al. 2006, Hegenauer et al. 2016). With their role during immunity signaling flg22 and CrCrip21 needed to be excluded as potential candidates that can influence the light output of the tested promoter-luciferase constructs. Especially CrCrip21 was interesting due to its origin in *Cuscuta spp*. cell walls, its recognition by CuRe1 and the known role during activation of immunity related processes in tomato. Flg22 is recognized by FLS2 that is present among other plants in the transiently transformed *N. benthamiana*. Throughout all assays the immunity response triggering peptides proved to be inactive (Figure 10).

To determine the sensitivity of the bioassay and respective sensors, the detection range was determined. Interestingly the application of higher volumes of Cuscuta Extract led to light quenching that reduced the level of detected light below the mock control, whereas the lowest detectable application was 0,03µl in pUMAMIT25:luc expressing *N. benthamiana* (Figure 12).

Auxin and cytokinin are known from their role during the meristem maintenance by a complex interplay of both plant hormones (Su et al. 2011). Besides the meristem maintenance auxin and cytokinin guide the lateral organ formation in roots (Moriwaki et al. 2011) and shoots (Shani et al. 2006) and were shown to be essential during plant grafting (Sharma and Zheng 2019). Auxin was shown to be induced by haustorium inducing factors in *P. japonicum* (Cui et al. 2020). The evidence that plant hormones could be utilized by parasitic plants to establish a plant-plant connection led to the necessity to exclude their involvement during the activation of the luciferase bioassay. Additionally, hormones that are involved in immunity related pathways were tested in form of Systemin, that is known as plant wide warning hormone upon insect feeding (Wang et al. 2018). Strigolactone plays a special role due to its function during symbiosis in arbuscular mycorrhizal fungi (Akiyama et al. 2005) and root parasitism, where it functions as chemical germination guide that is detected by root parasites, originating from the host root (Yoneyama et al. 2010) (Figure 14). Additionally, endogenous signals like carbohydrates and osmotic stresses were tested. Sugars play a major role in nutrition for the plant and therefore the detection of sugar might trigger transporters.

Chitin that occur in insect skeletons and fungi cell walls might activate the sensor due to their ability to trigger an immune response (Figure 13).

To correlate the light output with the luciferase transcription qRT-PCR was performed. The qRT-PCR showed that gene activation is visible after 30 minutes whereas after 2 hours and 14 hours only very low levels of transcript were detectable. The immediately initialized transcription is detectable after translation that leads to an increase of light emission over time (Figure 15).

The attachment Arabinogalactan Protein (attAGP) was shown to be activated during *Cuscuta* spp. attachment at the haustorium formation site via GUS-staining (Figure 16). The results of the promoter-luciferase bioassay reflect the result of the GUS-staining and lead to the conclusion that a molecular cue is transferred into the host and can activate transcription. *attAGP* upregulation so far is only described in resistant plants therefore the assay was repeated with *N. benthamiana* expressing CuRe1 to check if there might be a differential activation. The results suggest that CuRe1 is not involved in the accumulation at the attachment site. The slightly lower fold induction might be due to the additional expression of a 35S:CuRe1 in the transformed plants (Figure 17).

Stable plants were prepared to reduce the workload of transient transformation and a reduction in background variation that is owed to the transient transformation rate. Floral dipped *A. thaliana* did not react to any treatment this result aligned with early experiments performed with *A. thaliana* protoplasts that did not react with increased light output to any treatment (data not shown in this work, Figure 18). Since the assay is established and aimed at *N. benthamiana* it might be possible that a promoter-luciferase construct that proved active in *N. benthamina* does not respond in *A. thaliana*. There might be a signaling cascade that is missing in non-solanaceous plants that is needed to initiate the light production in the luciferase bioassay. Since the bioassay was established in *N. benthamina* stable transformed plants were produced and selected by BASTA® spraying. The survivors were tested by application of Cuscuta Extract and the stable transformed lines showed increased light output after Cuscuta Extract application (Figure 19). Positive tested plants were tested in the second generation as well to see possible silencing events that occurred just sporadically. Non-silenced candidates can be used for further experiments (Figure 20).

The promoter-luciferase construct pUMAMIT25:luc that yielded the most consistent bioassay results, that was not influenced by endogenous signals in form of sugars, plant hormones as well as osmotic stresses could be used for further experiments. pUMAMIT25:luc did not show any reaction to immunity related peptides and had a strong transcriptional upregulation that could be measured as increased light emission after 14 hours. Therefore pUMAMIT25:luc was used for further experiments

on various Cuscuta Extract preparations to screen for and to identify novel *Cuscuta*-derived molecular cues.

2.2.3 Purification of the parasitic signal

The first step was to verify the stability during the pre-purification based on Hegenauer et al 2016, that included boiling freeze-dried Cuscuta in 0,1M HCl to efficiently release CrGRP related molecular factors from Cuscuta. The harsh processing in HCl was not ideal for the following purification processes due to restrictions during buffer adjustment, therefore a milder approach by boiling in water was used. The water-based initial step provided an easy and repeatable platform for buffer adjustments. Boiling may result in protein denaturation therefore comparison between freshly prepared raw or crude Cuscuta Extract and the boiled Cuscuta Extract was needed. The comparison showed equal activation properties when tested in the promoter-luciferase bioassay and even a slight signal increase compared to the fresh material this result indicates a heat stability of the unknown molecular cue. Boiling freeze-dried material resulted in bigger amounts of starting material than the processing of raw material that would need thorough grinding and centrifugation to separate a smaller amount of raw extract and was thus used for further preparations (Figure 21).

Protein precipitation with ammonia sulfate to concentrate the proteins and reduce contaminations was used as initial step of the pre-purification. The precipitate was dialyzed with a small MWCO of 3500 to keep almost all bigger molecular cues since the approximate size was 5kDa as indicated by the gel-filtration. All steps during the pre-purification were monitored with the luciferase bioassay to track the bioactive compound and in addition the protein concentration was measured according to Bradford. The ammonia sulfate precipitation followed by dialysis did increase the protein concentration of the extract but not the light emission in the bioassay. The unknown molecular cue could be detected in the supernatant of the ammonia sulfate precipitation by a slightly increased light emission. The comparison of protein concentration and light emission of the bioassay implies that the light inducing molecular cue is not a protein that precipitates with an increased concentration of ammonia sulfate (Figure 22). Therefore, the initial purification methods focused on a molecular cue that does not precipitate but has a net charge that could be purified. The pre-purified Cuscuta Extract was loaded onto a strong cation exchange column with MES buffer adjusted to a pH of 5.5 to simulate intracellular conditions. These conditions were used in previous purifications of the CrGRP, the eluted fractions from the cation exchange column could not induce the light emission. The collected flowthrough was able to increase the light output in the bioassay (Figure 25). Interestingly, the ethylene levels are clearly increased by the eluted fractions, but no ethylene production was detectable for the flow through samples. This indicates that the strong cation exchange column did bind the CrGRP as shown in Hegenauer et al. 2020 but not the unknown molecular cue that is able to

activate the bioassay. The divergent activation shown by the ethylene assay and the luciferase bioassay indicates for a CuRe1 independent *Cuscuta*-derived molecular cue (Figure 23, Figure 26). To purify the unknown molecular cue, an anion exchange column was used with a more basic pH of 8.5 to bind the molecular cue to the column. The number of samples was reduced by collecting bigger fractions. However, none of the fractions did induce light emission in the bioassay. The ion exchange columns were thus not able to bind and to enrich the molecular cue. The molecular cue moved directly through the columns during sample application and could be found in the flow through (Figure 27). Since ion exchange columns did not enrich the molecular cue, it is assumed that it does not carry any charge to bind to the ion exchange columns.

The lack of binding to ion exchange columns led to alternative purification approaches. From the absorbent XAD16 the molecular cue could be eluted after a short wash with the running buffer. Still, most of the light inducing molecular cue rushed through the column during the sample application. The active fraction was loaded onto a cation exchange column to make sure the binding was not concentration dependent. The fractions were inactive and therefore the cation exchange column was not used for the further purification (Figure 28). The properties of XAD16 as an absorbent for organic substances led to the assumption that a reversed phase column might enrich the molecular cue. A reversed phase C18 column was loaded with the flow through of the XAD16 to bind the molecular cue to the column. Reversed phase C18 columns are dependent on pH as well as the organic solvent in the mobile phase, therefore a broad range of buffers was tested with pH 2.7, pH 5.5 and pH 10.2. Additionally, the mobile phases methanol and acetonitrile were used. All conditions resulted in the same result, that the reversed phase C18 column was not able to enrich the molecular cue. The activity was mainly in the flow through and not enriched in the eluted fractions (Figure 30). The molecular cue in the flow through of the C18 column led to the conclusion that the molecular cue should be polar.

To test whether the molecular cue is of proteinogenic nature the extract was digested with Proteinase K and tested in the luciferase bioassay, as control the digested Cuscuta Extract was tested in the ethylene assay. The luciferase assay has an increase of light emission despite the digestion with Proteinase K, the results of the ethylene assay clearly show that Proteinase K can destroy the in immunity involved CrGRP in the Cuscuta Extract (Hegenauer et al. 2016). Therefore, the molecular cue is not of proteidogenous nature or not digestible by Proteinase K as seen for the control protein CrGRP (Figure 31).

All purification techniques used during this work were not able to enrich the molecular cue to an extend that would result in the identification. In general, the different approaches lead to the

conclusion that the molecular cue is not of proteidogenous nature, does not carry any net charge and should be hydrophilic (Table 4).

2.2.4 "A New Hope" What does Cuscuta influence in the host?

The attempt to purify the molecular cue could not be accomplished but the activation of the sensor and the resulting light emission indicate a role of one or more *Cuscuta*-derived molecular cues during the haustoria establishment. Shortly before *Cuscuta* spp. is attaching to the host it is feeding on its own slowly decreasing reserves. A fast manipulation of the host, to free resources, would increase the survival chances during the initial attachment phase. The experiments suggest a *Cuscuta*-derived molecular cue to communicate with the host that is involved in the activation susceptibility enhancing processes. To get insights of the manipulation initiated by *Cuscuta* spp., the corresponding genes of the positively tested promoters were investigated.

In total three promoters did show increased light output upon Cuscuta Extract treatment: two of them, pRBP45B and pMTK, were described in Körner 2016 and one additional promoter, pUMAMIT25, was used in this study due to its stability during various tests and a strong and stable increase of light emission compared to the background. The promoter of pUMAMIT25:luc that has been characterized and used in this work, usually regulates the expression of an amino acid exporter UMAMIT25 that transfers phloem derived amino acids from the maternal tissue into the symplasmically isolated seeds in *A. thaliana* (Besnard et al. 2018, Karmann et al. 2018). *UMAMIT25* is exclusively expressed in the endosperm and the expression level directly correlates with the amino acid levels in the storing tissues (Besnard et al. 2018). *RBP45B* encodes an RNA binding protein that plays a role in in RNA metabolism, stability and translation during stress (Muthuramalingam et al. 2017). The processes controlled by RBP45B are directly involved in advantageous regulatory events of RNA biosynthesis during manipulation by *Cuscuta* spp.. MTK is a methylthioribose kinase and knock out experiments in *A. thaliana* showed that plants lacking MTK cannot utilize methylthioadenosine (MTA) as a sulfur source, which results in lower growth rates on sulfur deficient medium supplemented with MTA (Sauter et al. 2004). MTK is a key factor during the methionine salvage cycle and processing MTA into Methionine (Yang and Hoffman 1984)

These three genes seem not functionally related, but two of them are involved in nutrient relocation. Additionally, the RNA-sequencing data revealed that the major groups of upregulated host genes expressed during recognition of *Cuscuta* spp. seem to reflect these functions with protein modification, RNA biosynthesis and solute transport as the tree major upregulated molecular function groups. The molecular function including solute transporters fits in the model of C*uscuta* spp.

manipulating the host to increase the nutrition displacement to the newly connected sink-tissue-like parasite. Since UMAMIT25 is an amino acid exporter, the focus was on transporters that are known to be hijacked from other parasites like bacteria (Verdier et al. 2012) and root nematodes (Zhao et al. 2018). Further investigation of transporters was focused on sucrose transporters and two candidates were found and cloned. SWEET10 a passive transporter activated during floral transition (Andrés et al. 2020, Chen et al. 2012) and SUC2 an active phloem loading channel (Haupt et al. 2001). Both transporter genes were found in the RNA sequencing approach to be upregulated during *Cuscuta* spp. infection and implemented in the bioassay. The bioassay confirmed that the promoters of both genes responded to Cuscuta Extract application and initiated an increase of light emission. SWEET10 was described in the context of root parasitism to play a role in resistance by keeping the rhizosphere free from sugars and therefore limiting the carbohydrate content for soil pathogens (Chen et al. 2015). SWEETs or SWEET-likes additionally were reported as primary targets of pathogens derived effectors in rice (Chen et al. 2010). SWEETs seem to be a favorable target in parasitic interactions. The pSWEET10:luc sensor was tested with excessive sugar- and salt-levels due to reports that claim a sugar and salt inducibility (Sellami et al. 2019, Matsukura et al. 2000) but no increased light output could be detected. SWEET transporters are known from short distance passive transport (Chen et al. 2012), therefore it seems a good target for *Cuscuta* spp. during the early stages of infection. Apoplastic sugars that are available in high concentrations might be taken up by *Cuscuta* spp. to boost the invasion and feed the developing tissues of *Cuscuta* spp. haustoria before a proper connection to the phloem cells is established (Figure 32).

The Cuscuta Extract was also able to trigger the promoter of the active phloem loader SUC2 in the bioassay, that was used to illuminate the ability of haustoria connections to transfer macromolecules (GFP) from the host into the connected *Cuscuta* spp. (Figure 3, Haupt et al. 2001). The increased transcription of SUC2 transporters is important to redirect sucrose into the phloem, after an established connection of *Cuscuta* spp. to the phloem (Yoshida et al. 2016). *Cuscuta* spp. can profit from the increased levels of sucrose that is redirected to the *Cuscuta* spp. sink-like tissue. During the time course with two different preparations of Cuscuta Extract the activation of pSUC2:luc had two different patterns, the first one is comparable to other active sensors that lead to luciferase accumulation over time and show a strong induction of light emission after 14 hours. The treatment with the fraction 1A2 from the XAD16 column on the other hand induced the sensor very fast already after 4 hours 2.5 fold over the mock control. After 7h hours, the light emission seemed to plateau and was reduced again after 14h (Figure 33). This was the first hint that the Cuscuta Extract might contain several components which may play different roles during the attachment of *Cuscuta* spp.. pSUC2:luc was additionally tested with a wide range of concentrations of sucrose including the physiological

concentration to check for a sucrose dependent feedback loop as described in rice for *Oryza sativa* Sucrose Transporter 1 (OsSUT1) (Matsukura et al. 2000). The bioassay was clearly activated with increased light emission after treatment with sucrose, this might be a hint that sucrose gradients play a role during the attachment of *Cuscuta* spp. but sucrose is not the only *Cuscuta*-derived molecular cue since other sensors did not sense sucrose but were able to detect compounds of the Cuscuta Extract (Figure 34).

The tested transporter proteins are beneficial for *Cuscuta* spp. during attachment as well as in later developmental stages. The guiding or influencing of host transporter proteins during a parasite-host interactions is not jet described in shoot parasitic plants. However, in bacteria it is known that SWEETS are hijacked via transcription activation like (TAL)-Effectors that are known as susceptibility enhancing factors (Verdier et al. 2012). TAL-Effectors from *Xanthomonas* spp. were shown to induce the sugar transporter MeSWEET10a in Cassava (*Manihot esculenta*) (Cohn et al. 2014), therefore it would be possible to have *Cuscuta*-derived TAL-Effectors that could be discovered by a genome analysis based on the TAL-Effector-DNA binding code (Hutin et al. 2015).

Cuscuta spp. interestingly activates usually silent genes at the attachment side or manipulate gene expression otherwise involved in other processes. UMAMIT25 was shown to be expressed in seeds and is especially relevant for the endosperm loading with amino acids (Besnard et al. 2017). SWEET10 is distributed in all leaf veins and is activated by Suppressor of Overexpression of Constans 1 (SOC1) and Flowering Locus T (FT) to induce flowering; early flowering is also inducible by overexpression of SWEET10. An increased sugar level is beneficial for sink tissues like flowers or in a parasitic context with *Cuscuta* spp.. SUC2 is a sucrose transporter that facilitates the uptake from the apoplast into companion cells (Stadler and Sauer 2019). From the companion cells, the sugars are passively transferred into the thieve elements and from there are further distributed throughout the plant. Interestingly, while SWEET10 is helpful during early attachment, SUC2 is more important during later stages when *Cuscuta* spp. is fully connected to the vasculature after approximately 2-3 days. There might be a time-based misconception due to the application of Cuscuta Extract containing all molecular cues directly to the leaf. The bioassay might react to molecular cues that are derived from *Cuscuta* spp. at different timepoints of infection, but both activate the bioassay at the same time. The host-parasite interaction might be tightly regulated with a step by step procedure depending on the stage of attachment between host and *Cuscuta* spp..

2.2.4.1 CLE peptides and their impact during *Cuscuta* spp. attachment

CLE peptides are essential regulators during shoot apical meristem (SAM), root apical meristem (RAM) development and other developmental steps, but CLE-likes are also abused by parasites e.g. root

nematodes. Therefore, *Cuscuta*-derived CLE peptides might be involved during the attachment of *Cuscuta* spp. to the host plant. An *in silico* screen of the *Cuscuta australis* and *Cuscuta campestris* protein databases revealed 14 *Cuscuta* CLE-like peptides that were synthesized and tested for their ability to activate the light production in the luciferase bioassay. The *C. australis* CLE-like peptide CaCLE14 could be observed with a slightly increased light emission in pRLP2:luc, interestingly pRLP2:luc was not responsive to the Cuscuta Extract. The results need to be treated with caution since the low amplitude of the increased light emission is very close to the threshold of 2-3 fold of light induction. Small variations in between experiments led to a drop below the threshold and would therefore result in a difficult to interpretation. Compared to the increased light emission after treatment with Cuscuta Extract in other promoter-luciferase constructs the *Cuscuta* CLE-like peptide might play a minor role during the attachment. Still this is an additional hint towards multiple existent molecular cues that can be detected by the host plant during the attachment of *Cuscuta* spp.. The light inducing *Cuscuta* CLE-like peptide has a 75% sequence similarity with the *A. thaliana* AtCLE25 and AtCLE45 that are both described in the context of protophloem development. The protophloem is the precursor of the fully established phloem that relocates nutrients in developing and energy consuming tissues (Rodriguez-Villalon 2016, Ren et al. 2019). AtCLE25 is expressed in roots and moves to the leaves to initiates stomata closure during dehydration stress (Fletcher et al 2020, Takahashi et al. 2018). The guiding and establishing of a solute flow that is advantageous for *Cuscuta* spp. is an additional strategy that might be employed by *Cuscuta* spp. during the infection of the host. *Cuscuta* CLE-likes represent an additional molecular cue that is involved in the hijacking processes during the infection with *Cuscuta* spp. (Figure 35).

2.2.4.2 Summary

Cuscuta spp. can hijack essential feeding related genes and activate them during the infestation to profit from increased levels of carbohydrates and amino acids. *Cuscuta* spp. can redirect nutrients by sending out multiple molecular cues. These experiments suggest that the molecular cues might be sucrose gradients, *Cuscuta*-derived CLE-like peptides, TAL-effector-likes or a still elusive molecular trigger.

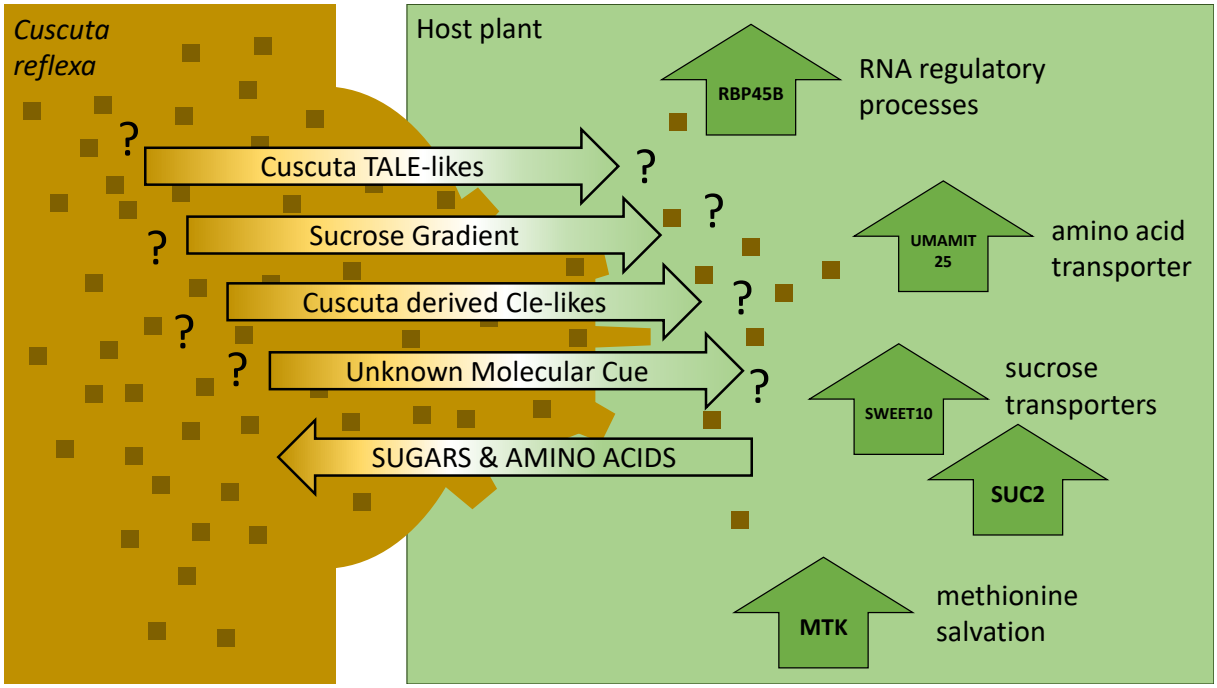

Figure 36 How does *Cuscuta reflexa* influence the host?

Hypothetical model of a *C. reflexa* haustorium penetrating a host plant stem. The figure shows the upregulated and tested genes (*RBP45B, UMAMIT25, SWEET10, SUC2, MTK*) during infection (bold green arrows)., the luciferase bioassay showed that the promoters of these genes could be influenced by Cucuta extracts and potential parasite derived molecular cues. The indicated genes are involved in RNA regulatory processes, amino acid transport, sugar transport and methionine salvage. The approach to identify the *Cuscuta*-derived molecular cue led to several interesting hypothetical candidates including *Cuscuta*-derived TALE-likes, Sucrose gradients, *Cuscuta*-derived CLE-likes and a still unknown molecular cue.

3 Analysis of the hydrophobic C-terminus of CuRe1

3.1 Results

3.1.1 Truncation of the CuRe1 C-terminal hydrophobic tail

CuRe1 is an LRR-RLP first identified in *Solanum lycopersicum* which confers resistance to *Cuscuta* spp. by recognizing the *Cuscuta reflexa* derived cell wall protein called CrGRP or its peptide epitope CrCrip21 (Hegenauer et al. 2020). CuRe1 consists of a C-terminal signal peptide and an LRR-N-terminal domain, followed by 35 LRRs interrupted by an island domain between the 31st and 32nd LRR, the transmembrane domain (TM) and the intracellular domain (Figure 37). The C-terminal intracellular domain consists of hydrophobic residues and might play a role as a 2nd transmembrane domain, the association with the membrane or the interaction with other proteins. Different deletions at the CuRe1 C-terminus were created and proteins were tested to get insights in the possible function of the hydrophobic tail of CuRe1 (Figure 37).

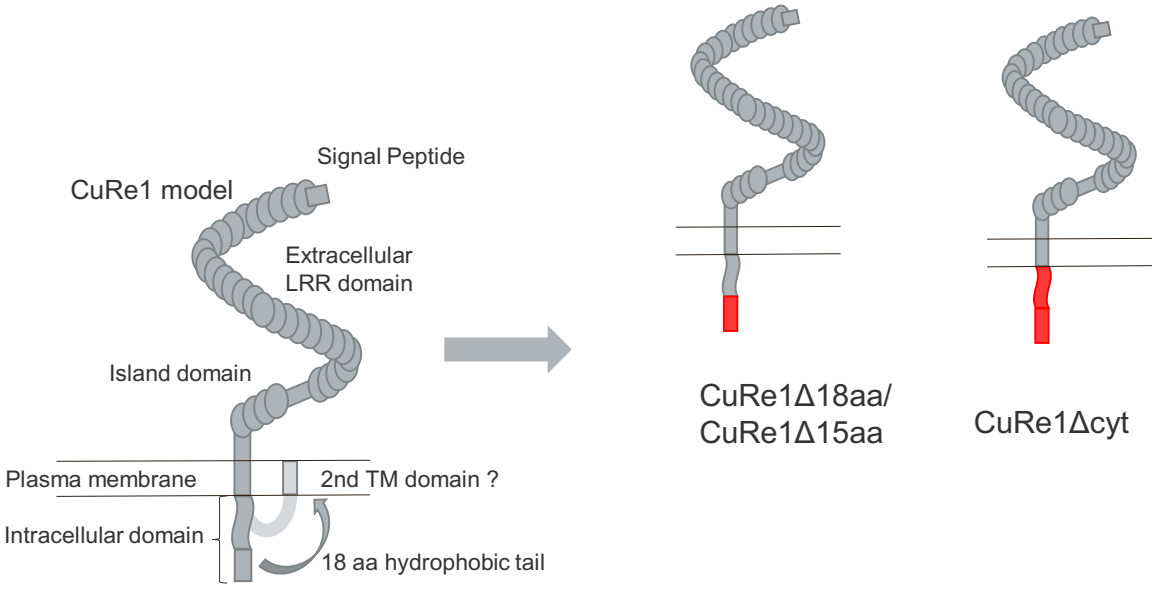

Figure 37 CuRe1 protein model (left) and C-terminal deletions (right).

CuRe1 extracellular domain consists of a C-terminal signal peptide and a LRR-N-terminal domain, followed by 35 LRRs interrupted by an island domain between the 31st and 32nd LRR. The transmembrane domain (TM) and the intracellular domain. The C-terminal intracellular domain consists of hydrophobic residues and might play a role in binding or as a 2nd transmembrane domain. The truncation of CuRe1 was performed by cutting 15/18 amino acids (aa) from the C-terminus (CuRe1Δ15aa/ CuRe1Δ18aa) or the whole cytosolic domain (CuRe1Δcyt) marked in red.

The hydrophobic tail is an obvious feature of CuRe1 and CuRe-likes, that seems to be absent in nearly all other LRR-RLPs (Fürst et al. 2016) (Figure 38).

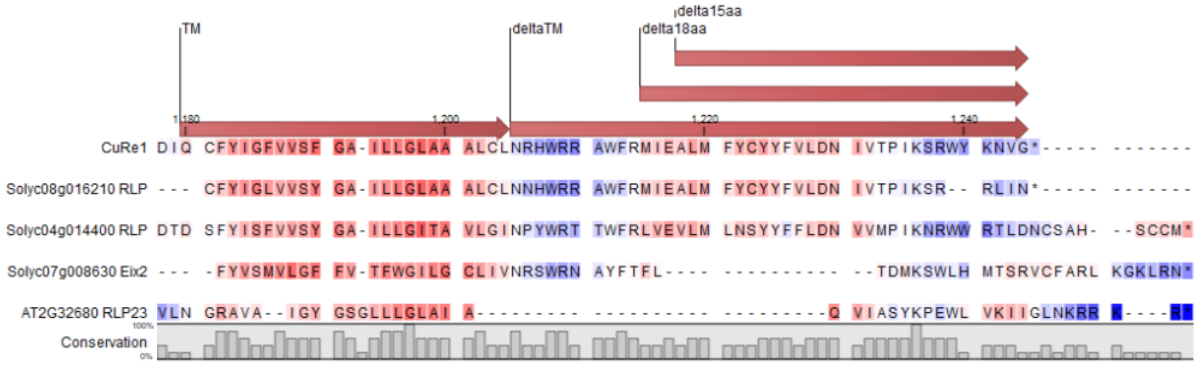

Figure 38 In silico analysis of CuRe1 and CuRe1-likes.

CuRe1 was aligned with CuRe1-likes (Solyc08g016210 and Solyc04g014400 share 64% - 81% amino acid identity (Fürst et al. 2016)). *S. lycopersicum* derived Eix2, a receptor for fungal Xylanase (Ron et al. 2004), as well as *A. thaliana* derived RLP23, a receptor for necrosis and ethylene-inducing peptide 1-like proteins from numerous bacterial, fungal, and oomycete (Albert I. et al. 2019), served as reference. The alignment is made with CLC Workbench using the Kyte-Doolittle amino acid annotation (window length: 9). Red color indicates hydrophobic residues. Eix2 and RLP23 lack the HT/ 2. TM.

3.1.1.1 Truncation of the hydrophobic tail of CuRe1 leads to reduced ethylene production

CuRe1 deletion constructs were transiently transformed in *N. benthamiana*, the transiently transformed leaves were used to perform Western Blot as well as an ethylene assay. The Western Blot suggest, that CuRe1 as well as CuRe1 deletions were expressed and detectable. Depending on the construct and the length of the deletion the ethylene production was reduced or absent (Figure 39).

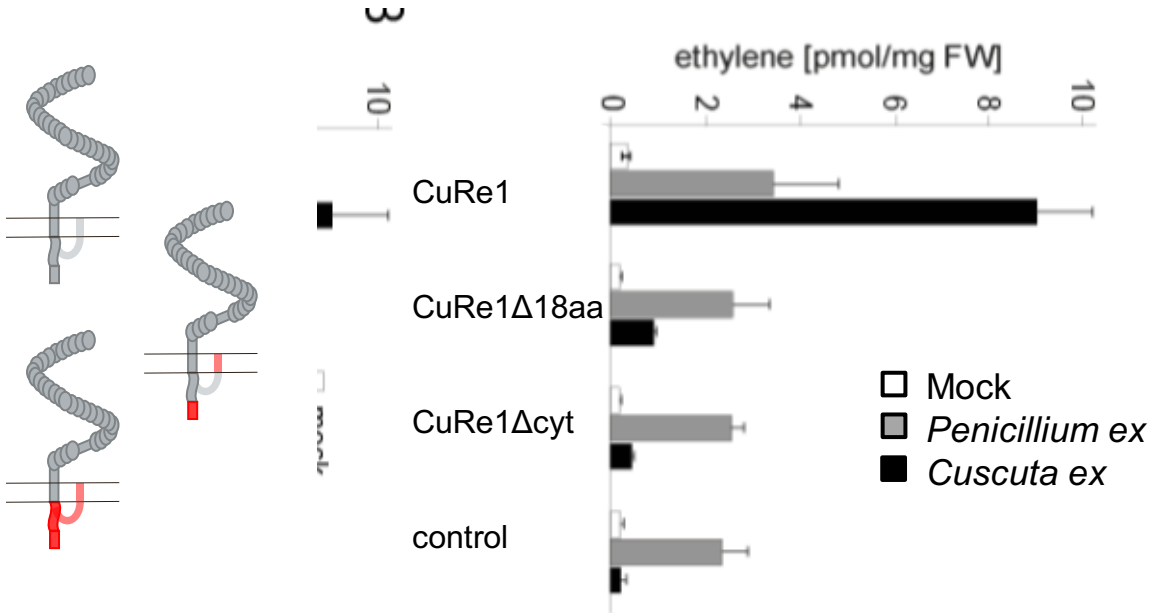

Figure 39 Ethylene production of truncated CuRe1's.

N. benthamiana leaves transiently expressing the full length CuRe1 or the C-terminal truncated CuRe1Δ18aa and CuRe1Δcyt were treated as indicated. The C-terminal truncated CuRe1Δ18aa and CuRe1Δcyt showed reduced

ethylene production after 3h hours of incubation with Cuscuta Extract. Bars represent ethylene production in pmol/mg fresh weight after 3 hours; whiskers are standard deviation.

3.1.1.2 Truncated CuRe1 does not interact with SOBIR1 in mass-spectrometry analysis

To get further insights in the interactome of CuRe1 and CuRe1 deletions the respective constructs were transiently transformed into *N. benthamiana*. The plants were then treated with *Cuscuta* Extract (pH adjusted with MES to pH 5.5) or MES (pH 5.5) as an additional control for any ligand dependent interactions. Immunoprecipitation was performed and sent to the Proteome-Center of Tübingen (PCT: core facility of the University of Tübingen and member of the Quantitative Biology Center Tübingen), where electron spray ionization liquid chromatography double mass spectrometry (ESI LC-MS/MS) was performed. The result was then screened for interacting proteins. One proven interactor of LRR-RLPs and CuRe1 is SOBIR1 (Hegenauer et al. 2016) which was detectable in a ligand independent manner for the full length CuRe1-GFP but turned out to be missing in all CuRe1 deletions independent of the treatment (Table 5).

Table 5 Detection of SOBIR1 via MS/MS with CuRe1, CuRe1Δ18aa and CuRe1Δcyt.

Detection of SOBIR1 via MS/MS				
Samples	Treatment	Intensity	iBAQ	Q-value
CuRe1-GFP	25mM MES	56221000	1606300	0
CuRe1-GFP	*Cuscuta* Extract	21099000	602840	0
CuRe1Δ18aa-GFP	25mM MES	0	0	0
CuRe1Δ18aa-GFP	*Cuscuta* Extract	0	0	0
CuRe1Δcyt-GFP	25mM MES	0	0	0
CuRe1Δcyt-GFP	*Cuscuta* Extract	0	0	0
P19	*Cuscuta* Extract	0	0	0

3.1.1.3 Interaction of SlSOBIR1 with CuRe1 truncations

To prove if there is a missing interaction between CuRe1 truncation and SlSOBIR1, a Co-IP followed by western blot analysis was performed. The Co-IP could not confirm the missing interaction and showed weak interaction between SlSOBIR1 and CuRe1 truncations which can be seen by weak signals on the western blots (Figure 40). Additionally, the Co-IP revealed strong variation in the expression pattern of the CuRe1 deletions (see input of MYC-tagged proteins in Figure 40) as well as changing expression strength (not shown in this work)

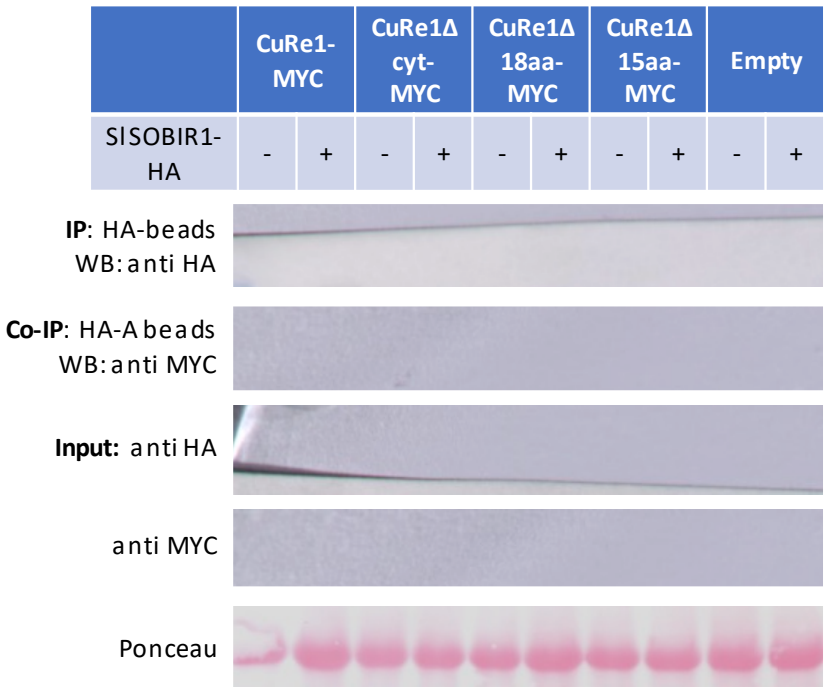

Figure 40 SlSOBIR1 forms a complex with CuRe1, but display variable interaction strength with CuRe1 truncations

Immunoblots of CuRe1Δcyt, CuRe1Δ18aa and CuRe1Δ15aa, co-immunoprecipitation with SlSOBIR1, pulldown at the C-terminal HA-tag of SlSOBIR1. Proteins were co-expressed in *N. benthamiana*. Input is sampled before adding IP-beads, equal load is shown by Ponceau S staining.

3.1.2 Truncation of the LRR-domain in addition to the hydrophobic tail

To make the expression of CuRe1 more stable the size of the whole protein was reduced by the deletion of the LRR domain. The main area of investigation, the hydrophobic tail, was additionally partially deleted. Full length CuRe1 has a size of approximately 160 kDa, with the deletion of the LRR the ΔLRRs were reduced to a size of approximately 20 kDa (Figure 41)

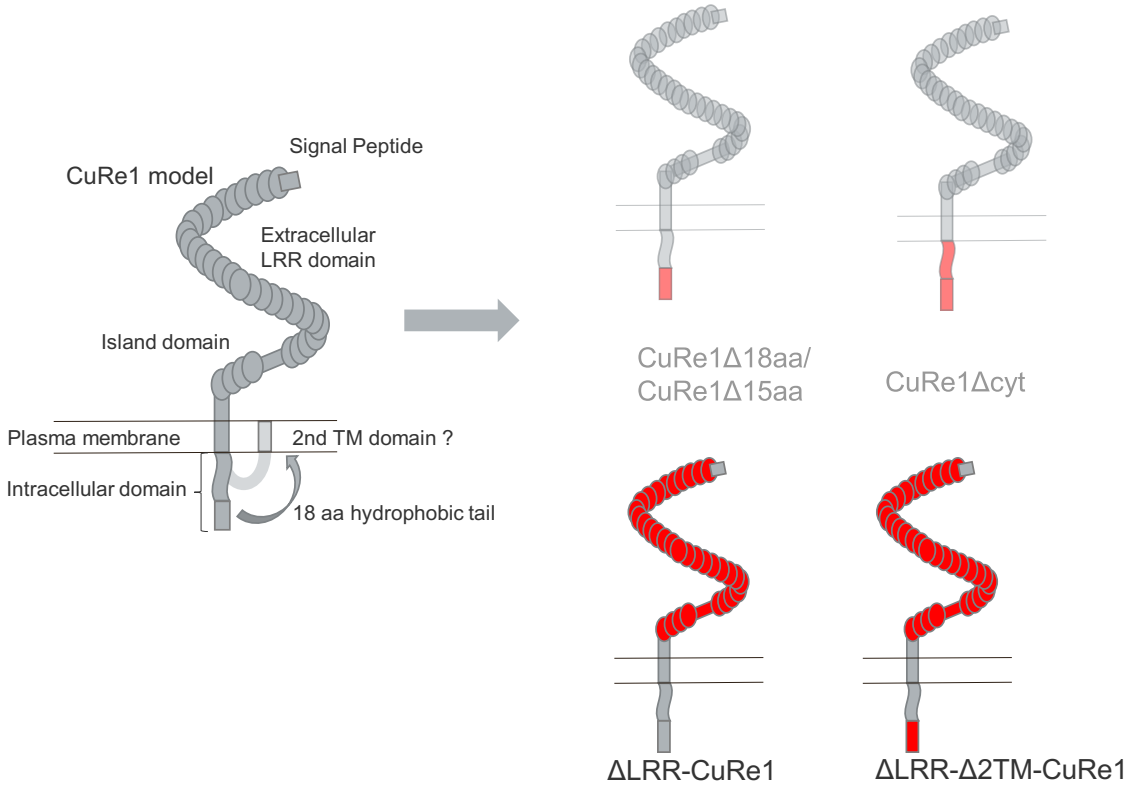

Figure 41 CuRe1 Structure and LRR deletion constructs.

The deletion constructs ΔLRR and ΔLRR-Δ2TM consist of the signal peptide directly followed by the transmembrane domain and the intracellular domain. ΔLRR has a full-length intracellular domain whereas ΔLRR-Δ2TM is missing the 2TM consisting of 18 hydrophobic amino acids. Red marks all deleted parts.

3.1.2.1 ΔLRR and ΔLRR-Δ2TM expression and ethylene production

Transient expression of the ΔLRR and ΔLRR-Δ2TM in *N. benthamiana* revealed a strong expression visible via fluorescence microscopy (Figure 42). Ethylene was measured to check for any auto activity (Figure 43).

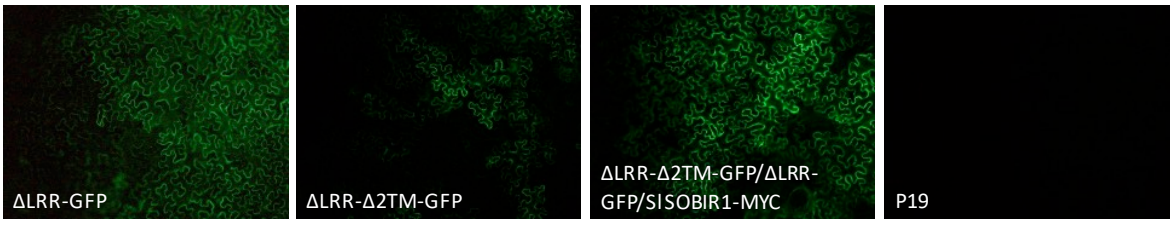

Figure 42 Fluorescence detection of the GFP tagged ΔLRR-GFP and ΔLRR-Δ2TM-GFP.

Transient expression in *N. benthamiana* was verified by fluorescence microscopy using the GFP-tag (488nm/ 507nm). Expression and co-expression as indicated.

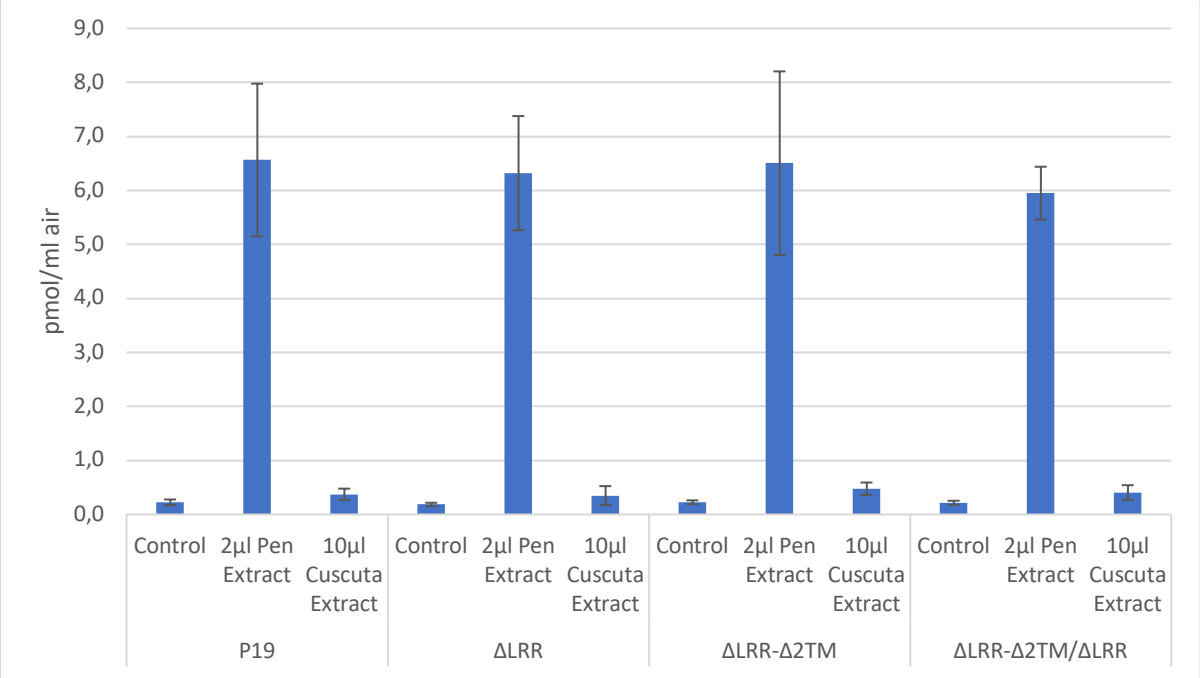

Figure 43 Ethylene production of *N. benthamiana* transiently expressing ΔLRR-GFP and ΔLRR-Δ2TM-GFP.

N. benthamiana leaf pieces were treated as indicated, mock is water, positive control is Penicillium Extract (Pen Extract). Bars represent pmol ethylene per ml air, ethylene was measured after 3 hours incubation, 1ml gas phase of a 6ml tube were measured, whiskers are standard deviation.

3.1.2.2 Interaction of ΔLRR and ΔLRR-Δ2TM with SlSOBIR1 via Co-IP and mass-spectrometry

The IP was performed against the MYC-tagged SlSOBIR1 with anti MYC-Agarose beads. ΔLRR-GFP and ΔLRR-Δ2TM-GFP then were detected with the Co-IP. Interaction of SlSOBIR1 was visible with ΔLRR-GFP and ΔLRR-Δ2TM-GFP alone as well as with the combination of both. All control lanes were empty and ponceau staining shows equal load (Figure 44).

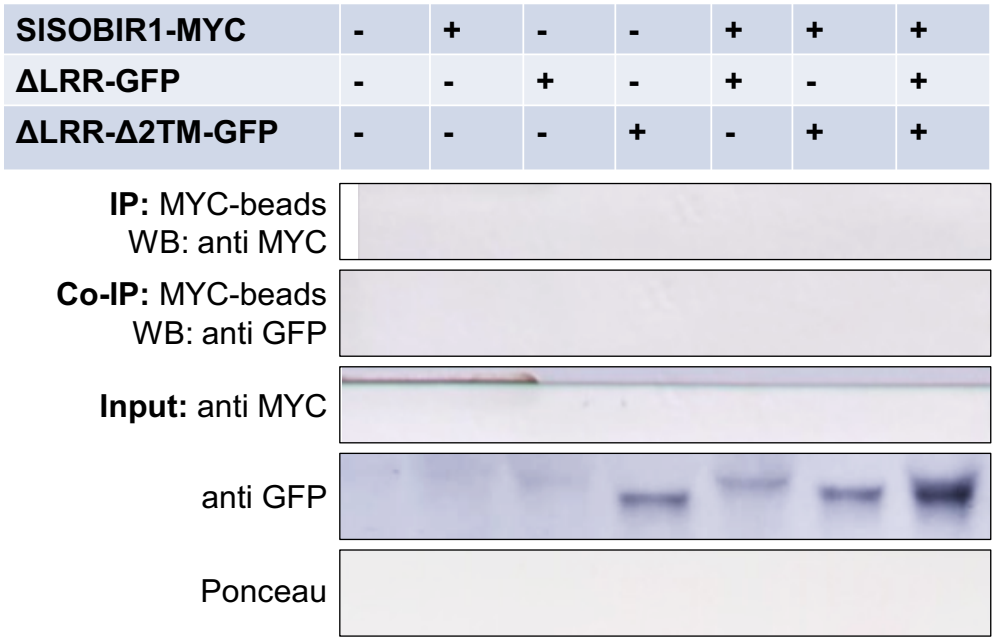

Figure 44 SlSOBIR1 forms a complex with ΔLRR-GFP and ΔLRR-Δ2TM-GFP.

Immunoblots of ΔLRR-GFP and ΔLRR-Δ2TM-GFP, co-immunoprecipitation with SlSOBIR1, pulldown at the C-terminal MYC-tag of SlSOBIR1. Proteins were co-expressed in *N. benthamiana*. Input is sampled before adding IP-beads, equal load is shown by Ponceau S staining.

Table 6 Detection of SOBIR1 via MS/MS with ΔLRR and ΔLRRΔ2TM

Detection of SOBIR1 via MS/MS							
	N. benthamiana		*N. sylvestris*		*N. attenuata*		
Samples	Intensity	iBAQ	Intensity	iBAQ	Intensity	iBAQ	Q-value
ΔLRR_GFP	6947600000	198500000	44391000	1268300	12221000	339470	0
ΔLRRΔ2TM-GFP	7469500000	213410000	42416000	1211900	27326000	759060	0
GFP-only	0	0	0	0	0	0	0

To prove if this interaction is detectable via MS/MS, immunoprecipitation was performed and sent to the Proteome-Center of Tübingen (PCT: core facility of the University of Tübingen and member of the Quantitative Biology Center Tübingen), where electron spray ionization liquid chromatography double mass spectrometry (ESI LC-MS/MS) was performed. The result is summarized in Table 6 and shows interaction of ΔLRR-GFP and ΔLRR-Δ2TM-GFP with SOBIR1. The MS/MS results were blasted against a database containing various solanaceous plants, therefore hits for SOBIR1 homologs origination from various *Nicotiana spp.* (*N. benthamiana, N. sylvestris, N. attenuata*) showed up in the analysis results (Table 6). Controls with GFP-only expressing *N. benthamiana* ended up empty and without unspecific binding.

3.1.2.3 ΔLRR does not interact with SlSERK3a/b

Since the ΔLRR-GFP constructs are strongly impaired it was important to exclude constitutive binding of SlSERKs to the short ΔLRR-GFP. Therefore, the ligand dependent interaction with SlSERK3a/b was used to check constitutive binding to ΔLRR-GFP (Figure 45). The ligand binding/ recognition and the resulting ethylene production are impaired due to the lack of the LRR-domain of CuRe1 (Figure 43).

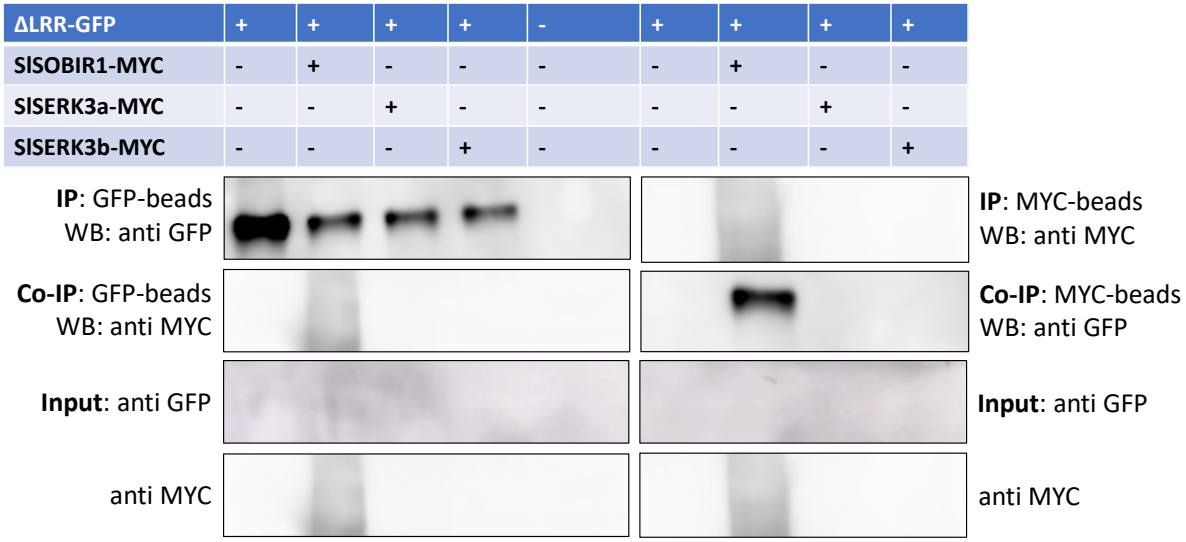

Figure 45 SlSERKs do not form a complex with ΔLRR-GFP.

Immunoblots of and SlSERKs and SlSOBIR1, co-immunoprecipitation with ΔLRR-GFP, pulldown at the C-terminal GFP-tag of ΔLRR-GFP. Proteins were co-expressed in *N. benthamiana*. Input is sampled before adding IP-beads, equal load is shown by Ponceau S staining.

3.2 Discussion

3.2.1 What is the role of the hydrophobic tail of CuRe1?

During the infection, *Cuscuta* spp. remain undetected by most plants. However, there is one host exception: the cultivated tomato *S. lycopersicum* can detect the *Cuscuta*-derived CrGRP or its minimal motif CrCrip21 by the tomato receptor protein CuRe1 (Hegenauer et al. 2020). CuRe1 was shown to interact with the Co-receptor SlSOBIR1 (Hegenauer et al. 2016) to induce immune responses in form of reactive oxygen species (ROS) and ethylene (Figure 5). One feature of CuRe1 and CuRe-likes is a hydrophobic stretch of amino acids at the C-terminal end that is absent in most other RLPs (Fritz-Laylin et al. 2005). The hydrophobic tail (HT) might act as secondary trans membrane domain (2.TM) or might serve as interaction domain for further downstream signaling components (Figure 38).

The aim was to determine the importance of the hydrophobic tail or 2. trans membrane domain (HT/ 2.TM) for functional CuRe1-initiated cellular signaling.

To determine the function of the HT/ 2. TM, three truncated versions of CuRe1 were created by deleting different parts of the HT/ 2.TM. The first two deletion constructs were relatively similar lacking 15 or 18 amino acids, respectively. The third construct lacks the full cytosolic domain (Figure 38). The initial experiment was performed by transiently expressing CuRe1Δ18aa and CuRe1Δcyt in *N. benthamiana* and measuring ethylene production after treatment with CrGRP containing Cuscuta Extract. The experiment showed a reduced or loss in ethylene production for CuRe1Δ18aa and CuRe1Δcyt, respectively. Based on these findings the hypothesis of a special role of the HT/ 2.TM was corroborated (Figure 39).

To investigate any difference of interaction partners between the truncated CuRe1 and the full length CuRe1 an IP followed by mass spectrometry analysis was performed (Table 5). Additionally, the interaction was investigated in context of the immunity inducing CuRe1 ligand CrGRP in the Cuscuta Extract. The mass spectrometry analysis revealed that the known interaction partner SlSOBIR1 was not detectable in the truncated samples CuRe1Δ18aa and CuRe1Δcyt. To confirm the findings of the mass spectrometry analysis, a Co-IP of SlSOBIR1 with the truncated and the full length CuRe1 was performed. Multiple Co-IPs revealed an extreme inconsistent expression of the different CuRe1 constructs which made it hard to get an equal expression and comparable results. Besides the inconsistent and unequal expression, the interaction with SlSOBIR1 was detectable in several experiments. The interaction was mostly weak but comparable to the expression level of CuRe1Δ18aa and CuRe1Δcyt (Figure 40).

The results left an inconclusive picture of the importance of the HT/ 2. TM, therefore, a new strategy was necessary.

3.2.2 Truncation of the LRR-domain in addition to the hydrophobic tail

The N-glycosylation of the LRR-domain, the size of CuRe1 of about 180kDa including a GFP-tag could influence the efficiency of transient expression in *N. benthamiana.* CuRe1 versions were c-terminally coupled to GFP to check for expression via fluorescence microscopy but all CuRe1-GFP versions were only barely visible or not detectable at all, which was underlined by the low expression levels when performing the IP. The main focus was still on the HT/ 2. TM., therefore, cloning a variant missing the HT/ 2. TM and the extracellular LRR-domain appeared to be the solution. The newly designed CuRe1 versions still contained the N-terminal signal peptide but lacked all 35 LRRs including the island domain but still contained the extracellular juxtamembrane region starting after the last LRR, the trans membrane domain and the intracellular domain. The variant with the full-length intracellular domain and therefore including the HT/ 2. TM domain was termed ΔLRR-CuRe1, the variant that lost the HT/

2.TM was termed ΔLRR-Δ2TM-CuRe1 (Figure 41). ΔLRR-CuRe1 and ΔLRR-Δ2TM-CuRe1 were transiently transformed into *N. benthamiana* and the expression was analyzed by detecting the GFP-tag visible as green fluorescence (Figure 42). Additionally, the transiently transformed *N. benthamiana* were used for an ethylene measurement and clearly showed that ΔLRR-CuRe1 and ΔLRR-Δ2TM-CuRe1 were not able to detect Cuscuta Extracts and initiate the ethylene production (Figure 43). Additionally, both constructs did not act in an auto active manner which became visible in background measurements. To determine if the SlSOBIR1 binding is influenced by the HT/ 2.TM, Co-IP was performed to investigate any interaction between SlSOBIR1, ΔLRR-CuRe1 and ΔLRR-Δ2TM-CuRe1. The Co-IP clearly showed the interaction of SlSOBIR1 with both variants ΔLRR-CuRe1 and ΔLRR-Δ2TM-CuRe1. In addition, SlSOBIR1 showed no preference for one or the other construct which is visible in the band intensity during the expression of SlSOBIR1, ΔLRR-CuRe1 and ΔLRR-Δ2TM-CuRe1 at the same time (Figure 44). An IP was performed and sent for mass spectrometry analyses to investigate the interaction partners of the novel ΔLRR-CuRe1 and ΔLRR-Δ2TM-CuRe1 versions. The obtained sequence data were blasted against several Solanaceous plants and SlSOBIR1 could be detected multiple times with a high intensity. The approach to investigate the interactions of ΔLRR-CuRe1 and ΔLRR-Δ2TM-CuRe1 turned out to be very successful. All experiments show a high expression ratio of the ΔLRR truncated CuRe1 constructs, starting with the detectability with the fluorescence microscope, to the strong expression in the IP that is supported by a 100-fold higher intensity in the mass spectrometry analysis by comparison with the full length CuRe1 constructs (Table 6). The additional experimental approach co-expressing SlSERK3a and SlSERK3b shows that no constitutive binding of ΔLRR-CuRe1 to the Co-Receptor takes place which confirmed the ethylene measurement that did not show a constitutively increased background ethylene level. The lack of ethylene production of ΔLRR-CuRe1 and ΔLRR-Δ2TM-CuRe1 after treatment with CrGRP containing extract as well as the lack of interaction with SlSERK3a and SlSERK3b despite the fully functional interaction with SlSOBIR1 leads to the conclusion that the ligand recognition must be impaired due to the lack of the LRR-domain (Figure 45).

These results lead to the conclusion that the initially expected loss of CuRe1 function in diverse deletion constructs displayed by the loss in ethylene production might be due to extreme low expression of CuRe1Δ18aa and CuRe1Δcyt. This would explain why no ethylene was detectable and in addition the loss of a detectable interaction in a mass spectrometry screen. Even with the low expression of CuRe1Δ18aa and CuRe1Δcyt it was possible to sometimes detect a weak interaction with SlSOBIR1 via Co-IP, which is in accordance with the interaction pattern of ΔLRR-CuRe1 and ΔLRR-Δ2TM-CuRe1. As shown for the interaction between *At*RLP23 and *At*SOBIR1 mainly the transmembrane or the juxtamembrane regions are necessary for the interaction of both proteins

(Albert et al. 2019). ΔLRR-CuRe1 and ΔLRR-Δ2TM-CuRe1 interact with SlSOBIR1 with a similar affinity which could be explained by the untouched outer juxtamembrane that was proposed to contribute by an electrostatic interaction (Gust and Felix 2014). Additionally, does the HT/ 2. TM. lack the GxxxGxxxG interaction motive that was shown to be necessary for the interaction *At*RLP23 and *At*SOBIR1 and others (Albert et al. 2019, Bi et al.2016). Since ΔLRR-CuRe1 and ΔLRR-Δ2TM-CuRe1 are lacking the extracellular LRR they might be not able to sense their ligand, initiate the SlSERK3a/b binding and therefore cannot induce downstream signaling (Smakowska-Luzan et al. 2018). The established ΔLRR-CuRe1 and ΔLRR-Δ2TM-CuRe1 variants still present an easy tool to investigate the role of the HT/ 2. TM.

3.2.3 "Back to the Future": What is the role of the hydrophobic tail of CuRe1?

The answer to one of our main research question remains in the dark: What is the function of the HT/ 2. TM? With the work on the ΔLRR-CuRe1 and ΔLRR-Δ2TM-CuRe1 variants this question might be answered in the future. The mass spectrometry analysis may serve as cornerstone for forthcoming research. Based on the mass spectrometry analysis, other possible interactors can be screened and tested. During this quest it is important to keep in mind that the mass spectrometry analysis only shows ligand independent interactions, no LRR means no ligand binding and therefore no Co-receptor recruitment.

Promising candidates might shed light on the interactome of CuRe1 and how it is connected to intriguing pathways to fend of *Cuscuta* spp. infection.

4 Material and Methods

4.1 Material

4.1.1 Peptides

Table 7: Peptide names and sequences (o: Hydroxyproline)

Symbol	Name	Sequence	Source
flg22	flg22	QRLSTGSRINSAKDDAAGLQIA	Felix et al. 1999
CrCrip21	CrCrip21	NCGNSGCCGGAYSNGQCKRCC	Hegenauer et al. 2020
CcCle1	Cc026640	RLVoSGoNPLHN	this work
CcCle2	Cc045050	RRVoSCoDPLHN	this work
CcCle3	Cc019175	RTVoKGoDPIHN	this work
CcCle4	Cc033921	RKVoNGoDPVHN	this work
CcCle5	Cc000094	KVVoGGoNPLHN	this work
CcCle6	Cc002183	RQSoGGoDPHHH	this work
CcCle7	Cc016733	RKILQGSDKDHN	this work
CaCle8	C011N0450E0	RRVRTGoNPLHN	this work
CaCle9	C018N0374E0	RRVoSCoDPLHN	this work
CaCle10	C018N0193E0	RKVoNGoDPVHN	this work
CaCle11	C019N0006E0	KVVoGGoNPLHN	this work
CaCle12	C023N0117E0	RVSoGGoDPHHH	this work
CaCle13	C061N0101E0	RTAoGGoDGQHH	this work
CaCle14	C097N0060M0	RKVSKGSDPIHN	this work

o: Hydroxyproline

4.1.2 Media and Antibiotics

Table 8: Media

Medium	Components
LB liquid/ LB solid	10 g/l Bacto-Tryptone, 5 g/l Bacto-Yeast extract, 5 g/l NaCl, to solidify add 15 g/l Agar
SOC	2.0 g/l Tryptone, 0.5 g/l Yeast extract, 10 mM NaCl, 2.5 mM KCl, 10 mM $MgCl_2$, 10 mM $MgSO_4$, 20 mM Glucose, set pH 7 with NaOH

Table 9: Antibiotics

Antibiotic	Stock	Final Concentration	Solvent
Kanamycin	50 mg/ml	50 µg/ml	H2O
Gentamycin	40 mg/ml	40 µg/ml	H2O
Spectinomycin	100 mg/ml	100 µg/ml	H2O
Rifampicin	50 mg/ml	100 µg/ml	DMSO

4.1.3 Bacterial strains

The Escherichia coli strain DH5α/ XL1-Blue were used for cloning experiments and amplification in Gate Way vectors, DH10B was used for all Golden Gate Cloning and amplifications. The Agrobacterium strain GV3101 was used for transient and stable expression in *Nicotiana benthamiana* and *Arabidopsis thaliana.*

Table 10: Bacterial strains and genotypes

Type	Strain	Genotype
Escherichia coli	DH5α	fhuA2 lac(del)U169 phoA glnV44 Φ80' lacZ(del)M15 gyrA96 recA1 relA1 endA1 thi-1 hsdR17
Escherichia coli	XL1-Blue	recA1 endA1 gyrA96 thi-1 hsdR17 supE44 relA1 lac [F´ proABlacIqZΔM15 Tn10 (Tetr)]
Escherichia coli	DH10B	F^- mcrA Δ(*mrr-hsd*RMS-*mcr*BC) Φ80d*lac*ZΔM15 Δ*lac*X74 *end*A1 *rec*A1 *deo*R Δ(*ara*,*leu*)7697 *ara*D139 *gal*U *gal*K *nup*G *rps*L λ^-
Agrobacterium thumefaciens	GV3101	T-DNA- vir+ rifr, pMP90 genr

4.1.4 Plasmid lists

Table 11: Entry and Donor Vectors

Insert	Reporter Gene	Source
p19	-	Voinnet et al. 2003
Empty pENTR-BsaI	-	Binder et al. 2014
Empty pBGWL7	luciferase	Karimi et al. 2005
Empty pB7FWG2.0	GFP	Karimi et al. 2002
Empty pGWB17	MYC	Nakagawa et al. 2007
Empty pGWB14	HA	Nakagawa et al. 2007
Empty pB7WGF2.0	GFP only	Karimi et al. 2002

Table 12: Constructs for the bioassay. All promoters were cloned in pBGWL7

		based on RNA analysis			
Locus ID	Abbreviation	Arabidopsis Name	Cloned/ Tested	Activity	Source
AT1G17240	RLP2	RECEPTOR LIKE PROTEIN 2	Yes	No	Körner 2016
AT5G25610	RD22	RESPONSIVE TO DESICCATION 22	Yes	No	Körner 2016
AT1G11650	RBP45B	RBP45B	Yes	Yes	Körner 2016

AT1G55 020	LOX1	LIPOXYGENASE 1	Yes	No	Körner 2016
AT4G40 060	HB16	HOMEOBOX PROTEIN 16	Yes	No	Körner 2016
AT4G30 960	SIP3	SNF1-RELATED PROTEIN KINASE 3	No	No	Körner 2016
AT5G26 340	STP13	SUGAR TRANSPORT PROTEIN 13	No	No	Körner 2016
AT1G28 110	SCPL45	SERINE CARBOXYPEPTIDASE-LIKE 45	Yes	No	Körner 2016
AT4G34 138	UGT73B1	UDP-GLUCOSYL TRANSFERASE 73B1	No	No	Körner 2016
AT1G49 820	MTK	5-METHYLTHIORIBOSE KINASE 1,	Yes	Yes	Körner 2016
AT5G04 040	SDP1	SUGAR-DEPENDENT1	Yes	No	this work
AT1G09 380	UMAMIT 25	USUALLY MULTIPLE ACIDS MOVE IN AND OUT TRANSPORTERS 25	Yes	Yes	this work
AT4G11 650	OSM34	OSMOTIN 34	Yes	No	this work
AT5G18 030	SAUR21	SMALL AUXIN UP RNA 21	Yes	No	this work
AT3G49 940	LBD38	LOB DOMAIN-CONTAINING PROTEIN 38	Yes	No	this work
AT2G13 610	ABCG5	ATP-BINDING CASSETTE G5	No	No	this work
AT3G03 770	LRR protein kinase	Leucine-rich repeat protein kinase family	No	No	this work
AT1G33 811	GGL7	Guard-cell-enriched GDSL Lipases	Yes	No	this work
AT2G38 530	CDF3, LTP2	CELL GROWTH DEFECT FACTOR-3, LIPID TRANSFER PROTEIN 2	No	No	this work
AT2G01 860	EMB975	EMBRYO DEFECTIVE 975	Yes	No	this work
AT2G19 190	FRK1	FLG22-INDUCED RECEPTOR-LIKE KINASE 1	Yes	No	this work based on Asai et al. 2002
AT4G03 230	G-LecRK	G-type lectin receptor kinase	Yes	No	this work
		Special Interest			
AT1G22 710	SUC2, SUT1	SUCROSE-PROTON SYMPORTER 2, SUCROSE TRANSPORTER 1	Yes	Yes	this work based on Hartenstein 2021
AT5G50 790	SWEET10	SUGARS WILL EVENTUALLY BE EXPORTED TRANSPORTERS 10	Yes	Yes	Klatt 2021
Solyc08g 078020	attAGP	attachment METHIONINE RICH ARABINOGALACTAN	Yes	Yes	this work based on Albert 2005

Table 13: Constructs for the analysis of the hydrophobic tail of CuRe1

Insert	Vector	Reporter Gene	Source

CuRe1	pB7FWG2.0	GFP	Hegenauer et al. 2016
CuRe1Δcyt	pB7FWG2.0	GFP	this work
CuRe1Δ18aa	pB7FWG2.0	GFP	this work
CuRe1	pGWB17	MYC	Hegenauer et al. 2016
CuRe1Δcyt	pGWB17	MYC	this work
CuRe1Δ18aa	pGWB17	MYC	this work
CuRe1Δ15aa	pGWB17	MYC	this work
CuRe1	pGWB14	HA	this work
CuRe1Δcyt	pGWB14	HA	this work
CuRe1Δ18aa	pGWB14	HA	this work
CuRe1Δ15aa	pGWB14	HA	this work
ΔLRR-CuRe	pB7FWG2.0	GFP	this work
ΔLRR-Δ2TM-CuRe	pB7FWG2.0	GFP	this work
Solanum lycopersicum (Sl) SOBIR1	pGWB14	HA	Liebrand et al. 2013
*Sl*SOBIR1	pGWB17	MYC	Liebrand et al. 2013
*Sl*SERK3a	pGWB17	MYC	Wang et al. 2016
*Sl*SERK3b	pGWB17	MYC	Wang et al. 2016

4.1.5 Oligonucleotide list

For cloning with commercial Gate Way cloning kits oligos were designed following the manufacturer instructions (Thermo Fischer Scientific manuals for K240020 and K250020). For cloning into pENTR-BsaI Golden Gate compatible oligos were designed, in the following lists marked with GG.

Table 14: Oligonucleotides for promoter cloning

Name	Sequence	Note
AT1G17240_P1	CATAGCAAGGAGAAGAAC	RLP2
AT1G17240_P2	ACAACACTGAGATAGAGG	
AT5G25610_P1	GGGAGTTGGAATAGAAATG	RD22
AT5G25610_P2	TGGTGAGCCATAAATGAG	
AT1G11650_P1	CGGAGAATAAGATAGAGAG	RBP45B
AT1G11650_P2	AAGCTTAACCTGATGGAC	
AT1G55020_P1	TGGGTGAAGTTGAAGTTTTG	LOX1
AT1G55020_P2	TGCTACAACTATCCCCGA	
AT4G40060_P1	AGTTCTACTCCAGCTTTTTC	HB16
AT4G40060_P2	CAATGGGTTTTGATTCGG	
AT4G30960_P1	GAAGAATTCGAGAGACGA	SIP3
AT4G30960_P2	GAGAATCTTCAGCAAACC	
AT5G26340_P1	AGAGAAGTTGAGGTAGTGAAG	STP13
AT5G26340_P2	TATATGGGGTGTTTTTAGGG	
AT1G28110_P1	GAAGAAGTGAAGAGGAGA	SCPL45
AT1G28110_P2	ATAGGAGCAAAACGAAGC	
AT4G34138_P1	TCCTGGTTTTTGTAGAGC	UGT73B1

AT4G34138_P2	TTCCTCAGCATCATCATC	
AT1G49820_P1	CTTCTCTGCTTCAGTTTC	MTK
AT1G49820_P2	CCAACTCCAAATACAAGC	
AT5G04040 (2077bp)	CGAAGATGAATTTGGGTG	SDP1
P2	TGAACAGTGATATGCGGC	
AT1G09380 (2010bp)	CTCCAAAATATGCCTCTC	(WAT1-like), UMAMIT25
P2	TAAAAATCACCGGCGGAA	
AT4G11650 (1831bp)	CATTTTAATAGGTTGGGGCG	OSM34
P2	ACTAGGATGTATGTGTGC	
AT5G18030 (2036bp)	TTGCTTGTTGTTGGTTGATG	SAUR21
P2	CTTGAAATGAAGGCTGGT	
AT3G49940 (2035bp)	GGTACAAGAAAGAGAAAGAG	LBD38
P2	TATCCCAATTAACAGCCC	
AT2G13610 (1974bp)	TTTGGAATCTTTAGGCGG	ABCG5
P2	TTCTTTCACATCTTCGGTTG	
AT3G03770 (2041bp)	AGCCACACAAGACCATAA	Leucine-rich repeat protein kinase family protein
P2	CCAGGTGGACTAAAATTTC	
AT1G33811 (2027bp)	GATTTGAGTGGAGTTCATAG	GDSL
P2	TGGTTTCGTTATTGGGTG	
AT2G38530 (2026bp)	TACGTTGGTTTGCAAGAG	CDF3, LTP2
P2	TTGATTACATTCTCGGGG	
AT2G01860 (2054bp)	AAACACACGAAGTTACGG	EMB975
P2	GGGACGATCTTTTTGTTG	
AT4G03230_P1	CTCAACTCAAAACGTGTC	G-type lectin S-receptor-like Serine/Threonine-kinase
AT4G03230_P2	CACCACCGGAACATGGGAAATA	
pFRK1 REV	GGAGTTATTGAGCTGCTTTCTC	FRK1
pFRK1 new FW	CACCCTGACAGTGAACTTCATTGTTCAA	
AtSUC2_FW1	ccGGTCTCtCACCGCATGCAAAATAGCACACCA	SUC2, GG
AtSUC2_Rev1	ccGGTCTCtCCTTATTTGACAAACCAAGAAAGTAAG AAAAA	GG

Table 15: Oligonucleotides for sequencing

Name	Sequence	Note
Primer_GFP	GACAACCACTACCTGAGCA	

Primer_BASTA	TCGATGTAGTGGTTGACG	
CuRe_seq568	GAACTCTGGTTTGAAGGCTATG	
CuRe_seq1311	GTACTTGGATATTGCGGATAACC	
CuRe_seq2083	CCAGGATGCACTAGGGATAACAG	
CuRe_seq2631	GCATTATCACGATAGTCATGGAC	
CuRe_seq2967	GGCAGTATTCAGTGTTGCATAC	
Gene Specific Basta II	ATGCCGGTCGATCTAGTAACA	
Gene Specific 35S II	TAGAGCCAAGCTGATCTCCTTTG	
M13 rev	CAGGAAACAGCTATGAC	
M13_fw	GTAAAACGACGGCCAG	
CuRe c-DNAseq B	CGATCGCGTATTTCGTCTCGC	
CuRe cDNA Seq A	CCTAAATTGTCAAATACCTCC	
CuRe1_cDNA-rev	AGTGACGAAAAGATGGTG	
GFP seq in T35S	CACTGGATTTTGGTTTTAGG	
Seq_pGWB_rev	CCAAGAAAGCCTCCTCATCTC	

Table 16: Oligonucleotides for genotyping

Name	Sequence	Note
Basta geno primer FW	ATGAGCCCAGAACGACGCC	
Basta geno primer Rev	ATCTCGGTGACGGGCAGGAC	

Table 17: Oligonucleotides for qRT-PCR

Name	Sequence	Note
LUC FW	CACATCTCATCTACCTCCCG	
LUC REV	GTGAGCCCATATCCTTGTCG	

Table 18: Oligonucleotides for CuRe deletion project

Name	Sequence	Note
CuRe_gDNA_FW_1	ccGGTCTCtCACCATGGGGAATATTAAGTTTTTGTTGTTAGT	GG
CuRe_gDNA_REV_3	ccGGTCTCtCCTTACCAACATTCTTGTACCATCTACT	GG
CuRe_deltaLRR_FW_2	ccGGTCTCtAGGTCAATTTGGAACTTTCAACAAAAGCA	GG
CuRe_deltaLRR_REV_1	ccGGTCTCtACCTGTTTCTAAGCTGCATTTTAC	GG
CuRe_deltaLRR_delta2TM_REV_1	ccGGTCTCtCCTTCTCTATCATCCTAAACCATGCTCT	GG
CuRE1-bef2TM-altern	CCTAAACCATGCTCTTCTCCAATG	
CuRe1-TM-rev	CAAGCAGAGCGCTGCAGCTAATCC	
cuRe1_FW	CACCATGGGGAATATTAAGTTTTTG	

CuRe1_before2TM_REV	CTCTATCATCCTAAACCATGC	
CuRe1_Rev	ACCAACATTCTTGTACCATCTAC	

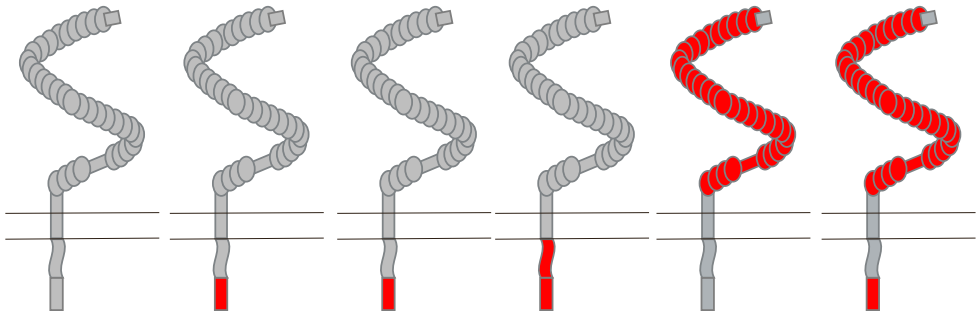

	CuRe1	CuRe1Δ18aa	CuRe1Δ15aa	CuRe1Δcyt	ΔLRR-CuRe1	ΔLRR-Δ2TM-CuRe1
Forward 1	CuRe1_FW	CuRe1_FW	CuRe1_FW	CuRe1_FW	CuRe_gDNA_FW_1	CuRe_gDNA_FW_1
Reverse 1	CuRe1_ Rev	CuRE1-bef2TM-altern	CuRe1_before2TM_REV	CuRe1-TM-rev	CuRe_deltaLRR_REV_1	CuRe_deltaLRR_REV_1
Forward 2					CuRe_deltaLRR_FW_2	CuRe_deltaLRR_FW_2
Reverse 2					CuRe_gDNA_REV_3	CuRe_deltaLRR_delta2TM_REV_1

Figure 46 Full length CuRe1 and deletion variants were cloned by using the described oligo pairs. For Golden Gate constructs multiple fragments were used (5'-3' numbered)

4.1.6 Antibodies

The antibodies were ordered from the respective companies. The antibodies were diluted in 1x PBS-T with 5% milk powder. Incubation of first antibodies was performed at 4°C over night. Secondary antibodies were incubated for 1-2 hours at room temperature.

Table 19: Primary antibodies

Primary Antibody	Origin	Use	Provider
α-GFP	goat	1:5000	Acris
α-MYC	rabbit	1:5000	Sigma-Aldrich
α-HA	mouse	1:5000	Sigma-Aldrich

Table 20: Secondary antibodies

Secondary Antibody	Conjugate amplifier	Use	Provider

α-goat IgG	AP	1:50000	Sigma-Aldrich
α-rabbit IgG	AP	1:50000	Sigma-Aldrich
α-mouse IgG	AP	1:50000	Sigma-Aldrich

4.1.7 Plant genotypes

Table 21: Plant genotypes

Genotype	Mutation	Source
Arabidopsis thaliana	Col-0	
Nicotiana benthamiana	CuRe1	Hegenauer et al 2016
Nicotiana benthamiana	Wild type	
Cuscuta reflexa	Wild type	

4.1.8 Chemicals and Consumables

All chemicals and expendable materials are from Carl Roth GmbH + Co. KG (Karlsruhe, Germany), Thermo Fischer Scientific (Karlsruhe, Germany), Greiner Bio-One (Frickenhausen, Germany), Eppendorf AG (Hamburg, Germany), Sarstedt AG & Co. KG (Nübrecht, Germany), Duran Group GmbH (Wertheim/Main, Germany), Qiagen (Hilden, Germany), Merck KGaA (Darmstadt, Germany), NEB Biolabs (Frankfurt am Main, Germany), D-Luciferin p.a. free acid (Art. Nr.: 102113): PJK GmbH (Kleinbittersdorf, Germany), Sigma-Aldrich (see Merck)

4.1.9 Purification Columns and Buffers

Table 22 Columns and Buffers used for FPLC purification

Method	Column	Running Buffer/ Elution Buffer	Activity
Ion exchange	HiTrap SP-FF 5ml *	25mM MES (pH 5,5)/ 500mM KCl	flow through
	HiTrap Q-FF 5ml *	25mM TRIS-HCl (pH 8,5)/ 500mM NaCl	flow through
		25mM MES (pH 5,5)/ 500mM KCl	
Reversed Phase	C4 (no brand)	0.1% formic acid (pH 2,7)/ Acetonitrile	flow through or lost
	Supelcosil LC-18 HPLC *	25mM MES (pH 5,5)/ MeOH	
	Resource 15 RPC	25mM MES (pH 5,5)/ Acetonitrile	
		100mM TRIS (pH 10,2)/ Acetonitrile	
Gel Filtration	Hi Load 26/600 Superdex 30pg	without buffer (water)	

		0.1% formic acid (pH 2.7); 100mM KCl	elution at half column volume ~5kDa
		25mM MES (pH 5,5); 100mM KCl	
		25mM Ammonium acetate (pH 6.5); 100mM KCl	
Hydrophobic Interaction	HiTrap Phenyl FF	3M Ammonium sulfate/ 50mM $MgSO_4$	
Various	XAD16N *	25mM MES (pH 5,5)/ MeOH	flow through and 1A2
	Concanavalin A	50mM Na-Acetate, 200mM NaCl, 1mM CaCl2, pH5.3/ 100mM α-Metylglucopyranoside	flow through
	GeneMatrix Universal RNA binding column	100µl DNA Binding Buffer+ 100µl Cuscuta Extrakt / 70% EtOH/ water	flow through
	Ethyl acetate	Ethyl acetate - Cuscuta Extract (1:1)	aqueous phase
	Ammonium sulfate *	0,6g/ml	precipitated

* shown in this work

4.2 Methods

4.2.1 DNA-Analysis

4.2.1.1 Plant genomic DNA preparation

A simple and rapid method for preparation of plant genomic DNA for PCR analysis (Edwards et al. 1991)

4.2.1.2 Plant RNA preparation

RNA was prepared following the instructions of the RNeasy Plant Mini Kit (Qiagen ID: 74904) the optional On-Column DNase digest was performed as described with the RNAse-Free DNase Set (Qiagen ID: 79254).

4.2.1.3 cDNA preperation

cDNA was prepared following the instructions of the RevertAid First Strand cDNA Synthesis Kit (ThermoFisher Scientific: K1622).

4.2.1.4 Quantitative Real-Time PCR (qRT-PCR)

Analysis of gene expression on transcript level was performed by qRT-PCR. A fluorescent dye binds to the double stranded DNA and with an increase in amplicon number during PCR, fluorescence intensity

increases. The released fluorescence is directly proportional to the amount of amplified nucleic acid. If the sample has a high number of transcribed gene copies, fluorescence will appear earlier during the PCR. The cycle at which the fluorescence can be detected first is termed as Quantitation cycle (Cq) or Threshold cycle (Ct) and is used for the calculation of transcript levels. Transcript levels of genes of interest (GOIs) are always calculated relative to reference genes (also called housekeeping genes).

Maxima™ SYBR™ Green/ROX 2x qPCR Master Mix (Thermo Fisher Scientific, Waltham, Massachusetts) was used for qRT-PCR in combination with gene specific primers. The binding specificity of the primers was always checked by BLAST search on NCBI, efficiency was tested and exclusivity of binding was analyzed via melting curve. For this work a qRT-PCR instrument (Rotor-Gene Q) from Qiagen was used. Data evaluation was done with Rotor Gene Q Series Software.

Target genes were normalized against a reference gene. The mean value of technical triplicates per sample was calculated and used for analyzing the relative expression of a gene in the sample. The negative potency of the ΔCt-value was finally calculated for more accuracy for gene expression.

4.2.1.5 Phusion PCR

The high fidelity Phusion polymerase offers high speed and a proofreading function. For one PCR reaction 0.2µL Phusion polymerase, 5µL 5x HF-Buffer were used. Per reaction 1µL forward (10mM), 1µL reverse oligonucleotides (10mM) and 1.5µL dNTP-mix (2.5mM each) were added. As template 15-20ng/µL gDNA were used. The reaction volume of 25µL was obtained with double distilled milli-Q water. The thermocycler program started with a
denaturation step (98°C, 7min), the cycle (34 repetitions) started with the denaturation (98°C, 30s), followed by the annealing (x°C (temperature depending on oligonucleotide characteristics), 30s) and the elongation (72°C, 30s/kb). The final elongation step (72°C, 4min) was followed by the storage step at 12°C.

4.2.1.6 Colony PCR

The colony PCR was used for direct amplification of cloned DNA from bacteria. Colonies were picked with a tip and mixed with the PCR reaction mix. For one PCR reaction 0.1µL taq polymerase, 2µL 10x taq-Buffer was used. Per reaction 1µL forward, 1µL reverse oligonucleotide (10mM each) and 1.5µL dNTP-mix (2.5mM each) was added. The reaction volume of 20µL was obtained with double distilled milli-Q water. The thermocycler program started with a denaturation step (94°C, 5min), the cycle (34 repetitions) started with the denaturation (94°C, 30s), followed by the annealing (x°C (temperature

depending on oligonucleotide characteristics), 30s) and the elongation (72°C, 60s/kb). The final elongation step (72°C, 4min) was followed by the storage step at 12°C.

4.2.1.7 Taq PCR

The taq polymerase was homemade and was used for genotyping. For one PCR reaction 0.1µL taq polymerase, 2µL 10x taq-Buffer was used. Per reaction 1µL forward, 1µL reverse oligonucleotide (10mM each) and 1.5µL dNTP-mix (2.5mM each) was added. As template 2µL gDNA were used. The reaction volume of 20µL was obtained with double distilled milli-Q water. The thermocycler program started with a denaturation step (94°C, 5min), the cycle (30 repetitions) started with the denaturation (94°C, 30s), followed by the annealing (x°C (temperature depending on oligonucleotide characteristics), 30s) and the elongation (72°C, 60s/kb). The final elongation step (72°C, 4min) was followed by the storage step at 12°C.

4.2.1.8 Plasmid Digest

Restriction enzymes and buffers were used as recommended by Thermo Scientific – Conventional Restriction Enzymes.

4.2.1.9 Agarose-Gels

DNA fragments were separated by size with the help of a 1% agarose gel. Here 1 g of agarose was mixed with 99 ml of 1 x TAE buffer (40 mM Tris, 50mM acetic acid, 1 mM EDTA pH 8.5, glacial). The agarose powder was melted in a microwave and afterwards supplemented with DNA stain GelRed (Biotium) in a dilution of 1:5. Agarose gels were run at 90-150 V in 1 x TAE buffer. A 1kb DNA GeneRuler ladder (Thermo Scientific) was used to compare the size of the respective DNA fragment. The visualization of DNA was achieved by using an UV Transilluminator (UVP GelStudio, Analytic Jena GmbH).

4.2.1.10 In Gel purification of DNA Fragments

After multiplication of a PCR-fragment via PCR, purification was performed according to the instruction from the GeneJet Gel Extraction Kit (Thermo Scientific).

4.2.1.11 Gateway TOPO cloning

Cloning with the pENTR™/D-TOPO™ Cloning Kit (K240020) or the pCR™8/GW/TOPO™ TA Cloning Kit (K250020) was performed as recommended by Thermo Fisher Scientific.

4.2.1.12 Gateway L/R-reaction

The Gateway L/R- reaction with the Gateway™ LR Clonase™ II Enzyme mix (11791100) was performed as recommended by Thermo Fisher Scientific.

4.2.1.13 GoldenGate cloning

The Golden Gate cloning method was introduced by Engler and Marillonnet in 2008 and makes use of type IIs endonucleases that cut DNA distal to their recognition site. By exploiting this unique way of site recognition and different sites for cutting, specific overhangs are created which allow unidirectional ligation of various fragments in one reaction. If the module to be inserted already contains type IIs restriction sites for BsaI, those need to be removed by targeted nucleotide exchange without interrupting the reading frame to avoid any kind of frame shift mutation (Engler et al. 2008).

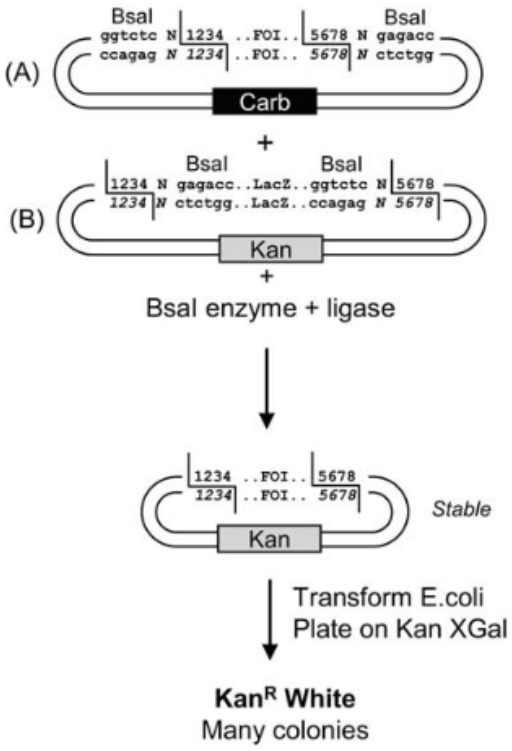

Figure 47 Golden Gate Cloning (modified after Engler et al. 2008).

Entry clone (A) and expression vector (B) are mixed in one tube together with BsaI and ligase. Only the desired product is stable. Numbers 1 to 8 denote any nucleotide of choice, and numbers in italics denote the complementary nucleotides. FOI means DNA fragment of interest.

4.2.1.14 Plasmid extraction from bacteria

2ml of a 5ml over night culture of *E. coli* containing the plasmid of interest were centrifuged at full speed (Eppendorf 5427R) at room temperature and processed as recommendet in the GeneJET Plasmid Miniprep Kit (K0503) by Thermo Fisher Scientific.

4.2.1.15 Sequencing

Sequencing was outsourced to Eurofins Genomics (Ebersberg, Germany). The investigated fragment (50-100ng/µL) was mixed with 2.5µL oligonucleotide (10mM). The total volume of 10µL was obtained with double distilled milli-Q water.

4.2.1.15.1 RNA-Sequencing (provided by Krause Lab Tromsø)

The quality of the sequences was checked by using FastQC. For trimming and cleaning Trimmomtaic was used. The cleaned sequences were again checked by FastQC. In most of the remaining sequence were strange nucleotides at the first and the last position which were then clipped away manually. In addition to this all sequences were checked for rRNA and tRNA contamination. The transcripts were then mapped against the *N. tabacum* genome (Nitab4.5). The *N. benthamiana* draft genome (v1.0.1) was not used because it is not yet published. Thus, anything based on this genome cannot be published since this genome is published (Data Agreement). In addition, the genome is not as good as the *N. tabacum* genome. After mapping, the read count analysis, the transformation and the normalization the expression changes were statistically analysed (DGE 1.1 (EdgeR), FDR correction based on the method from Benjamini and Hochberg) In addition to the available genome annotation, a bincode annotation was generated and further blast annotations were done were necessary.

4.2.2 Bacterial growth and transformation

4.2.2.1 Bacterial growth, O/N-cultures

For cultivation of bacteria in liquid cultures LB media was prepared as described in (Table 8), for cultivation on plates agar was added to the LB media. LB media liquid and solid were steam-pressure autoclaved at 121°C. For overnight cultures, the liquid media was mixed with the antibiotics as shown in Table 11. For plates LB solid was boiled in the microwave until the agar was liquefied, then cooled to 60°C and mixed with antibiotics.

4.2.2.2 Transformation of *Escherichia coli*

For the transformation of *Escherichia coli* chemical competent cells (200µL vials stored at -80°C) were slowly defrosted on ice, mixed with 2-4µL of plasmid DNA and incubated on ice for 20-30 minutes. The incubation was followed by heat-shocking at 42°C for 50s, after 3 minutes on ice, 300µL SOC-medium was added and the solution was incubated at 37°C for 1 hour. Colonies were grown over night at 37°C on selective LB plates containing the appropriate antibiotics.

4.2.2.3 Transformation of *Agrobacterium thumefaciens*

For the transformation of *Agrobacterium thumefaciens* electro-competent cells (50µL vials stored at -80°C) were slowly defrosted on ice and mixed with 1µL of plasmid DNA. After 5 minutes of incubation the cells were transferred into electroporation cuvettes and treated with 1500V. The cells were resuspended in 300µL SOC-medium and incubated for 1 hour at 30°C. 15µL were incubated overnight to 2 days at 30°C on selective LB plates containing the appropriate antibiotics.

4.2.3 Protein Analysis

4.2.3.1 Protein Extraction

All protein extractions were performed on ice and in refrigerated centrifuges (4°C).

4.2.3.1.1 Protein extraction for checking expression level

To determine the Expression level of respective proteins a “crude extraction” was performed. For the crude extraction plant material was ground at -80°C (in liquid nitrogen) into a fine light green powder. 100mg fine ground powder was mixed with double the amount of 3x SDS-buffer (total volume of 40 ml: 12 ml glycerol, 12 ml SDS 10%, 7,5 ml 0,5 M TRIS/HCl pH 6,8, 2 ml 1% bromophenol blue, 6,5 ml ddH_2O). The samples were thawed on ice and then boiled at 95°C for 5 minutes. Before loading 20µL onto an SDS-PAGE the samples were centrifuged for 5 minutes at full speed.

4.2.3.1.2 Protein extraction for Co-immunooprecipitation

For Co-Immunoprecipitation plant material was ground in liquid nitrogen into a fine powder (the finer the better). 200mg of the powder were mixed with 1ml ice cold extraction-buffer (10% glycerol, 150 nM Tris-HCl, pH 7,5, 1 mM EDTA, 150 mM NaCl, 10 mM DTT, 0,2% Nonidet P-40, 2% PVPP, proteinase inhibitor cocktail (Sigma, P9599) 33µl per gram plant material), thawed on ice and then incubated for 1 hour in an overhead shaker at 4°C.

Bead transfers were always carried out with a cut tip to prevent damaging the beads.

During the incubation 20µL GFP-coupled agarose/ magnetic beads (Chromotek) were transferred into a new tube. The transferred beads were washed 3 times with 1ml GTEN-buffer (10% glycerol, 150 mM Tris/HCl, pH 7,5, 1 mM EDTA, 150 mM NaCl, 10 mM DTT, 0,2% Nonidet P-40) to remove the storage buffer. For Agarose beads sedimentation of beads in between the washing steps was carried out by centrifugation at 2500g (4°C) for 2 minutes, for magnetic beads the DynaMag-2 Magnet rack (Thermo, 12321D) was used. After the last washing step, the beads were resuspended in 100µl per sample GTEN-buffer and kept on ice.

After the one-hour incubation at 4°C the samples were centrifuged at 5000g for 20 minutes at 4°C to get rid of the cell debris. The supernatant was filtered through a one-layer Miracloth (Merck Millipore) into a fresh 1,5ml Eppendorf tube. 40µL were transferred into a new reaction tube and mixed with 40µL 3x SDS-buffer, this was used as input control.

The washed beads were added to the samples (100µl each) and the mixture was incubated for 1 hour in an overhead shaker at 4°C to bind the tagged proteins. To get rid of unspecific binding the beads were washed two times with 500µl Buffer A (50 mM Tris/HCl, 150 mM NaCl) followed by one additional washing step with 500µl Buffer B (50 mM Tris/HCl, 50 mM NaCl). After the last washing step, the supernatant was removed and 40µl 3x SDS-buffer was added. The samples were boiled for 5 minutes at 95°C, centrifuged at full speed and ready for loading onto an SDS-PAGE.

4.2.3.1.3 Protein extraction for mass specrometry analysis

For the MS/MS analysis higher amounts of protein were needed, therefore the protocol extraction for Co-immunoprecipitation was scaled up. Depending on the expression instead of 200mg plant material at least 1g or more plant material was used. The extraction Buffer was scaled up accordingly and the extraction was performed in higher volume reaction tubes. For the upscaled experiments 50µl beads were used, all steps were performed as described in Protein extraction for Co-immunooprecipitation.

4.2.3.2 Protein Detection

4.2.3.2.1 SDS-Polyacrylamide gel electrophoresis (SDS-PAGE)

Protein extracts were boiled before loading 20µl at 95 °C for 5 minutes. The gels consisted of a 8% stacking gel and a 10% loading gel, for size determination 4µl page ruler (Thermo) were loaded into one pocket. The gels were run for 45 to 60 minutes in the BioRad Mini-Protean system with the

PowerPac HC (BioRad) at 25mA per gel using a 1x SDS running buffer (25 mM Tris base, 192 mM glycine, 0.1% (w/v) SDS).

4.2.3.2.2 Coomassie gel staining

Coomassie staining solution (0.125% (w/v) Coomassie blue R-250, 25% (v/v) 2-Propanol and 10% (v/v) acetic acid) was used to stain proteins in gels directly. After 30 minutes in Coomassie solution was replaced with the destaining solution (45% (v/v) isopropanol, 10% (v/v) acetic acid) until single bands were visible.

4.2.3.2.3 Gel preparation for mass specrometry analysis

The samples were loaded onto an 10% SDS-page, the run was terminated after the running front had migrated 1cm into the gel. The gel was staind with coomassii and the resulting band was cut from the gel and placed in an 1,5ml reaction tube. The Proteomcenter of Tübingen performed an in gel trypsin digest and used ESI LC-MS/MS for a whole protein analysis.

4.2.3.2.4 Immunoblot analysis

Proteins separated in an SDS-Page were transferred to a nitrocellulose membrane with the BioRad Mini-Protean tank blotting system. The membrane was preincubated in the transfer buffer (25 mM Tris base, 192 mM glycine, 20% methanol), the tank blot system was assembled and run for 1 hour at 100V (BioRad, PowerPac HC). To block unspecific binding sites on the blotting membrane, the membrane was incubated for 1 hour at room temperature in 5% milk powder solved in PBS-T (137 mM NaCl, 27 mM KCl, 10 mM Na_2HPO_4, 2 mM KH_2PO_4, pH 7.4, 0.1% Tween 20). The first antibody was diluted in 5% milk powder solved in PBS-T and incubated over night at 4°C. The membrane was washed 3 times for 5 minutes with PBS-T followed by an incubation for 1 hour with the secondary antibody coupled to alkaline phosphatase (diluted in 5% milk in PBS-T). The membrane was washed in PBS-T two times for 5 minutes followed by two washings with assay buffer (20mM Tris/HCl pH 9, 2mM $MgCl_2$). The assay buffer was used to dilute the NitroBlock (1:20), the mixture was then spread on the membrane that was placed on a foil (Leitz) for 5 minutes. The NitroBlock was washed off the membrane by placing the membrane in assay buffer for 2 minutes, this step was followed by the application of CDP-Star (1:50 in assay buffer). After 5 minutes the membrane was wrapped in foil ready to be detected in the UVP ChemStudio (AnalytikJena). Protocol says detect nice and correct bands.

4.2.3.2.5 Ponceau S

As transfer control on the nitrocellulose membrane Ponceau S (0,1% Ponceau S, in 5% acetic acid) as a reversible staining was used. The Ponceau S solution was added to the membrane incubated for 5 minutes, detaining by tap water was individual adjusted until single bands were visible.

4.2.3.2.6 Protein concentration

The protein concentration was measured by Bradford's protein assay ($OD_{595/450}$) with a BSA calibration series. (Bradford 1976). Roti®Nanoquant (Roth) was used for low amounts of protein, the assay was prepared as recommended by the manufacturer.

4.2.4 Plant growth conditions and transformation

4.2.4.1 Plant growth conditions

Nicotiana benthamiana was grown in P-soil (pH 5.5-6.5; Salt [g/l] 1.5; N [mg/l] 100-250; P_2O_5 [mg/l] (plant ready) 100-250; K_2O [mg/l] 100-250) in 6er pods up to a size of 20 cm. Bigger plants were transferred into 10er pods and grown in T-soil (pH 5.5-6.5; Salt [g/l] 3.0; N [mg/l] 250-300; P_2O_5 [mg/l] (plant ready) 250-450; K_2O [mg/l] 300-500). The plants were grown with a 14/10-hour light/dark rhythm (6 in the morning to 8 in the evening) at 23°C during light hours and 20°C during dark hours (60% humidity). All plants were treated with a 0,3 % Wuxal solution (8% N; 8% K; 6% K; Microelements) two times a week. (Provided by the Central Facilities of the ZMBP, Tübingen, Germany)

4.2.4.2 Transient transformation of *Nicotiana benthamiana*

A. thumefaciens GV3101 containing the investigated constructs as well as *A. thumefaciens* GV3101 containing the silencing suppressor P19 were grown as a 5ml liquid culture in their respective antibiotics for 2 days. The 5ml liquid culture were then transferred into 50ml reaction tubes and centrifuged at 4°C for 15 minutes at 4000g. The supernatant was discarded, and the cell pellet was resuspended in 10mM $MgCl_2$ containing 150µM Acetosyringone and adjusted to an OD_{600} of 1. The adjusted suspension was kept at room temperature for 90 minutes (do not close lid tightly) and afterwards diluted 1:10 in $MgCl_2$ to an OD_{600} of 0,1, to each investigated construct P19 was added with an OD_{600} of 0,1. P19 only was used as empty control.

4.2.4.3 Stable transformation of Nicotiana benthamiana and A. thaliana

Stable transformation of *N. benthamiana* and *A. thaliana* was carried out by Birgit Löffelhardt (ZMBP) according to the stable transformation protocols provided by the plant transformation unit of the central facilities of the ZMBP.

4.2.5 Functional assays

4.2.5.1 Proteinase digest

Cuscuta Extract was digested with Proteinase K (ProK) by mixing 10µl Cuscuta Extract with 80µl reaction buffer (5mM $CaCl_2$ and 50mM Tris/ HCl pH 7.5) and 10µl ProK (50µg/ml). The mixture was incubated at 37°C (O/N), afterwards the ProK was deactivated by boiling at 95°C for 15 minutes.

4.2.5.2 Promoter:Luciferase Bioassay

For the promoters of the promoter:luciferase Bioassay were cloned into pBGWL7 containing the luciferase gene. The promoter:luciferase construct was transiently transformed into *N. benthamina* and one day after infiltration the leaves were cut into 2x2mm pieces (need to fit in a 96-well plate). The leaf pieces were incubated in petri dishes overnight in water. The next day the 96-well plate was prepared by freshly mixing the reaction buffer (25mM MES pH 5.5; 200 µM D-Luciferin p.a. free acid (pjk biotech GmbH)) and distributing 100µl in each well. The leaf pieces were carefully added with a spatula. Treatment was done as described in the main text.

4.2.5.3 Ethylene biosynthesis

Ethylene assays were performed as previously described (Albert et al. 2010, Felix et al. 1999), using samples of 3 leaf pieces (~3 x 4 mm each) in 6 ml glass reaction tubes with 500µl H2O. Samples were treated with Cuscuta Extract or other elicitors as indicated, sealed with rubber plugs and incubated for 3h at room temperature on a shaker (130 rpm). Ethylene was measured by injecting 1 ml of the air phase into a gas chromatograph (Shimadzu GC-2014) and analyzed as described (Albert et al. 2010).

4.2.6 Technical devices

Western Blot

BioRad Mini-Protean Tetra Vertical Electrophoresis Cell and the Mini Trans-Blot

Electroporation

BioRad Gene Pulser 2

Luminometer

Berthold Tristar 5 Multimode Reader (Inject port)

Berthold Centro LB960 Luminometer

Gas chromatograph

Shimadzu GC-2014 (FID; DINJ); Glass Column (1,6mx3mm), Column bed: Al_2O_3

Ethylene_800min: Multi-Inject program 800min runtime with peak calculation (inject in alternating ports in 20s intervals)

Camera

Canon EOS 80D + Canon RF 24-70mm F2.8L IS USM

Gel and Blot detection

UVP GelStudio 230V (AnalytikJena)

Amersham ImageQuant 600 (GE/Cytiva)

UVP ChemStudio, 815 f/0.95 25mm lens, 230V (AnalyticJena)

Power Supply

BioRad PowerPac Basic Power Supply

BioRad PowerPack HC High-Current Power Supply

Pipettes

Eppendorf ResearchPlus (0,1-2,5µL; 0,5-10 µL; 2-20 µL; 20-200 µL; 100-1000 µL; 1-10mL

Mettler Toledo Pipet-Lite XLS+ manual 8-channel (2-20µL; 20-200µL)

Centrifuges

Eppendorf 5427R

Eppendorf 5810R

Sorvall WX 80 ULTRA 230V

Biozym Color Sprout Plus MiniCentrifuge light green

5 Summary

Parasitic plants are a constraint on agriculture worldwide. Plants of the genus *Cuscuta* are obligate holoparasites with a broad host spectrum for nearly all dicotyledonous plants. As leaf- and rootless plants, *Cuscuta* spp. wind around stems of host plants and penetrate host tissue with haustoria. They directly connect to the vasculature and exhaust water, nutrients and carbohydrates. Thus, the haustorium development and the establishment of a connection to the host represent essential steps in the parasite's life cycle. To date, little is known concerning the development of such host-parasite connections on molecular level. The aim of this work was to gain knowledge about specific molecular signals of *Cuscuta* spp. that get sensed by host plants and manipulate hosts towards susceptibility. On the host plant side, the major focus was to identify *Cuscuta*-derived transcription factor targets or receptors that recognize parasitic molecules and further induce cellular signaling programs related to susceptibility or development. To shed light on the transcriptomic reprogramming during the early stages of infection with *Cuscuta* spp., a transcriptome analysis by RNA sequencing after infiltration of Cuscuta Extract into *N. benthamiana* leaves has been performed. Additionally, an intense literature search with a focus on RNA sequencing data providing regulated transcripts of host and parasite genes was initiated. To investigate the molecular cues that might be necessary to switch-on host responses, intracellular processes and the connection to the host vascular system, promoters of upregulated host genes at the *Cuscuta* spp. infection site have been used to control the expression of the luciferase reporter gene. To establish a promoter:luciferase based bioassay to screen for inducing *Cuscuta*-derived molecular cues, a promoter was needed to control luciferase expression leading to significantly increased light emission after treatment with Cuscuta Extract. The promoter:luciferase construct of USUALLY MULTIPLE ACIDS MOVE IN AND OUT TRANSPORTER 25 (pUMAMIT25:luc) that showed a specific reaction to Cuscuta Extract was used to purify the *Cuscuta*-derived molecular cue. The purification and identification of the *Cuscuta*-derived molecule is part of an ongoing project. The molecule seems to be difficult to isolate since it did not bind to most of the tested chromatography columns. A characterization showed that the molecular cue had no charge, was hydrophilic and was not of proteidogenous nature. An *in silico* analysis of the host UMAMIT25 which seems manipulated by *C. reflexa* revealed its involvement in amino acid transport, that can be relevant for *Cuscuta* spp. nutrition and growth. Additional beneficial transporter genes like sucrose transporters were analyzed and the corresponding promoter:luciferase constructs showed increased light emission upon Cuscuta Extract treatment. The experiments of this work leave it open whether the molecular cue might be a sucrose gradient, a *Cuscuta*-derived CLE peptide, a Transcription activator-like (TAL) effector-like or a still elusive molecular trigger.

Cultivated tomato is a notable exception and represents one of few resistant host plants for *C. reflexa*. This is partially due to the presence of the membrane-bound leucine-rich repeat receptor-like protein (LRR-RLP) Cuscuta Receptor 1 (CuRe1). In this work, an additional project was to investigate the early downstream signaling and receptor activation of CuRe1 with a special interest in the C-terminal hydrophobic tail that could be a possible interaction site for downstream signaling partners. After construction and expression of four CuRe1 deletion variants, it could be clearly demonstrated that SlSOBIR1 binding was not dependent on the extra hydrophobic C-terminal tail. The expression of two deletion variants lacking parts of the extracellular LRR-domain in *N. benthamiana* and a co-immunoprecipitation followed by mass spectrometry analysis has been performed. The large hit list will probably reveal promising candidates of the CuRe1 interactome and will help to decipher how CuRe1 is connected to known or un-known signaling pathways to defend against *Cuscuta* spp..

6 Zusammenfassung

Parasitäre Pflanzen führen zu drastischen Ernteeinbußen und stellen daher eine Gefahr für die weltweite Landwirtschaft dar. Pflanzliche Parasiten aus dem Genus *Cuscuta* sind obligate Holoparasiten die beinahe alle zweikeimblättrigen Pflanzen befallen können. Als Blatt- und Wurzellose Pflanze windet sich *Cuscuta* spp. um den Stiel des Wirtes und verbindet sich durch das sogenannten Haustorium mit dem Leitgewebe des Wirtes um diesem Wasser, Nährstoffe und Kohlenhydrate zu entziehen. Die Entwicklung des Haustoriums sowie die Etablierung einer Verbindung zwischen Parasit und Wirt stellen essentielle Schritte im Lebenszyklus von *Cuscuta* spp. dar. Bis heute ist wenig über die molekularen Schritte während der Verbindung zwischen Parasit und Wirt bekannt. Das Ziel dieser Arbeit war die Erforschung der parasitischen molekularen Signale und Botenstoffe, die durch den Wirt wahrgenommen werden und diesen hin zur Suszeptibilität beeinflussen. Auf Seiten des Wirtes lag der Fokus in der Aufklärung von *Cuscuta* aktivierten Transkriptionsfaktoren oder Rezeptoren, die den parasitischen Botenstoff wahrnehmen können und intrazelluläre Signalkaskaden aktiveren, die zur Suszeptibilität beitragen. Um die transkriptionelle Neuprogrammierung in der frühen Phase der Infektion aufzuklären, wurden *N. benthamiana* Blätter mit Cuscuta Extrakt infiltriert und die regulierten Transkripte durch eine RNA Sequenzierung analysiert. Zusätzlich wurde eine intensive, auf RNA Sequenzierungen fokussierte Literaturrecherche initiiert, mit dem Ziel regulierte Transkripte von Parasitischen- und Wirts-Genen zu finden. Um herauszufinden, welche Rolle die, durch den Parasiten ausgesendeten, Botenstoffe im Wirt während der Verbindung der Leitgewebe spielt, wurden Promotoren von hochregulierten Genen, genutzt, um ein Luciferase Reportergen zu kontrollieren. Um ein Promotor:Luciferase basiertes Bioassay zu etablieren, wurde ein Promotor benötigt der durch die Behandlung mit Cuscuta Extrakt die Luciferase Produktion aktivieren konnte und dadurch eine signifikant erhöhte Lichtemission induzierte Das Promotor:Luciferase Konstrukt von USUALLY MULTIPLE ACIDS MOVE IN AND OUT TRANSPORTER 25 (pUMAMIT25:luc) konnte durch seine spezifische Reaktion auf Cuscuta Extrakt verwendet werden, um den von *Cuscuta* ausgesendete Botenstoff aufzuklären. Die Aufreinigung und Identifikation des, von *Cuscuta* ausgesendeten, Botenstoffs ist Teil eines fortlaufenden Projekts, da die meisten der verwendeten chromatographischen Säulen den Botenstoff nicht binden konnten. Eine Charakterisierung des parasitären Botenstoffs zeigte jedoch, dass er keine Ladung aufweist, hydrophil und von nicht-proteinogener Natur ist. Eine *in silico* Analyse des durch *Cuscuta* manipulierten UMAMIT25 des Wirtes, zeigte dessen Beteiligung am Aminosäuretransport, der für die Nährstoffversorgung und das Wachstum wichtig ist. Weitere interessante und für *Cuscuta* nützliche, zu den Zuckertransportern zählende, Gene wurden analysiert. Die korrespondierenden Promotor:Luciferase Konstrukte wurden kloniert, in *N. benthamiana* exprimiert und zeigten eine erhöhte durch Cuscuta Extrakt induzierte

Lichtemission. Die Experimente dieser Arbeit lassen es offen, ob der von *Cuscuta* ausgesendete wirtsmanipulierende Botenstoff ein Zuckergradient, ein *Cuscuta* CLE Peptid, ein Transcription activator-like (TAL) effector-like oder ein weiterhin unbekannter Botenstoff ist.

Die Kulturtomate ist eine bemerkenswerte Ausnahme und repräsentiert einen von wenigen resistenten Wirten für *C. reflexa*. Diese Teilresistenz kann auf den membrangebundenen Leucin reichen Rezeptor (Leucine-Rich Repeat Rezeptor Like Protein, LRR-RLP) Cuscuta Receptor 1 (CuRe1) zurückgeführt werden. Ein zusätzliches Projekt dieser Arbeit war die Untersuchung der CuRe1 Aktivierung und der darauffolgenden Signaltransduktionskaskade. Im Fokus stand dabei der hydrophobe C-Terminus, der eine mögliche Schnittstelle für die Interaktion mit Co-Rezeptoren und nachgeschalteten Signalschritten darstellt. Durch die Klonierung und Expression von vier verkürzten CuRe1 Varianten konnte klar gezeigt werden, dass die Interaktion mit SlSOBIR1 nicht in Abhängigkeit des zusätzlichen hydrophoben C-Terminus stattfindet. Die Expression von zwei Deletionsvarianten, die eine zusätzlich verkürzte extrazelluläre LRR-Domäne aufwiesen, gefolgt von einer Co-Immunpräzipitation und einer massenspektrometrischen Analyse, könnte interessante Interaktionskandidaten von CuRe1 aufdecken. Des Weiteren wird diese Analyse dabei helfen zu verstehen wie CuRe1 in Verbindung zu bekannten oder unbekannten Signalwegen zur Verteidigung gegen *Cuscuta* stehen.

7 References

AKIYAMA, K., MATSUZAKI, K.-I. & HAYASHI, H. 2005. Plant sesquiterpenes induce hyphal branching in arbuscular mycorrhizal fungi. *Nature,* 435**,** 824-827.

ALAKONYA, A., KUMAR, R., KOENIG, D., KIMURA, S., TOWNSLEY, B., RUNO, S., GARCES, H. M., KANG, J., YANEZ, A. & DAVID-SCHWARTZ, R. 2012. Interspecific RNA interference of SHOOT MERISTEMLESS-like disrupts Cuscuta pentagona plant parasitism. *The Plant Cell,* 24**,** 3153-3166.

ALBERT, I., BÖHM, H., ALBERT, M., FEILER, C. E., IMKAMPE, J., WALLMEROTH, N., BRANCATO, C., RAAYMAKERS, T. M., OOME, S. & ZHANG, H. 2015. An RLP23–SOBIR1–BAK1 complex mediates NLP-triggered immunity. *Nature plants,* 1**,** 1-9.

ALBERT, I., ZHANG, L., BEMM, H. & NÜRNBERGER, T. 2019. Structure-function analysis of immune receptor at RLP23 with its ligand nlp20 and coreceptors at SOBIR1 and At BAK1. *Molecular Plant-Microbe Interactions,* 32**,** 1038-1046.

ALBERT, M., JEHLE, A. K., MUELLER, K., EISELE, C., LIPSCHIS, M. & FELIX, G. 2010. Arabidopsis thaliana pattern recognition receptors for bacterial elongation factor Tu and flagellin can be combined to form functional chimeric receptors. *Journal of Biological Chemistry,* 285**,** 19035-19042.

ANDRÉS, F., KINOSHITA, A., KALLURI, N., FERNÁNDEZ, V., FALAVIGNA, V. S., CRUZ, T., JANG, S., CHIBA, Y., SEO, M. & METTLER-ALTMANN, T. 2020. The sugar transporter SWEET10 acts downstream of FLOWERING LOCUS T during floral transition of Arabidopsis thaliana. *BMC Plant Biology,* 20**,** 1-14.

ARAYA, T., MIYAMOTO, M., WIBOWO, J., SUZUKI, A., KOJIMA, S., TSUCHIYA, Y. N., SAWA, S., FUKUDA, H., VON WIRÉN, N. & TAKAHASHI, H. 2014. CLE-CLAVATA1 peptide-receptor signaling module regulates the expansion of plant root systems in a nitrogen-dependent manner. *Proceedings of the National Academy of Sciences,* 111**,** 2029-2034.

ASAI, T., TENA, G., PLOTNIKOVA, J., WILLMANN, M. R., CHIU, W.-L., GOMEZ-GOMEZ, L., BOLLER, T., AUSUBEL, F. M. & SHEEN, J. 2002. MAP kinase signalling cascade in Arabidopsis innate immunity. *Nature,* 415**,** 977-983.

BESNARD, J., ZHAO, C., AVICE, J.-C., VITHA, S., HYODO, A., PILOT, G. & OKUMOTO, S. 2018. Arabidopsis UMAMIT24 and 25 are amino acid exporters involved in seed loading. *Journal of experimental botany,* 69**,** 5221-5232.

BETHKE, G., THAO, A., XIONG, G., LI, B., SOLTIS, N. E., HATSUGAI, N., HILLMER, R. A., KATAGIRI, F., KLIEBENSTEIN, D. J. & PAULY, M. 2016. Pectin biosynthesis is critical for cell wall integrity and immunity in Arabidopsis thaliana. *The Plant Cell,* 28**,** 537-556.

BI, G., LIEBRAND, T. W., BYE, R. R., POSTMA, J., VAN DER BURGH, A. M., ROBATZEK, S., XU, X. & JOOSTEN, M. H. 2016. SOBIR1 requires the GxxxG dimerization motif in its transmembrane domain to form constitutive complexes with receptor-like proteins. *Molecular plant pathology,* 17**,** 96-107.

BINDER, A., LAMBERT, J., MORBITZER, R., POPP, C., OTT, T., LAHAYE, T. & PARNISKE, M. 2014. A modular plasmid assembly kit for multigene expression, gene silencing and silencing rescue in plants. *PLoS One,* 9**,** e88218.

BLUME, B., NÜRNBERGER, T., NASS, N. & SCHEEL, D. 2000. Receptor-mediated increase in cytoplasmic free calcium required for activation of pathogen defense in parsley. *The Plant Cell,* 12**,** 1425-1440.

BOLLER, T. & FELIX, G. 2009. A renaissance of elicitors: perception of microbe-associated molecular patterns and danger signals by pattern-recognition receptors. *Annual review of plant biology,* 60**,** 379-406.

BOLLER, T. & HE, S. Y. 2009. Innate immunity in plants: an arms race between pattern recognition receptors in plants and effectors in microbial pathogens. *Science,* 324**,** 742-744.

BRADFORD, M. M. 1976. A rapid and sensitive method for the quantitation of microgram quantities of protein utilizing the principle of protein-dye binding. *Analytical biochemistry,* 72**,** 248-254.

CHANG, M. & LYNN, D. G. 1986. The haustorium and the chemistry of host recognition in parasitic angiosperms. *Journal of Chemical Ecology,* 12**,** 561-579.

CHEN, H. Y., HUH, J. H., YU, Y. C., HO, L. H., CHEN, L. Q., THOLL, D., FROMMER, W. B. & GUO, W. J. 2015. The Arabidopsis vacuolar sugar transporter SWEET 2 limits carbon sequestration from roots and restricts Pythium infection. *The Plant Journal,* 83**,** 1046-1058.

CHEN, L.-Q., HOU, B.-H., LALONDE, S., TAKANAGA, H., HARTUNG, M. L., QU, X.-Q., GUO, W.-J., KIM, J.-G., UNDERWOOD, W. & CHAUDHURI, B. 2010. Sugar transporters for intercellular exchange and nutrition of pathogens. *Nature,* 468**,** 527-532.

CHEN, L.-Q., QU, X.-Q., HOU, B.-H., SOSSO, D., OSORIO, S., FERNIE, A. R. & FROMMER, W. B. 2012. Sucrose efflux mediated by SWEET proteins as a key step for phloem transport. *Science,* 335**,** 207-211.

CHINCHILLA, D., BAUER, Z., REGENASS, M., BOLLER, T. & FELIX, G. 2006. The Arabidopsis receptor kinase FLS2 binds flg22 and determines the specificity of flagellin perception. *The Plant Cell,* 18**,** 465-476.

CHINCHILLA, D., ZIPFEL, C., ROBATZEK, S., KEMMERLING, B., NÜRNBERGER, T., JONES, J. D., FELIX, G. & BOLLER, T. 2007. A flagellin-induced complex of the receptor FLS2 and BAK1 initiates plant defence. *Nature,* 448**,** 497-500.

CHISHOLM, S. T., COAKER, G., DAY, B. & STASKAWICZ, B. J. 2006. Host-microbe interactions: shaping the evolution of the plant immune response. *Cell,* 124**,** 803-814.

COHN, M., BART, R. S., SHYBUT, M., DAHLBECK, D., GOMEZ, M., MORBITZER, R., HOU, B.-H., FROMMER, W. B., LAHAYE, T. & STASKAWICZ, B. J. 2014. Xanthomonas axonopodis virulence is promoted by a transcription activator-like effector–mediated induction of a SWEET sugar transporter in cassava. *Molecular Plant-Microbe Interactions,* 27**,** 1186-1198.

CUI, S., KUBOTA, T., NISHIYAMA, T., ISHIDA, J. K., SHIGENOBU, S., SHIBATA, T. F., TOYODA, A., HASEBE, M., SHIRASU, K. & YOSHIDA, S. 2020. Ethylene signaling mediates host invasion by parasitic plants. *Science advances,* 6**,** eabc2385.

DAVID-SCHWARTZ, R., RUNO, S., TOWNSLEY, B., MACHUKA, J. & SINHA, N. 2008. Long-distance transport of mRNA via parenchyma cells and phloem across the host–parasite junction in Cuscuta. *New Phytologist,* 179**,** 1133-1141.

DEPAMPHILIS, C. W. & PALMER, J. D. 1990. Loss of photosynthetic and chlororespiratory genes from the plastid genome of a parasitic flowering plant. *Nature,* 348**,** 337-339.

DEPAMPHILIS, C. W., YOUNG, N. D. & WOLFE, A. D. 1997. Evolution of plastid gene rps2 in a lineage of hemiparasitic and holoparasitic plants: many losses of photosynthesis and complex patterns of rate variation. *Proceedings of the National Academy of Sciences,* 94**,** 7367-7372.

DEPUYDT, S., RODRIGUEZ-VILLALON, A., SANTUARI, L., WYSER-RMILI, C., RAGNI, L. & HARDTKE, C. S. 2013. Suppression of Arabidopsis protophloem differentiation and root meristem growth by CLE45 requires the receptor-like kinase BAM3. *Proceedings of the National Academy of Sciences,* 110**,** 7074-7079.

DESAKI, Y., KOHARI, M., SHIBUYA, N. & KAKU, H. 2019. MAMP-triggered plant immunity mediated by the LysM-receptor kinase CERK1. *Journal of General Plant Pathology,* 85**,** 1-11.

DESAKI, Y., MIYATA, K., SUZUKI, M., SHIBUYA, N. & KAKU, H. 2018. Plant immunity and symbiosis signaling mediated by LysM receptors. *Innate Immunity,* 24**,** 92-100.

DÖRR, I. 1969. Feinstruktur intrazellular wachsenderCuscuta-Hyphen. *Protoplasma,* 67**,** 123-137.

DÖRR, I. 1972. Der Anschluß derCuscuta-Hyphen an die Siebröhren ihrer Wirtspflanzen. *Protoplasma,* 75**,** 167-184.

EDWARDS, K., JOHNSTONE, C. & THOMPSON, C. 1991. A simple and rapid method for the preparation of plant genomic DNA for PCR analysis. *Nucleic acids research,* 19**,** 1349.

ENGLER, C., KANDZIA, R. & MARILLONNET, S. 2008. A one pot, one step, precision cloning method with high throughput capability. *PloS one,* 3**,** e3647.

FELIX, G., DURAN, J. D., VOLKO, S. & BOLLER, T. 1999. Plants have a sensitive perception system for the most conserved domain of bacterial flagellin. *The Plant Journal,* 18**,** 265-276.

FLETCHER, J. C. 2020. Recent advances in Arabidopsis CLE peptide signaling. *Trends in Plant Science,* 25**,** 1005-1016.

FLETCHER, J. C., BRAND, U., RUNNING, M. P., SIMON, R. & MEYEROWITZ, E. M. 1999. Signaling of cell fate decisions by CLAVATA3 in Arabidopsis shoot meristems. *Science,* 283**,** 1911-1914.

FRITZ-LAYLIN, L. K., KRISHNAMURTHY, N., TÖR, M., SJÖLANDER, K. V. & JONES, J. D. 2005. Phylogenomic analysis of the receptor-like proteins of rice and Arabidopsis. *Plant physiology,* 138**,** 611-623.

FÜRST, U., HEGENAUER, V., KAISER, B., KÖRNER, M., WELZ, M. & ALBERT, M. 2016. Parasitic Cuscuta factor (s) and the detection by tomato initiates plant defense. *Communicative & Integrative Biology,* 9**,** 478-481.

FURUHASHI, K., IWASE, K. & FURUHASHI, T. 2021. Role of Light and Plant Hormones in Stem Parasitic Plant (C uscuta and Cassytha) Twining and Haustoria Induction. *Photochemistry and Photobiology,* 97**,** 1054-1062.

GENRE, A., CHABAUD, M., BALZERGUE, C., PUECH-PAGÈS, V., NOVERO, M., REY, T., FOURNIER, J., ROCHANGE, S., BÉCARD, G. & BONFANTE, P. 2013. Short-chain chitin oligomers from arbuscular mycorrhizal fungi trigger nuclear C a2+ spiking in M edicago truncatula roots and their production is enhanced by strigolactone. *New Phytologist,* 198**,** 190-202.

GÓMEZ-GÓMEZ, L. & BOLLER, T. 2000. FLS2: an LRR receptor–like kinase involved in the perception of the bacterial elicitor flagellin in Arabidopsis. *Molecular cell,* 5**,** 1003-1011.

GÓMEZ-GÓMEZ, L., FELIX, G. & BOLLER, T. 1999. A single locus determines sensitivity to bacterial flagellin in Arabidopsis thaliana. *The Plant Journal,* 18**,** 277-284.

GRESSEL, J., HANAFI, A., HEAD, G., MARASAS, W., OBILANA, A. B., OCHANDA, J., SOUISSI, T. & TZOTZOS, G. 2004. Major heretofore intractable biotic constraints to African food security that may be amenable to novel biotechnological solutions. *Crop protection,* 23**,** 661-689.

GUAN, Y. & NOTHNAGEL, E. A. 2004. Binding of arabinogalactan proteins by Yariv phenylglycoside triggers wound-like responses in Arabidopsis cell cultures. *Plant Physiology,* 135**,** 1346-1366.

GUO, Y., NI, J., DENVER, R., WANG, X. & CLARK, S. E. 2011. Mechanisms of molecular mimicry of plant CLE peptide ligands by the parasitic nematode Globodera rostochiensis. *Plant Physiology,* 157**,** 476-484.

GUST, A. A. & FELIX, G. 2014. Receptor like proteins associate with SOBIR1-type of adaptors to form bimolecular receptor kinases. *Current opinion in plant biology,* 21**,** 104-111.

HAUPT, S., OPARKA, K. J., SAUER, N. & NEUMANN, S. 2001. Macromolecular trafficking between Nicotiana tabacum and the holoparasite Cuscuta reflexa. *Journal of Experimental Botany,* 52**,** 173-177.

HEGENAUER, V., FÜRST, U., KAISER, B., SMOKER, M., ZIPFEL, C., FELIX, G., STAHL, M. & ALBERT, M. 2016. Detection of the plant parasite Cuscuta reflexa by a tomato cell surface receptor. *Science,* 353**,** 478-481.

HEGENAUER, V., KÖRNER, M. & ALBERT, M. 2017. Plants under stress by parasitic plants. *Current opinion in plant biology,* 38**,** 34-41.

HEGENAUER, V., SLABY, P., KÖRNER, M., BRUCKMÜLLER, J.-A., BURGGRAF, R., ALBERT, I., KAISER, B., LÖFFELHARDT, B., DROSTE-BOREL, I. & SKLENAR, J. 2020. The tomato receptor CuRe1 senses a cell wall protein to identify Cuscuta as a pathogen. *Nature communications,* 11**,** 1-7.

HEGENAUER, V., WELZ, M., KÖRNER, M. & ALBERT, M. 2017. Growth Assay for the Stem Parasitic Plants of the Genus Cuscuta. *Bio-protocol,* 7.

HETTENHAUSEN, C., LI, J., ZHUANG, H., SUN, H., XU, Y., QI, J., ZHANG, J., LEI, Y., QIN, Y. & SUN, G. 2017. Stem parasitic plant Cuscuta australis (dodder) transfers herbivory-induced signals among plants. *Proceedings of the National Academy of Sciences,* 114**,** E6703-E6709.

HIBBERD, J. M. & DIETER JESCHKE, W. 2001. Solute flux into parasitic plants. *Journal of experimental botany,* 52**,** 2043-2049.

HIRAKAWA, Y., SHINOHARA, H., KONDO, Y., INOUE, A., NAKANOMYO, I., OGAWA, M., SAWA, S., OHASHI-ITO, K., MATSUBAYASHI, Y. & FUKUDA, H. 2008. Non-cell-autonomous control of

vascular stem cell fate by a CLE peptide/receptor system. *Proceedings of the National Academy of Sciences,* 105**,** 15208-15213.

HUTIN, M., PÉREZ-QUINTERO, A. L., LOPEZ, C. & SZUREK, B. 2015. MorTAL Kombat: the story of defense against TAL effectors through loss-of-susceptibility. *Frontiers in plant science,* 6**,** 535.

ISHIDA, J. K., WAKATAKE, T., YOSHIDA, S., TAKEBAYASHI, Y., KASAHARA, H., WAFULA, E., DEPAMPHILIS, C. W., NAMBA, S. & SHIRASU, K. 2016. Local auxin biosynthesis mediated by a YUCCA flavin monooxygenase regulates haustorium development in the parasitic plant Phtheirospermum japonicum. *The Plant Cell,* 28**,** 1795-1814.

JESCHKE, W. D., BAIG, A. & HILPERT, A. 1997. Sink-stimulated photosynthesis, increased transpiration and increased demand-dependent stimulation of nitrate uptake: nitrogen and carbon relations in the parasitic association Cuscuta reflexa-Coleus blumei. *Journal of Experimental Botany,* 48**,** 915-925.

JESCHKE, W. D., BÄUMEL, P., RÄTH, N., CZYGAN, F.-C. & PROKSCH, P. 1994. Modelling of the flows and partitioning of carbon and nitrogen in the holoparasite Cuscuta reflexa Roxb. and its host Lupinus albus L. II. Flows between host and parasite and within the parasitized host. *Journal of Experimental Botany,* 45**,** 801-812.

JONES, J. D. & DANGL, J. L. 2006. The plant immune system. *nature,* 444**,** 323-329.

KARIMI, M., DE MEYER, B. & HILSON, P. 2005. Modular cloning in plant cells. *Trends in plant science,* 10**,** 103-105.

KARIMI, M., INZÉ, D. & DEPICKER, A. 2002. GATEWAY™ vectors for Agrobacterium-mediated plant transformation. *Trends in plant science,* 7**,** 193-195.

KARMANN, J., MÜLLER, B. & HAMMES, U. Z. 2018. The long and winding road: transport pathways for amino acids in Arabidopsis seeds. *Plant reproduction,* 31**,** 253-261.

KIM, G., LEBLANC, M. L., WAFULA, E. K., DEPAMPHILIS, C. W. & WESTWOOD, J. H. 2014. Genomic-scale exchange of mRNA between a parasitic plant and its hosts. *Science,* 345**,** 808-811.

KÖRNER, M., SLABY, P. & ALBERT, M. 2020. Quinones shuffling the CARDs. *Nature Plants,* 6**,** 1074-1075.

LEMOINE, R., CAMERA, S. L., ATANASSOVA, R., DÉDALDÉCHAMP, F., ALLARIO, T., POURTAU, N., BONNEMAIN, J.-L., LALOI, M., COUTOS-THÉVENOT, P. & MAUROUSSET, L. 2013. Source-to-sink transport of sugar and regulation by environmental factors. *Frontiers in plant science,* 4**,** 272.

LIEBRAND, T. W., VAN DEN BERG, G. C., ZHANG, Z., SMIT, P., CORDEWENER, J. H., AMERICA, A. H., SKLENAR, J., JONES, A. M., TAMELING, W. I. & ROBATZEK, S. 2013. Receptor-like kinase SOBIR1/EVR interacts with receptor-like proteins in plant immunity against fungal infection. *Proceedings of the National Academy of Sciences,* 110**,** 10010-10015.

LISCUM, E., ASKINOSIE, S. K., LEUCHTMAN, D. L., MORROW, J., WILLENBURG, K. T. & COATS, D. R. 2014. Phototropism: growing towards an understanding of plant movement. *The Plant Cell,* 26**,** 38-55.

LIU, L., ADRIAN, J., PANKIN, A., HU, J., DONG, X., VON KORFF, M. & TURCK, F. 2014. Induced and natural variation of promoter length modulates the photoperiodic response of FLOWERING LOCUS T. *Nature communications,* 5**,** 1-9.

MATSUKURA, C.-A., SAITOH, T., HIROSE, T., OHSUGI, R., PERATA, P. & YAMAGUCHI, J. 2000. Sugar uptake and transport in rice embryo. Expression of companion cell-specific sucrose transporter (OsSUT1) induced by sugar and light. *Plant Physiology,* 124**,** 85-94.

MATSUMOTO-KITANO, M., KUSUMOTO, T., TARKOWSKI, P., KINOSHITA-TSUJIMURA, K., VÁCLAVÍKOVÁ, K., MIYAWAKI, K. & KAKIMOTO, T. 2008. Cytokinins are central regulators of cambial activity. *Proceedings of the National Academy of Sciences,* 105**,** 20027-20031.

MORIWAKI, T., MIYAZAWA, Y., KOBAYASHI, A., UCHIDA, M., WATANABE, C., FUJII, N. & TAKAHASHI, H. 2011. Hormonal regulation of lateral root development in Arabidopsis modulated by MIZ1 and requirement of GNOM activity for MIZ1 function. *Plant Physiology,* 157**,** 1209-1220.

MOTT, G. A., SMAKOWSKA-LUZAN, E., PASHA, A., PARYS, K., HOWTON, T. C., NEUHOLD, J., LEHNER, A., GRÜNWALD, K., STOLT-BERGNER, P. & PROVART, N. J. 2019. Map of physical interactions between extracellular domains of Arabidopsis leucine-rich repeat receptor kinases. *Scientific data,* 6**,** 1-6.

MUTHURAMALINGAM, M., WANG, Y., LI, Y. & MAHALINGAM, R. 2017. Interacting protein partners of Arabidopsis RNA-binding protein At RBP 45b. *Plant Biology,* 19**,** 327-334.

NAESSENS, E., DUBREUIL, G., GIORDANENGO, P., BARON, O. L., MINET-KEBDANI, N., KELLER, H. & COUSTAU, C. 2015. A secreted MIF cytokine enables aphid feeding and represses plant immune responses. *Current Biology,* 25**,** 1898-1903.

NAKAGAWA, T., KUROSE, T., HINO, T., TANAKA, K., KAWAMUKAI, M., NIWA, Y., TOYOOKA, K., MATSUOKA, K., JINBO, T. & KIMURA, T. 2007. Development of series of gateway binary vectors, pGWBs, for realizing efficient construction of fusion genes for plant transformation. *Journal of bioscience and bioengineering,* 104**,** 34-41.

NICKRENT, D. L. 2020. Parasitic angiosperms: how often and how many? *Taxon,* 69**,** 5-27.

OKA-KIRA, E. & KAWAGUCHI, M. 2006. Long-distance signaling to control root nodule number. *Current opinion in plant biology,* 9**,** 496-502.

OLSEN, S., STRIBERNY, B., HOLLMANN, J., SCHWACKE, R., POPPER, Z. & KRAUSE, K. 2016. Getting ready for host invasion: elevated expression and action of xyloglucan endotransglucosylases/hydrolases in developing haustoria of the holoparasitic angiosperm Cuscuta. *Journal of experimental botany,* 67**,** 695-708.

PÉRON, T., CANDAT, A., MONTIEL, G., VERONESI, C., MACHEREL, D., DELAVAULT, P. & SIMIER, P. 2017. New insights into phloem unloading and expression of sucrose transporters in vegetative sinks of the parasitic plant Phelipanche ramosa L.(Pomel). *Frontiers in plant science,* 7**,** 2048.

POULIN, R. & MORAND, S. 2000. The diversity of parasites. *The quarterly review of biology,* 75**,** 277-293.

POULSEN, C. P., DILOKPIMOL, A. & GESHI, N. 2015. Arabinogalactan biosynthesis: Implication of AtGALT29A enzyme activity regulated by phosphorylation and co-localized enzymes for nucleotide sugar metabolism in the compartments outside of the Golgi apparatus. *Plant signaling & behavior,* 10**,** e984524.

REN, S. C., SONG, X. F., CHEN, W. Q., LU, R., LUCAS, W. J. & LIU, C. M. 2019. CLE25 peptide regulates phloem initiation in Arabidopsis through a CLERK-CLV2 receptor complex. *Journal of integrative plant biology,* 61**,** 1043-1061.

ROBATZEK, S., CHINCHILLA, D. & BOLLER, T. 2006. Ligand-induced endocytosis of the pattern recognition receptor FLS2 in Arabidopsis. *Genes & development,* 20**,** 537-542.

RODRIGUEZ-VILLALON, A. 2016. Wiring a plant: genetic networks for phloem formation in Arabidopsis thaliana roots. *New Phytologist,* 210**,** 45-50.

RODRIGUEZ-VILLALON, A., GUJAS, B., KANG, Y. H., BREDA, A. S., CATTANEO, P., DEPUYDT, S. & HARDTKE, C. S. 2014. Molecular genetic framework for protophloem formation. *Proceedings of the National Academy of Sciences,* 111**,** 11551-11556.

RUNYON, J. B., MESCHER, M. C. & DE MORAES, C. M. 2006. Volatile chemical cues guide host location and host selection by parasitic plants. *Science,* 313**,** 1964-1967.

SAUTER, M., CORNELL, K. A., BESZTERI, S. & RZEWUSKI, G. 2004. Functional analysis of methylthioribose kinase genes in plants. *Plant Physiology,* 136**,** 4061-4071.

SELLAMI, S., LE HIR, R., THORPE, M. R., VILAINE, F., WOLFF, N., BRINI, F. & DINANT, S. 2019. Salinity effects on sugar homeostasis and vascular anatomy in the stem of the Arabidopsis thaliana inflorescence. *International journal of molecular sciences,* 20**,** 3167.

SHANI, E., YANAI, O. & ORI, N. 2006. The role of hormones in shoot apical meristem function. *Current opinion in plant biology,* 9**,** 484-489.

SHARMA, A. & ZHENG, B. 2019. Molecular responses during plant grafting and its regulation by auxins, cytokinins, and gibberellins. *Biomolecules,* 9**,** 397.

SHEN, Y. & DIENER, A. C. 2013. Arabidopsis thaliana RESISTANCE TO FUSARIUM OXYSPORUM 2 implicates tyrosine-sulfated peptide signaling in susceptibility and resistance to root infection. *PLoS genetics,* 9**,** e1003525.

SHIMIZU, K., HOZUMI, A. & AOKI, K. 2018. Organization of vascular cells in the haustorium of the parasitic flowering plant Cuscuta japonica. *Plant and Cell Physiology,* 59**,** 720-728.

SLABY, P., KÖRNER, M. & ALBERT, M. 2021. A cell wall-localized glycine-rich protein of dodder acts as pathogen-associated molecular pattern. *Communicative & integrative biology,* 14**,** 111-114.

SMAKOWSKA-LUZAN, E., MOTT, G. A., PARYS, K., STEGMANN, M., HOWTON, T. C., LAYEGHIFARD, M., NEUHOLD, J., LEHNER, A., KONG, J. & GRÜNWALD, K. 2018. An extracellular network of Arabidopsis leucine-rich repeat receptor kinases. *Nature,* 553**,** 342-346.

SMEEKENS, S. 1998. Sugar regulation of gene expression in plants. *Current opinion in plant biology,* 1**,** 230-234.

SPALLEK, T., MELNYK, C. W., WAKATAKE, T., ZHANG, J., SAKAMOTO, Y., KIBA, T., YOSHIDA, S., MATSUNAGA, S., SAKAKIBARA, H. & SHIRASU, K. 2017. Interspecies hormonal control of host root morphology by parasitic plants. *Proceedings of the National Academy of Sciences,* 114**,** 5283-5288.

SPALLEK, T., MUTUKU, M. & SHIRASU, K. 2013. The genus S triga: a witch profile. *Molecular plant pathology,* 14**,** 861-869.

SPANU, P., GROSSKOPF, D. G., FELIX, G. & BOLLER, T. 1994. The apparent turnover of 1-aminocyclopropane-1-carboxylate synthase in tomato cells is regulated by protein phosphorylation and dephosphorylation. *Plant Physiology,* 106**,** 529-535.

STADLER, R. & SAUER, N. 2019. The AtSUC2 promoter: a powerful tool to study phloem physiology and development. *Phloem.* Springer.

SU, Y.-H., LIU, Y.-B. & ZHANG, X.-S. 2011. Auxin–cytokinin interaction regulates meristem development. *Molecular plant,* 4**,** 616-625.

TADA, Y., SUGAI, M. & FURUHASHI, K. 1996. Haustoria of Cuscuta japonica, a holoparasitic flowering plant, are induced by the cooperative effects of far-red light and tactile stimuli. *Plant and cell physiology,* 37**,** 1049-1053.

TAKAHASHI, F., SUZUKI, T., OSAKABE, Y., BETSUYAKU, S., KONDO, Y., DOHMAE, N., FUKUDA, H., YAMAGUCHI-SHINOZAKI, K. & SHINOZAKI, K. 2018. A small peptide modulates stomatal control via abscisic acid in long-distance signalling. *Nature,* 556**,** 235-238.

TRUSCOTT, F. H. 1958. On the regeneration of new shoots from isolated dodder haustoria. *American Journal of Botany***,** 169-177.

VAN DER BURGH, A. M., POSTMA, J., ROBATZEK, S. & JOOSTEN, M. H. 2019. Kinase activity of SOBIR1 and BAK1 is required for immune signalling. *Molecular plant pathology,* 20**,** 410-422.

VERDIER, V., TRIPLETT, L. R., HUMMEL, A. W., CORRAL, R., CERNADAS, R. A., SCHMIDT, C. L., BOGDANOVE, A. J. & LEACH, J. E. 2012. Transcription activator-like (TAL) effectors targeting Os SWEET genes enhance virulence on diverse rice (Oryza sativa) varieties when expressed individually in a TAL effector-deficient strain of Xanthomonas oryzae. *New Phytologist,* 196**,** 1197-1207.

VOINNET, O., RIVAS, S., MESTRE, P. & BAULCOMBE, D. 2003. Retracted: An enhanced transient expression system in plants based on suppression of gene silencing by the p19 protein of tomato bushy stunt virus. *The plant journal,* 33**,** 949-956.

WAKATAKE, T., OGAWA, S., YOSHIDA, S. & SHIRASU, K. 2020. An auxin transport network underlies xylem bridge formation between the hemi-parasitic plant Phtheirospermum japonicum and host Arabidopsis. *Development,* 147**,** dev187781.

WANG, L., ALBERT, M., EINIG, E., FÜRST, U., KRUST, D. & FELIX, G. 2016. The pattern-recognition receptor CORE of Solanaceae detects bacterial cold-shock protein. *Nature plants,* 2**,** 1-9.

WANG, L., EINIG, E., ALMEIDA-TRAPP, M., ALBERT, M., FLIEGMANN, J., MITHÖFER, A., KALBACHER, H. & FELIX, G. 2018. The systemin receptor SYR1 enhances resistance of tomato against herbivorous insects. *Nature plants,* 4**,** 152-156.

WESTWOOD, J. H., YODER, J. I., TIMKO, M. P. & DEPAMPHILIS, C. W. 2010. The evolution of parasitism in plants. *Trends in plant science,* 15**,** 227-235.

WICKE, S., MÜLLER, K. F., DEPAMPHILIS, C. W., QUANDT, D., BELLOT, S. & SCHNEEWEISS, G. M. 2016. Mechanistic model of evolutionary rate variation en route to a nonphotosynthetic lifestyle in plants. *Proceedings of the National Academy of Sciences,* 113**,** 9045-9050.

WINKELMÜLLER, T. M., ENTILA, F., ANVER, S., PIASECKA, A., SONG, B., DAHMS, E., SAKAKIBARA, H., GAN, X., KUŁAK, K. & SAWIKOWSKA, A. 2021. Gene expression evolution in pattern-triggered immunity within Arabidopsis thaliana and across Brassicaceae species. Oxford University Press.

YAMAGUCHI, Y. L., ISHIDA, T. & SAWA, S. 2016. CLE peptides and their signaling pathways in plant development. *Journal of Experimental Botany,* 67**,** 4813-4826.

YAMAMOTO, Y. Y., ICHIDA, H., MATSUI, M., OBOKATA, J., SAKURAI, T., SATOU, M., SEKI, M., SHINOZAKI, K. & ABE, T. 2007. Identification of plant promoter constituents by analysis of local distribution of short sequences. *BMC genomics,* 8**,** 1-23.

YANG, S. F. & HOFFMAN, N. E. 1984. Ethylene biosynthesis and its regulation in higher plants. *Annual review of plant physiology,* 35**,** 155-189.

YODER, J. I. & SCHOLES, J. D. 2010. Host plant resistance to parasitic weeds; recent progress and bottlenecks. *Current opinion in plant biology,* 13**,** 478-484.

YONEYAMA, K., AWAD, A. A., XIE, X., YONEYAMA, K. & TAKEUCHI, Y. 2010. Strigolactones as germination stimulants for root parasitic plants. *Plant and Cell Physiology,* 51**,** 1095-1103.

YOSHIDA, S., CUI, S., ICHIHASHI, Y. & SHIRASU, K. 2016. The haustorium, a specialized invasive organ in parasitic plants. *Annual review of plant biology,* 67**,** 643-667.

YU, C.-P., LIN, J.-J. & LI, W.-H. 2016. Positional distribution of transcription factor binding sites in Arabidopsis thaliana. *Scientific reports,* 6**,** 1-7.

ZHAO, D., YOU, Y., FAN, H., ZHU, X., WANG, Y., DUAN, Y., XUAN, Y. & CHEN, L. 2018. The role of sugar transporter genes during early infection by root-knot nematodes. *International journal of molecular sciences,* 19**,** 302.

ZIPFEL, C. & FELIX, G. 2005. Plants and animals: a different taste for microbes? *Current opinion in plant biology,* 8**,** 353-360.

ZIPFEL, C., KUNZE, G., CHINCHILLA, D., CANIARD, A., JONES, J. D., BOLLER, T. & FELIX, G. 2006. Perception of the bacterial PAMP EF-Tu by the receptor EFR restricts Agrobacterium-mediated transformation. *Cell,* 125**,** 749-760.

ZIPFEL, C., ROBATZEK, S., NAVARRO, L., OAKELEY, E. J., JONES, J. D., FELIX, G. & BOLLER, T. 2004. Bacterial disease resistance in Arabidopsis through flagellin perception. *Nature,* 428**,** 764-767.

8 Supplementary Information

8.1 List of Figures

Figure 1 *Cuscuta* spp. in different habitats growing on various host plants. 1
Figure 2 Parasitic plants attached to their host plants (top panel) and sections of the haustorium (bottom panel). 2
Figure 3 Haustoria development in *Cuscuta reflexa.* 3
Figure 4 *C. reflexa* growing on *N. tabacum* shoots expressing pSUC2:GFP. 4
Figure 5 Roles of GRPs in plants and how CrGRP can initiate host defense during haustorium formation. 7
Figure 6 Principal Components Analysis of the individual samples. 10
Figure 7 Up- and Downregulation of host genes by exposition to Cuscuta Extract. 11
Figure 8 Plate preparation and measuring overview of the luciferase-based bioassay. 15
Figure 9 Light emission over time with one measurement per hour. 16
Figure 10 Light emission after incubation using an endpoint measurement (representative selection). 18
Figure 11 *N. benthamiana* plant age effects on the detection of Cuscuta Extract with transient transformed pUMAMIT25:luc. 19
Figure 12 Dose dependent detection range of the sensor pUMAMIT25:luc to applied Cuscuta Extract. 20
Figure 13 Effects of endogenous signals (carbohydrats, osmotic signals and pathogen related molecules) on pUMAMIT25:luc. 22
Figure 14 The effects of plant hormones on the sensor pUMAMIT25:luc. 23
Figure 15 Quantitative analysis of luciferase transcription via qRT-PCR. 24
Figure 16 Promoter attAGP:GUS expression in stable transformed moneymaker. 25
Figure 17 pattAGP in stable with CuRe1 transformed and wildtype *N. benthamina*. 25
Figure 18 Stable transformed pRBP45B:luc and pMTK:luc in *A. thaliana* treated with Cuscuta Extract. 26
Figure 19 Stable transformed pUMAMIT25:luc in *N. benthamiana* treated with Cuscuta Extract. 27
Figure 20 Stable transformed pUMAMIT25:luc in *N. benthamiana* treated with Cuscuta Extract. 28
Figure 21 Workflow of the pre-purification. 29
Figure 22 Correlation of protein concentration and the induced light emission of the pre-purification steps (pUMAMIT25:luc, 14h). 30
Figure 23 Ethylene production in *N. benthamiana* leaves expressing CuRe1 treated with the Cuscuta Extract pre-purification preparations. 31
Figure 24 Workflow of the chromatographic purification and characterization 32
Figure 25 Cation Exchange column (HiTrap SP-FF, 5ml) fractions applied to the sensor pUMAMIT25:luc. 33
Figure 26 Ethylene production of *N. benthamiana* expressing CuRe1, treated with Cuscuta Extract preparations from the cation exchange column. 34
Figure 27 Anion Exchange column (HiTrap Q-FF, 5ml) fractions applied to the sensor pUMAMIT25:luc. 35
Figure 28 Activity of XAD16 fractions and dilutions applied to the sensor pUMAMIT25:luc 36
Figure 29 Luciferase-dependent light production in leaves containing the sensor pUMAMIT25:luc and treated with fractions from the CEC (HiTrap SP-FF, 1ml). 37
Figure 30 Light emission of the sensor pUMAMIT25:luc after application to the fractions from the C18 column (Supelcosil LC-18 HPLC). 38

Figure 31 Light emission induced by Proteinase K digested Cuscuta Extract applied to the sensor pUMAMIT25:luc (left) and ethylene production of Proteinase K digested Cuscuta Extract applied to CuRe1 expressing *N. benthamiana* (right) 39
Figure 32 The promoter of the bidirectional sucrose transporter SWEET10 coupled to luciferase initiates light emission upon treatment with Cuscuta Extract but not with the established stresses. 41
Figure 33 The promoter of the sucrose transporter SUC2, responsible for phloem loading and long-distance transport, coupled to luciferase initiates a distinct light emission after treatment with Cuscuta Extract or Fraction 1A2. 42
Figure 34 Light emission of *N. benthamiana* leaves transiently expressing pSUC2:luc is initiated by Cuscuta Extract and a high concentration of Sucrose. 43
Figure 35 Light emission of promoter-luciferase constructs treated with *Cuscuta*-derived CLE peptides. 44
Figure 35 How does *Cuscuta reflexa* influence the host? 57
Figure 36 CuRe1 protein model (left) and C-terminal deletions (right). 58
Figure 37 In silico analysis of CuRe1 and CuRe1-likes. 59
Figure 38 Ethylene production of truncated CuRe1's. 59
Figure 39 SlSOBIR1 forms a complex with CuRe1, but display variable interaction strength with CuRe1 truncations 61
Figure 40 CuRe1 Structure and LRR deletion constructs. 62
Figure 41 Fluorescence detection of the GFP tagged ΔLRR-GFP and ΔLRR-Δ2TM-GFP. 62
Figure 42 Ethylene production of *N. benthamiana* transiently expressing ΔLRR-GFP and ΔLRR-Δ2TM-GFP 63
Figure 43 SlSOBIR1 forms a complex with ΔLRR-GFP and ΔLRR-Δ2TM-GFP. 64
Figure 44 SlSERKs do not form a complex with ΔLRR-GFP. 65
Figure 45 Full length CuRe1 and deletion variants were cloned by using the described oligo pairs. For Golden Gate constructs multiple fragments were used (5'-3' numbered) 75
Figure 46 Golden Gate Cloning (modified after Engler et al. 2008). 80

8.2 List of Tables

Table 1 Upregulated genes sorted by their Gene Ontology (GO) molecular function in resistant plants (CuRe1 containing *N. benthamiana*) 2 hours after CrGRP containing extract infiltration (1124 genes were upregulated and 505 had a designated molecular function). 11
Table 2 Genes selected for the bioassay 13
Table 3 Promoter-Luciferase construct cloned and tested in the bioassay to detect Cuscuta Extract 17
Table 4 Purification Methods tested for the enrichment of the molecular cue. 40
Table 5 Detection of SOBIR1 via MS/MS with CuRe1, CuRe1Δ18aa and CuRe1Δcyt. 60
Table 6 Detection of SOBIR1 via MS/MS with ΔLRR and ΔLRRΔ2TM 64
Table 7: Peptide names and sequences (o: Hydroxyproline) 69
Table 8: Media 69
Table 9: Antibiotics 69
Table 10: Bacterial strains and genotypes 70
Table 11: Entry and Donor Vectors 70
Table 12: Constructs for the bioassay. All promoters were cloned in pBGWL7 70
Table 13: Constructs for the analysis of the hydrophobic tail of CuRe1 71
Table 14: Oligonucleotides for promoter cloning 72
Table 15: Oligonucleotides for sequencing 73
Table 16: Oligonucleotides for genotyping 74
Table 17: Oligonucleotides for qRT-PCR 74
Table 18: Oligonucleotides for CuRe deletion project 74
Table 19: Primary antibodies 75
Table 20: Secondary antibodies 75
Table 21: Plant genotypes 76
Table 22 Columns and Buffers used for FPLC purification 76

8.3 Supplemental Datasets

Supplemental Datasets are stored on the server of the Molecular Plant Physiology, University of Erlangen-Nuernberg, 91058 Erlangen, Germany (Chair: Prof. Markus Albert)

S1 Dataset_RNA sequencing (Supplemental for RNA sequencing)

S2 Dataset_0744MaAl_R03R09_Table5 (Supplemental for Table 5)

S3 Dataset_0936MaAl_R01R03_Table6 (Supplemental for Table 6)

Mein Dank gilt…

…Prof. Dr. Markus Albert für sein Vertrauen in meine Arbeit, die Unterstützung für mein Thema und die Idee für das p:Luc Bioassay.

…Prof. Dr. Georg Felix (Jürg) für die vielen intensive Diskussionen während meiner Zeit in Tübingen.

…Prof. Dr. Katharina Markmann für ihre Expertise im Thesis Komitee.

…Dr. Julien Bruckmüller für seine Auswertung der RNA-Sequenzierung.

…der gesamten Gruppe Albert.

…allen Mitgliedern der Molekularen Pflanzenbiologie (ZMBP, Tübingen).

…allen Mitgliedern der Molekularen Pflanzenphysiologie (FAU).

…allen Stammgästen der Tübinger Happy Hour.

…meinen Eltern.